# Structural and functional brain plasticity for acquisition of drumming expertise

Department of Psychological Sciences

University of Liverpool

Manal Alosaimi

This dissertation is submitted for the degree of

*Doctor of Philosophy*

*April 2021*

# Declaration

I declare that this thesis has been composed by myself and that the work contained within has not been submitted for any other degree or professional qualification. I confirm that the work submitted is my own work.

Alosaimi, Manal

# Acknowledgements

# Abstract

Magnetic resonance imaging (MRI) has greatly extended the study of neuroplasticity in the human brain. Imaging studies conducted over recent years uncovered structural changes that occur in both grey and white matter, with most of these studies focusing on changes that occur after learning new skills. Learning, including learning to play a musical instrument, has been shown to trigger functional and structural brain plasticity. Neurological research into the effects of music have of late grown considerably and provided valuable insight into neural mechanisms that govern perception, as well as motor production of music in the healthy brain. The main goal of this project was to quantify functional and structural changes in response to learning a new musical motor task, in this case drumming. For this, we investigated the effects of drum playing on structural and functional plasticity over a six-months drumming learning course.

15 healthy volunteer non-drummers received a 45-minute drumming training session each week over 21 weeks, delivered by the professional drumming tutor. High resolution T1-weighted structural and task-based functional magnetic resonance imaging (fMRI) measurements were acquired at the baseline (pre), mid and post-learning stages of the course. In addition, a diffusion tensor imaging (DTI) scan was also performed multiple times throughout the training course to assess various measures of water diffusion within brain tissue.

Following training, the superior and middle temporal gyrus, and supramarginal gyrus, showed an increase in BOLD response signal and grey matter volume. Diffusivity values also decreased in these regions. These changes may reflect increased synaptogenesis and dendritic growth, generation of new axon collaterals, and neuron formation, which would support enhanced functional demands needed to facilitate musical training, indicating that the adult brain can be modified via learning. Clinical focus on the neural basis of music processing in the abnormally developed or degenerating brain, or in neurological illness such as, might enable exploration of the effects of music-based interventions in neurological rehabilitation.

# Contents

# List of Figures

# List of Tables

# Frequently used abbreviations:

AD        Axial Diffusivity

RD        Radial Diffusivity

MD        Mean diffusivity

FA        Fractional anisotropy

DTI        Diffusion Tensor Imaging

GM        Gray matter

IFG        Inferior Frontal Gyrus

fMRI        functional Magnetic Ressonance Imaging

SMA        Supplementary Motor Area

SMG        Supramarginal Gyrus

STG        Superior Temporal Gyrus

MTG        Middle Temporal Gyrus

VBM        Voxel-Based Morphometry

WM        White matter

BA        Brodmann Area

# Chapter 1    General Introduction

## 1.1 Thesis structure

This thesis has been divided into six chapters. Chapter 1 gives an overview of A) Brain Plasticity Imaging Studies, which includes previous functional and structural brain plasticity studies with different types of learning tasks, B) Music and Brain Plasticity, with this section focusing on the brain plasticity that could occur with musical training, C) Mechanisms in plasticity, discussing cellular and molecular level changes underlying brain plasticity, and D) Methodological background, covering the basic information about the neuroimaging modalities that have been used in this project to capture brain plasticity over the six months drumming course. Later in chapter 2, details about the drumming task, participants and the different performance methods used to evaluate the participants' progress are presented. Chapter 3 describes (study 1), which used two functional MRI tasks to capture functional plasticity with drumming learning. The functional MRI data pre, mid and post-training was analysed to investigate functional plasticity during the learning process. Following this, chapter 4 then explains (study 2), which was designed to track grey and white matter volume changes with drumming training and investigate if the brain regions showing functional changes also showed changes in grey matter volume (GMV). Additionally, chapter 5 looks more closely at the micro structural changes in white matter volume (WMV) using the diffusion tensor modality, and includes an analysis of the DTI data before, mid ,and after training to investigate structural plasticity (study 3). Finally, in chapter 6, a summary of these three studies and general discussion of how these findings could advance our understanding of the brain is explored.

## 1.2 Brain Plasticity Imaging Studies

The human brain has been found to be plastic in response to experience and behaviour, including any kind of sensory and motor activity. The training tasks employed in these Brain Plasticity Studies range from visuomotor tasks, such as juggling (for e.g., Draganski et al., 2004), golf (Bezzola et al., 2011) or balancing (Taubert et al., 2010), to cognitive tasks, such as deciphering Morse code (Schmidt-Wilcke et al., 2010), working memory (for e.g., Takeuchi et al., 2010), and learning for an exam (Draganski et al., 2006). Other studies have recruited musicians, jugglers and bilinguals, and compared their brains to those of non-musicians, non-jugglers and monolinguals, respectively (Munte et al., 2002; Gaser and Schlaug, 2003; Draganski et al., 2004; Mechelli et al., 2004).

## 1.3 Structural Brain Plasticity

Structural brain plasticity effects can be briefly illustrated by the London Taxi Drivers study, which indicated that practise-induced changes can occur over a sufficient period of time (Maguire et al., 2000). The study concluded that regularly navigating the many streets of London was associated with greater GMV in the posterior hippocampi, as well as reduced in anterior hippocampal regions when London taxi drivers were compared with age-matched controls. The degree of modification was also linked with the amount of time spent as a taxi driver (Maguire et al., 2000). A note of caution is due here since the sample of this study did not include females or left-handed people. This is a limitation as there are likely to be female London taxi drivers, and it may be that female navigational ability may be different from males due to stereotype views about female drivers. This means that any conclusions drawn will not be representative of all London taxi drivers and so the study cannot be generalised of the whole population.

In 2004, Draganski and colleagues reported increases in GMV in bilateral temporal visual motion areas and the left intraparietal sulcus in response to juggling practice. This was the first longitudinal study evidence of learning-induced structural plasticity in humans following three months of juggling training. The main limitation of this study is that, lacks population validity (i.e. the sample was including 21 females and 3 males only).

Several papers have indeed identified WM organisational features present before training that influences the degree or type of plasticity that emerges post-learning. Keller & Just (2009) showed that approximately 100 hrs of intensive reading remediation led to increased fractional anisotropy (FA) in the left frontal lobe, and this change was correlated with changes in reading ability among children (Keller and Just, 2009). In addition, Scholz et al. (2009) concluded that six weeks of juggling training in adults resulted in FA increases in the WM beneath the right intraparietal sulcus. Additional studies suggest adult FA increases following balance training (Taubert et al., 2010), working memory training in ageing participants (Lövdén et al., 2010, Engvig et al., 2011), and meditation training (Tang et al., 2010).

However, it remains unclear whether brain structural properties at baseline are associated with subsequent complex skill acquisition, and also whether the degree of brain structural change with long-term training depends on factors such as the amount of practice time and the performance outcome. As well, the lifestyle factors such as exercise and sleep have been found to correlate with brain structural measures and are potentially important mediators of Brain plasticity.

Another weakness is that the improvement of specific cognitive mechanisms can not be distinguished from a purely attentional effect. In face of the consistency of improvement on attentional variables, the possibility of an exclusive or largely predominant impact of attention on executive processes can not be ruled out.

## **1.4  Functional Brain Plasticity**

Functional neuroimaging studies have demonstrated both increases and decreases in brain activity with respect to training design (e.g. repeated practise, guided skill learning, problem-solving techniques) and targeted behaviour (e.g. motor skills, cognition, and sensory-perceptual abilities). The activation maps show training-related increases and decreases across both motor and cognitive domains (Patel et al., 2013). Changes following training have revealed several brain areas associated with increases and/or decreases in brain activity. Patel, et al., (2013) reviewed the functional neuroimaging studies of cognitive and motor skills training in adults (N = 38) and found a number of brain areas associated with increased and/or decreased activation following training. Functional MRI studies of perceptual learning with pitch tasks have shown both increases (Gaab et al., 2006) and decreases (Jäncke et al., 2001) of activity in auditory areas, as is also the case with other types of perceptual learning (Kelly & Garavan, 2005).

### 1.4.1  **Increases in Brain Activity**

Left medial prefrontal cortex (BA9), left posterior cingulate (BA31), left inferior parietal lobule (angular gyrus; BA39), and right postcentral gyrus (BA40) are frequently reported to demonstrate increased activation following motor learning. Higher levels of activity within these regions have been shown in several studies in which subjects had to learn the task without external feedback, such as drawing tasks (Van Mier et al., 1999). These activation increases were linked with greater task ease and mind wandering, whereby participants were able to perform a task well whilst simultaneously recollecting past events or imagining personal future events, processes supported by the default network (Mason et al., 2007). Post-training increases were also identified in both the lingual gyri (BA18) and fusiform gyri (left: BA19; right: BA37) bilaterally, as well as the putamen, bilaterally, and right caudate and anterior cerebellum bilaterally. Greater involvement of the basal ganglia after training is

thought to reflect a shift in the balance of corticostriatal activity from untrained to trained task performance (Carter et al., 1998; Penhune et al., 2002; Floyer-Lea et al., 2005).

## 1.4.2 **Decreases in Brain Activity**

On the other hand, bilateral areas of the frontal lobe, including the dorsolateral prefrontal cortex [PFC], ([BA] 9/46), inferior frontal gyrus (BA9), dorsal anterior cingulate cortex [ACC], (BA6), and the right lateral frontal pole (BA10) are associated with reduced activation following training. These areas are highly involved in controlled attention, and reduced recruitment of these regions may reflect activation shifting from controlled to more automatic forms of task performance following training. Significant decreases were also observed in the premotor cortex (BA6) and superior parietal lobule (BA7) bilaterally. This means that "good" learners of a motor sequence learning task exhibited a quicker decrease in activation of prefrontal regions as compared with "poor" performers (Sakai et al., 1998). There is, however, little consensus regarding which areas of the brain are consistently activated during the acquisition of motor skills. This may be a result of the diverse range of experimental paradigms that have been used to examine motor learning. Fitts and Posner (1967) proposed a three-phase motor learning model (i.e. the cognitive, associative, and autonomous phases). 1) The cognitive phase, when the learner is actively trying to figure out what exactly needs to be complete. At this stage, learners tend to pay attention to the step-by-step execution of the skill, which requires a considerable attentional capacity. 2) The associative phase, when the learner has acquired the basic movement pattern. At this stage, attention is gradually reduced, and the movement becomes more economical. 3) The autonomous phase, which is characterised by fluent and seemingly effortless motions following extensive practise. At this stage, the skill movements are performed largely automatically and require little or no attention.

## 1.5  Cross-sectional and Longitudinal Plasticity Studies

According to the experimental design, studies on brain plasticity can be divided into two types: cross-sectional studies with a single data acquisition time point, and longitudinal studies with repeated measurements of data acquisition over time. While inferences from cross-sectional studies remain at the descriptive level of correlation analysis, longitudinal studies have the potential to reveal how behavioural changes result from the temporal dynamic of interaction between brain regions. However, due to the nature of the design, cross-sectional studies are unable to distinguish between experience-dependent structural changes and pre-existing structural conditions that determine behaviour and performance. In other words, the main limitation of the cross-sectional analysis is that it cannot differentiate the effects of training on the brain from pre-existing environmental and/or genetic differences.

Longitudinal studies, which are able to test directly for experience-driven changes in grey matter (GM) or white matter (WM) structure, have provided some evidence that learning can induce structural plasticity in humans' brains. However, the complex changes in MRI-derived metrics observed with age need to be taken into account when interpreting brain-behaviour correlates (see Table 1).

| Authors/years | Modality | Sample Characteristics | Task/Group | Results |
|---|---|---|---|---|
| **Cross- sectional studies** | | | | |
| **Maguire et al. (2000)** | VBM | Male group<br><br>N = 35;<br><br>Mean age =35y. | London taxi drivers | Drivers had greater GMV in the posterior hippocampi, and reduced anterior hippocampal compared to the control. |
| **Maguire et al. (2006b)** | VBM | Mix group<br><br>N=38<br><br>Mean age =30y. | London taxi drivers | |
| **Tudor Popescu et al. (2019)** | VBM | Mix group<br><br>N =43<br><br>Mean age =30y. | Mathematicians | Mathematicians had higher GMV in the right superior parietal lobule compared to the control. |
| **Bermudez and Zatorre, (2005)** | VBM | Male group<br><br>N=40<br><br>Mean age= 24y. | Musicianship | Musician had a higher GMV in auditory regions compared to the control group. |
| **Gaser and Schlaug, (2003)** | VBM | Male group<br><br>N = 35<br><br>Mean age= 35y. | Musicianship | |
| **Cannonieri et al., (2007)** | VBM | Mix group<br><br>N= 17<br><br>Mean age =34y. | Professional typists | GMV in the SMA, PFC, and cerebellum were positively linearly correlated with time of typing training. |
| **Jancke et al., (2009)** | VBM | Male group<br><br>N=40<br><br>Mean age= 26y. | Golf players | Golf players had a greater GMV in premotor and parietal cortices compared to the control group. |

| | | | | |
|---|---|---|---|---|
| **Park et al., (2009)** | Volume analysis | Male group N=19 Mean age= 20y. | Basketball players | Basketball players have larger vermian lobules VI–VII than controls. |
| **Han et al., (2009)** | VBM | Mix group N=19 Mean age= 22y. | Musicianship | Pianists had higher GMV in the left primary sensorimotor cortex and right cerebellum. |
| **Schmithorst and Wilke (2002)** | DTI | Male group N=11 Mean age =32y. | Musicianship | Musicians had a greater fractional anisotropy (FA) in the genu of the corpus callosum. |
| **Longitudinal studies** | | | | |
| **Lei cui et al. (2019)** | VBM and Re-fMRI. | Mix group N =20 Mean age= 20y. | 8-week aerobic exercise program | Increased GMV in left superior temporal gyrus and right middle temporal gyrus compared to the control group. |
| **Midori Kodama et al. (2018)** | VBM | Mix group N=15 Mean age= 21y. | 5-day visuo-motor learning task | Participants had a greater GMV in the primary motor, primary sensory and in the hippocampal areas. |
| **Timothy A. Keller et al. (2016)** | DTI and fMRI. | Mix group N=29 Mean age= 22y. | 45-min spatial route-learning task | Participants had a MD decreased in the dentate gyrus of the left hippocampus, accompanied by an increase in fMRI-measured BOLD signal. |
| **Weronika D. et al. (2016)** | DTI and fMRI. | Mix group | 3-week tactile training based | Participants had a FA increased in the primary |

| | | N= 21<br><br>Mean age =23y. | on Braille reading | somatosensory cortex accompanied by an increase in fMRI-measured BOLD signal. |
|---|---|---|---|---|
| **Taubert et al. (2016)** | VBM | Mix group<br><br>N =57<br><br>Mean age =26y. | 1-hour of body balancing task | An increase in motor cortical thickness detected after practise in the balancing task. |
| **Taubert et al. (2010)** | DTI and VBM. | Mix group<br><br>N=28<br><br>Mean age =25y. | 2-week body balancing task | GMV increase in the prefrontal cortex correlated positively with subject's performance. |
| **Bezzola et al., (2011)** | VBM | Mix group<br><br>N =22<br><br>Mean age =57y. | 40-hours of golf practise | The golf novices showed a decrease in hemodynamic responses during the mental rehearsal of the golf swing in non-primary motor areas. |
| **Kwoka et al., (2011)** | VBM | Mix group<br><br>N= 19<br><br>Mean age = 20y. | Learning new colour names for 3-days | Increased GMV in the left visual cortex by comparing pre and post T1 scans. |
| **Erickson et al., (2011a)** | Volume analysis. | Mix group<br><br>N=60<br><br>Mean age =67y. | 1-2 year aerobic exercise program | An increase in hippocampus volume for the aerobic exercise group. |
| **Draganski et al., (2004)** | VBM | Mix group<br><br>N=15<br><br>Mean age = 22y. | 3-months three-ball juggling | Juggler showed a bilateral expansion in GMV in the mid-temporal area and in the left posterior intraparietal sulcus comparing between |
| **Driemeyer et al., (2008)** | VBM | Mix group | 3-months juggling | |

| | | N=20<br><br>Mean age = 26y. | | pre and post T1 scans. |
|---|---|---|---|---|
| **Boyke et al., (2008)** | VBM | Mix group<br><br>N=44<br><br>Mean age = 60y. | 7-days juggling | Juggler showed a increased GMV in middle temporal and nucleus accumbens bilaterally. |
| **Scholz et al., (2009)** | VBM and DTI. | Mix group<br><br>N=24<br><br>Mean age =24y. | 6-weeks juggling | Increased GMV in medial occipital and parietal cortex, overlying the FA increase comparing between the pre and post T1 scans. |
| **Zhang (2011)** | fMRI | Mix group<br><br>N=14<br><br>Mean age=22y. | 2-week motor imagery training experiment | Functional alterations induced by training were found in the fusiform gyrus. |
| **Takeuchi (2011)** | VBM and fMRI. | Mix group<br><br>N =36<br><br>Mean age=22y. | Processing speed training | Training group showed an increasesin GMV in STG and in functional activity in the left perisylvian region. |
| **Jolles (2011)** | fMRI | Mix group<br><br>N=15<br><br>Mean age =12y. | 6-weeks of working memory task | Increased activation in default-mode regions after practice. |
| **Raboyeau (2010)** | fMRI | Mix group<br><br>N=10<br><br>Mean age =22y. | 5-days of learned second-language (80 Spanish words) | Significant activations in the left IFG and Broca's area after learning. |

| Schmidt-Wilcke (2010) | VBM and fMRI. | Mix group<br><br>N=16<br><br>Mean age =30y. | Learned to decipher Morse code | After training learners showed a GMV increased the left occipito-temporal region and activity in the inferior parietal cortex bilaterally and the medial parietal cortex. |
| --- | --- | --- | --- | --- |

Table 1. Provides an overview of previous studies that investigated brain plasticity using various tasks and neuroimaging modalities. Abbreviations : DTI= diffusion tensor images, GMV= Gray Matter volume,FA= Fractional Anisotropy,VBM = voxel-based morphometry, N= number of the subject, Mix group = group were made up of both males and females, MD = Mean Diffusivity , y=years.

## 1.6 Music and Brain Plasticity

Brain plasticity that is caused by musical training is at the heart of the research reported here. Learning to play an instrument requires extensive practise incorporating various brain regions and functions, resulting in neuroplastic structural and functional changes over time. Brain changes in response to musical practise is therefore an example of training-induced plasticity, a plasticity that is most pronounced in children but can be induced throughout the life-span in a healthy brain. It has been claimed that justifiable reasons for using musical training to explore neuroplasticity are that:

1) Playing music is unlike other everyday motor activities, as it involves multiple sensory modalities and motor planning, preparation, and execution systems (Schlaug et al., 2010). Listening to music also requires specific perceptual abilities, such as pitch discrimination, and auditory memory (Zatorre et al., 2007).

2) Musical instrumental training is a physical movement which requires very accurate coordination of numerous parts of the human body (Sibylle et al., 2012); "The precise physical movement required by musical performances requires very accurate coordination of numerous parts of the body bolstered by detailed feedback at all levels" (Jourdain, 1998).

3) There is minimal risk to safety, and musical performance skills can be easily measured, allowing for the link between brain function and musical performance or ability to be examined (Sibylle et al., 2012).

4) Finally, most of the recent neuroimaging conclusions indicate that music listening is traceable in terms of network connectivity and activations of target regions in the brain (Reybrouck, 2018).

Music is therefore becoming more and more of an area of investigation in the cognitive neurosciences and research into neuroplasticity.

### 1.6.1 Music processing in the brain

Several studies involving healthy individuals indicate that cortical language networks are involved in the processing of music, with right hemispheric dominance in the musical domain and left hemispheric dominance in the language domain. A right hemisphere dominance was proposed for brain processing of music (relatively independent of musical knowledge and training), and a variable dominance was proposed for musical perception (Schlaug, 2001; 2015). Cross-sectional studies provided evidence that extensive training in professional musicians is associated with GMV changes in sensorimotor, premotor cortex, auditory, and the cerebellum regions relative to non-musicians. The volume of the cerebellum in male musicians is larger than in male non-musicians. In addition, musicians have higher GM and WM density in the left primary sensory-motor cortex and right cerebellum (Gaser and Schlaug 2003a; Gaser and Schlaug 2003b; Bermudez and Zatorre, 2005; Han et al., 2009). And the anterior portion of the corpus callosum (the thick part of the brain that connects the two hemispheres) was larger in musicians, especially those who began their training at a young age (Schlaug et al., 1995).

Not only cross-sectional, but also longitudinal studies have revealed musical training to be a suitable paradigm for exploring neuroplasticity, whether it be monitoring a beginner training

to play sequences on a piano keyboard (Lahav et al., 2007; Chen et al., 2012; Herholz et al., 2015), learning to listen to and imitate different auditory rhythms (Chen et al., 2007), or developing drumming expertise (Ahmed et al., 2016; Petrini et al., 2011). In 2008, Lappe et al. carried out a study of non-musician adults who learned to play a piano over a 2-week period, and found an increase in the volume of the auditory cortex compared to baseline.

In addition to anatomical differences, functional differences in cortical representation areas have been demonstrated in musicians. Functional differences in musicians' brains, or an enhanced neural response, was observed in the somatosensory cortex (Elbert et al., 1995), auditory cortex (Pantev et al., 1998; Koelsch et al., 1999; Rüsseler et al., 2001), and hippocampus (Herdener et al., 2010).

A significant difference in the degree of activation between musicians and non-musicians was noted in the temporal regions, and for musicians the degree of activation was correlated with the age at which the person had begun musical training (Ohnishi et al. 2001). Functional MRI has also been used to explore brain activations of novices trained to play sequences on a piano keyboard (Lahav et al. 2007; Chen et al. 2012; Herholz et al. 2015) and those listening to and imitating different auditory rhythms (Chen et al. 2007; Chu et al. , 2014). The studies indicate that musical training is associated with enhancing effects on various cognitive functions spanning from executive control to creativity, even if sometimes only restricted to the auditory domain. A common finding across these studies is that nearly all of those brain areas involved in the control of musical expertise (motor cortex, auditory cortex, and cerebellum) show specific anatomical and functional features in professional and semi-professional musicians. Moreover, It is well known that the inferior frontal gyrus, premotor cortex, supplementary motor area, somatosensory cortex, parietal cortex, and temporal lobes, all are hypothesised to house the human mirror system (MNs) (Fujioka, Ross, Kakigi, Pantev, & Trainor, 2006; Koelsch & Siebel, 2005; Overy & Molnar-Szakacs, 2009; Zatorre, Chen, & Penhune, 2007). There is probably no other activity studied to date that activates as many neuronal networks as music (see Fig. 1. and Table 2.).

According to a considerable body of literature, factors that shape neuroplasticity in musicians include age of commencing musical tuition (Schlaug et al., 1995a, Amunts et al., 1997, Jancke et al., 1997, Pantev et al., 1998, Schlaug et al., 1998, Ohnishi et al., 2001, Schlaug, 2001, Lotze et al., 2003, Koeneke et al., 2004, Bengtsson et al., 2005, Imfeld et al., 2009), duration of musical performance (Sluming et al., 2002, Hutchinson et al., 2003, Aydin et al., 2005, Abdul-Kareem et al., 2011), instrument specialty (Elbert et al., 1995, Pantev et al., 2001, Schneider et al., 2005, Bangert and Schlaug, 2006, Shahin et al., 2008), and musical expertise.
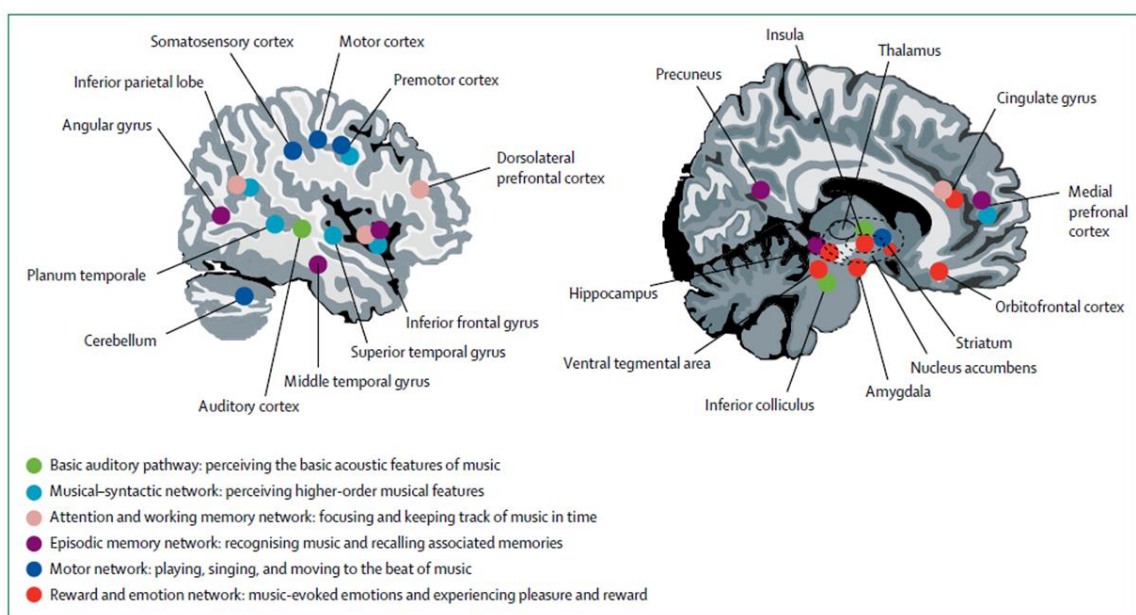


Figure 1. Locations of key brain areas involved in processing musical information. Areas identified from neuroimaging studies of healthy people (adapted from Särkämö et al., 2013).

| Brain regions | Location | Brodmann areas | Specific role |
|:---:|:---:|:---:|:---|
| **Auditory Network** | Superior and Middle Temporal Gyrus | BA21 and BA22 | Processing sounds and language (Schneider et al., 2002; Schneider et al., 2005). |
| **Motor Planning cortex** | Frontal Lobe and Cerebellum | BA4 and BA6 | Controlling smooth motor coordination, posture, and balance. Execution of absolute timing (Bermudez et al., 2009; Gaser & Schlaug, 2003). |
| **Visual cortex** | Occipital Lobe | BA17, 18 and 19 | Reading musical notation, which involves fine recognition of relative vertical and horizontal positions of musical notes on the score (Anaya et al., 2017; Rodrigues et al., 2010). |
| **Somatosensory cortex** | Parietal Lobe | BA1, 2 and 3 | Engaging in sensorimotor transformations and planning that are relevant for playing a musical instrument (Foster & Zatorre, 2010; Gaser & Schlaug, 2003; James et al., 2014). |
| **Corpus callosum** | White-Matter | * | It is the primary white-matter pathway connecting the two hemispheres. |
| **Insula** | * | * | Sub-serving the integration of sensorimotor information, emotional expression, and cognitive control during music performance (Kleber et al., 2013, 2017; Koelsch, 2014; Thaut et al., 2014). |
| **Hippocampus** | * | * | Acting as a novelty detector to the temporal domain of the acoustic modality and expanding previous findings on the impact of musical expertise on brain functions (Elbert et al., 1995; Pantev et al., 1998; Schneider et al., 2002; Parbery-Clark et al., 2009) to the hippocampal region. |

Table 2. Anatomical differences in the brains of musicians. Brain regions found to show structural differences in musicians compared to non-musicians.

## 1.7 Mechanisms in plasticity

The two major structural compartments of the human brain are grey matter (GM) and white matter (WM). GM primarily harbours the cell bodies of different neuronal cell types, whereas WM is majorly comprised of long-range myelinated axonal tracts. The role of the axons is information transfer from one neuron to another. The three basic parts of a neuron are the cell body and two extensions called an axon and a dendrite. The axon looks like a long tail and transmits messages from the cell (see Fig. 2). Dendrites look like the branches of a tree and receive messages for the cell. Dendrites are the region where one neuron receives messages from the axons of other neurons.

The cell body or 'soma' contains the nucleus and the other organelles necessary for cellular function. The axon is a key component of nerve cells over which information is transmitted from one part of the neuron (e.g., the cell body) to the terminal regions of the neuron. Axons can be rather long, extending up to a meter or so in some human sensory and motor nerve cells. The synapse is the terminal region of the axon and it is here where one neuron forms a connection with another and conveys information through the process of synaptic transmission (Rusznák et al., 2016; Scholl &Priene, 2015).
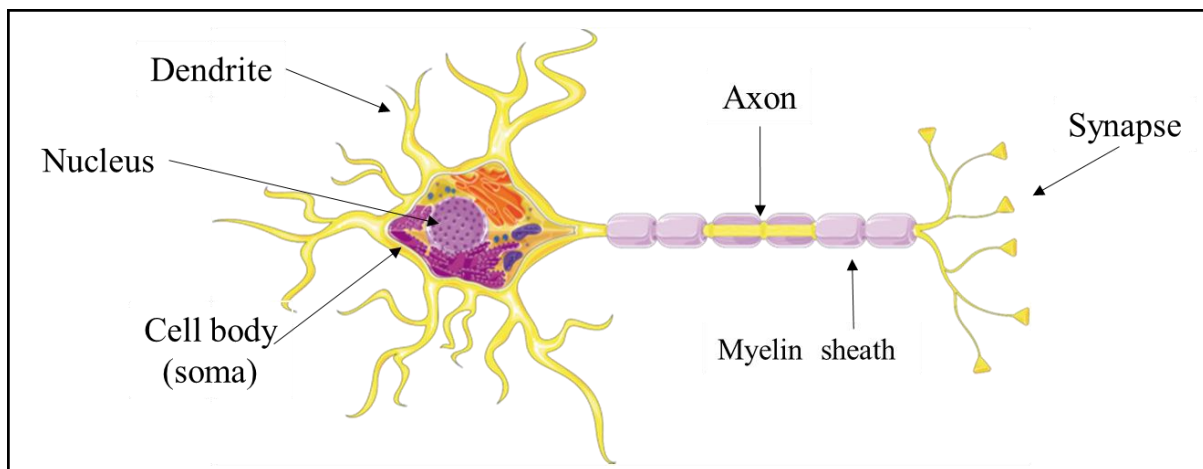
Figure 2. The Architecture of the Neuron.

## 1.8 Neural plasticity

Neural plasticity can be defined as the brain's ability to adapt and change with time. Plasticity is more likely to occur when there is stimulation of the neural system, such as when learning new skills, meaning that the brain must be active to adapt. In other words, plasticity is mainly driven by a mismatch between existing functional supply and environmental demand, or caused by primary changes in functional supply (Lovden et al., 2010). The functional and structural reorganisation capacity of the brain may occur during maturation, general learning, specific skill acquisition, environmental challenges, or pathology (Zilles, 1992, Lledo et al., 2006). The process of neuroplasticity may occur at several levels (from molecular to regional changes) and may occur in both GM and WM. The scope of neuroplasticity is wide, ranging from short-term weakening and strengthening of existing synapses, through induction of long-term potentiation (LTP), to formation of long-lasting new neuronal connections. It can occurring at the molecular, synaptic, electrophysiological, and structural organisation levels.

The candidate structural mechanisms for neuroplasticity in GM detected by MRI during learning include neurogenesis, synaptogenesis and changes in neuronal morphology (Zatorre, Fields, & Johansen-Berg, 2012; Rusznák et al., 2016). In addition, mechanisms for neuroplasticity in WM include axon branching, packing density, axon diameter, fibre crossing and the number of axons, myelination of unmyelinated axons, myelin thickness and morphology, and changes in astrocyte morphology or number (see Fig. 3).

## I. Synaptogenesis

Synaptogenesis is the process of increasing synapse number and dendritic complexity (Chang et al., 1991, Toni et al., 1999), and it can occur over periods of minutes to hours. Synapses are specialised asymmetric cell–cell connections permitting the controlled transfer of an electrical or chemical signal between a presynaptic neuronal cell and a postsynaptic target cell (Fu and Zuo, 2011; Holtmaatand Svoboda, 2009; Johansen-Berg et al., 2012; Zhao et al., 2008). Sufficient synapse function is vital for all neuronal processing, including higher cognitive functions, such as learning and memory. Though learning may be primarily related to synaptogenesis and dendritic branching, physical exercise may affect capillaries without increasing neural tissue (Black et al., 1990) (see Fig. 3a).

## II.Neurogenesis

Neurogenesis is the process by which new neurons are formed in the brain. It can modify neuronal connectivity in specific brain areas, which may include formation of new connections by dendritic spine growth (synaptogenesis). The process of neurogenesis in humans has only been successfully reported in few brain regions, such as the hippocampus and the olfactory bulb, but not in the cerebral cortex (Eriksson et al., 1998). Therefore, neurogenesis is unlikely to play a large role in MRI-detected experience-dependent change

outside the hippocampus. Neuroscientific progress in the decades since has made adult neurogenesis in the hippocampus and olfactory system a widely accepted phenomenon (Lepousez, et al., 2015) (see Fig. 3a).

## III.Myelin

White matter (WM) is mainly composed of long-range myelinated axonal cells that connect cortical portions of the brain. The majority of the myelination process occurs during the first two years of life. This process then continues through childhood, adolescence and adulthood, reaching peak myelination in the second or third decade of life (Yakovlev and Lecours, 1967), and undergoing refinements throughout the lifespan thereafter. The primary function of myelination is to speed conduction of the electric impulse along an axon, allowing the action potential to travel long distances faster (reviewed in Freeman et al., 2016; Hartline and Colman, 2007).

The candidate structural mechanisms for neuroplasticity in WM include increases in the number of axons, axon diameter, the packing density of fibres, axon branching, axon trajectories and myelination. Alterations in the axon structural properties give rise to changes in physiological properties such as conduction speed, which will have relevance to behaviour (Fields, 2015). These changes (i.e. myelination of unmyelinated axons, or modification of the myelin sheath on myelinated axons) may be caused by oligodendrocyte progenitor cells. The oligodendrocyte cells remain resident in large numbers in the adult brain after adolescence (Wedeen et al., 2005). These cells participate in repair following myelin damage, but they could in theory participate in learning if myelination of unmyelinated axons is stimulated by functional activity. Lastly, extra-neuronal changes may result from increases in glial cell size and number, and angiogenesis (see Fig. 3b).
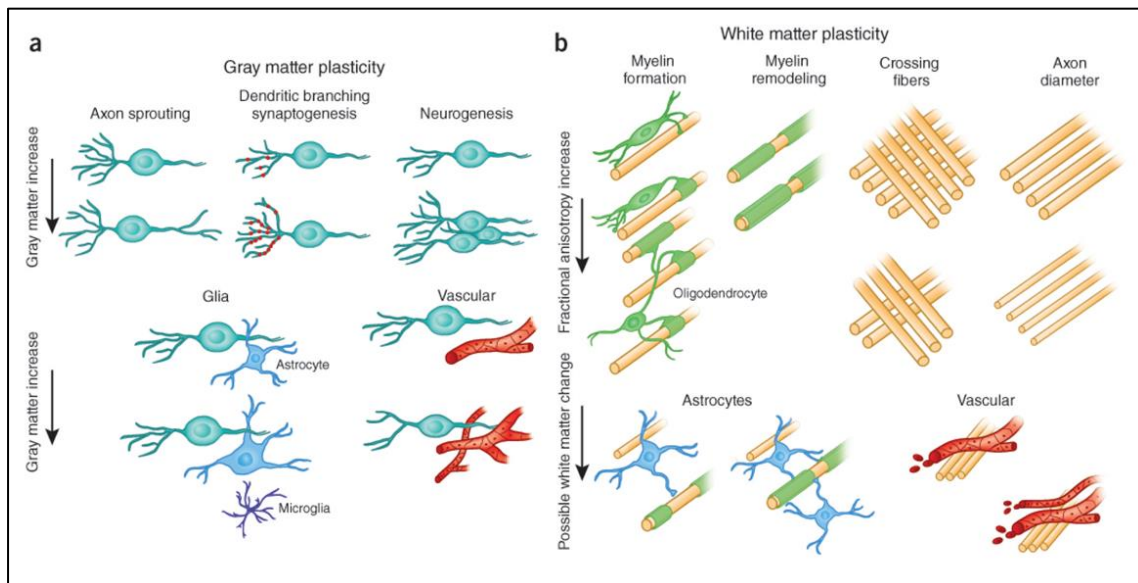
Figure 3. The candidate structural mechanisms for neuroplasticity in (a) GM regions include axon sprouting, dendritic branching and synaptogenesis, neurogenesis, changes in glial number and morphology, and angiogenesis (b) white matter include axon branching, packing density, axon diameter, fibre crossing, and the number of axons, myelination of unmyelinated axons, myelin thickness and morphology, and changes in astrocyte morphology or number (adapted from Zatorre et al., 2012).

# 1.9  Methodological background

The discovery that neuroplastic brain changes are detectable with MR imaging has opened up new avenues for research. Brain plasticity can be studied at different scales, from the micro- and macroscopic up to the systems level through the perspective of either brain structure and/or function. Anatomical imaging focuses on the brain structures and tissues, whereas functional imaging detects physiological changes that indicate brain activity. The field of neural reorganisation associated with training is strongly influenced by the current brain imaging techniques. These techniques include: 1) Functional Magnetic Resonance Imaging (fMRI), a functional method confined to exploring GM, 2) Voxel Based Morphometry (VBM), a structural method used to assess both GM and WM, and 3) Diffusion Tensor Imaging (DTI), a structural method confined to studying WM. The goal of this section is to give a basic and broad overview of brain imaging techniques that were used in this thesis.

## 1.9.1  Functional Magnetic Resonance Imaging (fMRI)

The term functional MRI (fMRI) generally refers to the imaging of brain activation detectable by changes in cerebral blood flow (CBF) (Gross, Sposito, Pettersen, Panton, & Fenstermacher, 1987). The presentation of a stimulus can elicit changes in brain activity observable by fMRI, changes which are induced by alterations in the synaptic and electrical activities of neurons. The focal increase in CBF can be considered to relate directly to neuronal activity because glucose metabolism and CBF changes are closely coupled (Raichle, 2011). Since the 1890s (Roy and Sherrington, 1896), it has been known that changes in blood flow and blood oxygenation in the brain are closely linked to neural activity, i.e. during brain activity, an increase in cerebral blood flow (CBF) can be observed.

Increased blood flow alters the local ratio of (paramagnetic) deoxy-haemoglobin to (diamagnetic) oxy-haemoglobin. Paramagnetic deoxy-haemoglobin produces a small local magnetic gradient (magnetic susceptibility), which distorts the magnetic field locally. This magnetic susceptibility enhances T2*- relaxation, resulting in decreased signalling in T2*-weighted images. In contrast, diamagnetic (non – paramagnetic) oxy-haemoglobin causes *decreased* magnetic susceptibility, leading to slower T2*-relaxation and, consequently, elevated signalling in T2*-weighted images, as detected by the MRI scanner. Signal intensity variations in the MR image result from this 'blood oxygen level dependent' (known as 'BOLD') contrast (Ogawa, Lee, Nayak, & Glynn, 1990). The Hemodynamic Response Function (HRF) typically follows a well-characterised shape and takes a few seconds to occur after neuronal activation. It is demonstrates a small initial dip, followed by a tall peak, and then a variable post-stimulus undershoot as shown in Fig.4.

The increase in neuronal activity in a brain area results in an initial increase in oxygen consumption. After a delay of about 2 sec, a large increase in localized cerebral blood flow is triggered, which over-compensates the oxygen consumption. Therefore, localized increases in blood flow increase blood oxygenation and consequently reduce deoxyhaemoglobin. As a result, better visibility in MRI images is thought to correlate with neuronal activity. The BOLD signal takes approximately 6s to peak, and then returns to baseline after an initial undershoot.
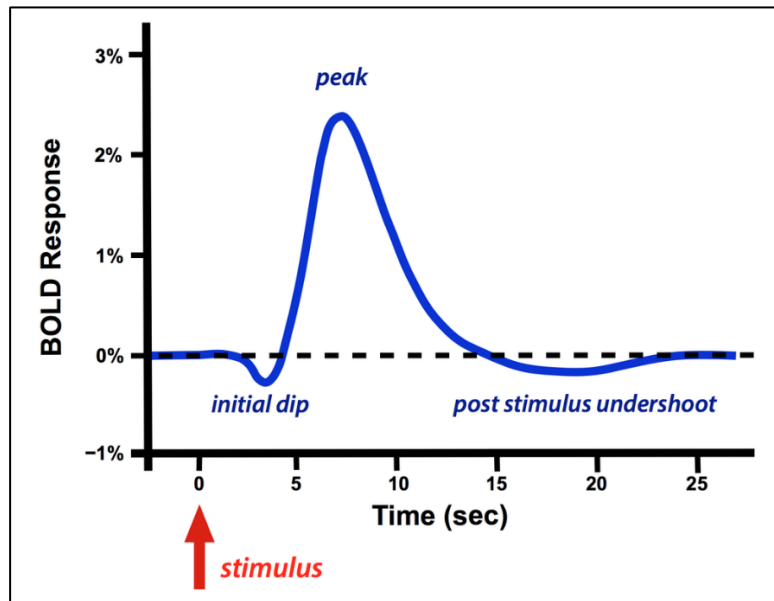
Figure 4. BOLD Hemodynamic Response Function (HRF) following a single brief stimulus.

This BOLD contrast allows us to measure the ratio between the oxygenated and deoxygenated haemoglobin in the blood. Thus, the measurement of CBF change induced by stimulation has been used for mapping brain activity, which in turn has been applied to the extensive investigation of various brain functions, including visual, motor, language, and cognitive functions.

There are two primary types of fMRI studies – 1) those in which a cognitive task is used to modulate specific neuronal activity (Task-based MRI), and 2) resting-state studies (rs-fMRI). Task-based MRI employs sensory stimuli to cue the participant to perform a behavioural task whilst lying in the MRI scanner. Then, a statistical comparison of pattern of activity across the whole brain between two conditions (e.g., verb generation vs control condition) allows the generation of activation maps that can be overlaid on the anatomical image in vivo. Block design and event-related design are the two common design approaches of the task-based fMRI (see amaro jr. and barker, 2006 for an overview of designs). On the other hand, the resting state MRI involves a subject that's resting in the absence of conscious mentation. Both types of task-based, as well as resting state studies, have become indispensable tools for

studying cognition in healthy as well as diseased brains, and tens of thousands of studies incorporating these designs have been published (Landi et al., 2010; Monzalvo et al., 2012).

In either case, a dynamic series of T2*-weighted scans (Echo-planar gradient) is acquired, resulting in a time series of signals for every brain voxel (Kruger et al. 2001). These time series are submitted to various levels of correction and de-noising (pre-processing steps) before model- or data-driven analyses are applied to obtain maps of activity. Functional MRI is a very powerful method for mapping brain functions, and has relatively high spatial and temporal resolution. There are of course physical limitations, for instance, how quickly and accurately pulses and magnetic fields can be turned on and off. More importantly, temporal and spatial resolution are antagonists, that is, increasing the spatial resolution means that it will take more time to acquire a single brain volume, thus decreasing the temporal resolution. This in turn will increase the whole time of the experiment, which is limited by how long a participant can be expected to stay in the scanner.

Major advantages of fMRI include: (a) it has an excellent spatial resolution that allows for the precise anatomical location of neural activation within the brain, (b) it comes with sufficient temporal resolution to detect neural correlates of behaviour on the basis of experimental trials, (c) it is very sensitive and can therefore measure subtle differences in neural activation between experimental conditions, which is a prerequisite to test theories on human behaviour, and (d) it is non-invasive and safe to use in human research participants because it does not require any pharmacological contrast agents or the lowering of signal detecting devices into the cranium.

### 1.9.2 **Voxel based morphometry (VBM)**

Voxel-based morphometry (VBM) is a whole-brain, automatic technique that enables the analysis of each voxel in the MR data. At its simplest, VBM involves a voxel-wise statistical comparison of regional GM between groups of subjects or time points (i.e. it enables monitoring of the brain structures' changes over time using repeated measurements) (Colcombe et al., 2006). In this technique, T1-weighted structural brain images are provided as input to the standard VBM processing stream (Ashburner and Friston, 2000), and statistical parametric maps (SPM) indicating differences in the density or volume of brain tissue are provided as the output.

VBM incorporates different pre-processing steps: (1) Spatial normalisation to a reference brain (e.g. MNI), which means that all subjects' brains are adjusted by means of a spatial normalisation to a standard anatomical space (i.e. each voxel relates to the same corresponding anatomical structure across all brains). This allows the comparison of anatomical localisations between different brains and even different studies. (2) Tissue classification (segmentation) into separate anatomical tissue compartments, such as GM, WM and CSF, after removing non-brain parts. To guide tissue segmentation, additional tissue probability maps can be used to consider prior anatomical knowledge about the spatial distribution of different tissues (Ashburner and Friston 2005). (3) Bias correction of intensity non-uniformities (Ashburner and Friston, 2005).

VBM is most often applied to investigate the local distribution of GM, but can also be used to examine WM. However, the sensitivity for detecting effects in WM is limited due to the low-intensity contrast in large homogeneous WM regions with only small changes in intensity. It can be used to assess local changes by comparing tissue previously classified either in cross-sectional or longitudinal studies (Ashburner and Friston 2000; Ashburner and Friston 2005; Draganski and May 2008).

### 1.9.3 **Diffusion-weighted imaging (DWI)**

Diffusion-weighted imaging (DWI) is a modern Magnetic Resonance Imaging (MRI) technique for measuring the translational displacement of water molecules in the brain in the presence of a spatially varying magnetic field (known as a gradient). Diffusion of water molecules was first observed by the Scottish botanist Robert Brown in 1827, who interpreted the movement as "essence of life"; a scientific explanation of molecular diffusion was then given by Albert Einstein almost 80 years later (Einstein, 1905).

The motion of water molecules in the CSF and GM are the same in all directions (isotropic), whereas in WM, motion is hindered due to the physical boundaries of the fibre bundles formed by the myelin sheaths (anisotropic) (Basser & Pierpaoli, 1996) (see Fig.5). Therefore, the diffusion varies with direction (anisotropic). The term 'isotropic diffusion' describes the equal rate of molecular motion in all directions and may occur in the CSF and GM (Pierpaoli et al., 1996), as no dominant underlying structural orientation exists in these tissues (Pierpaoli et al., 1996, Alexander et al., 2007). Conversely, in anisotropic diffusion, such as that which occurs in WM fibre tracts where axonal membranes and myelin sheaths present barriers to the diffusion of water, movement of water molecules is not equal in all directions. This contrast between WM and GM allows for modelling the diffusion as an ellipsoid, and subsequently quantifies the local WM integrity (Le Bihan et al., 2001). The orientation of the ellipsoid is defined by the three eigenvectors of the tensor, and its shape, and is characterised by the three eigenvalues (Basser et al., 1994b).

Diagonalisation of the tensor matrix results in a set of three orthogonal eigenvectors, $\hat{e}1$, $\hat{e}2$, and $\hat{e}3$ representing the major, medium and minor principal axes of diffusivity modelling respectively. The corresponding eigenvalues, $\lambda1$, $\lambda2$, and $\lambda3$ quantify the apparent diffusivities along these axes. Several diffusion metrics can be obtained from the three eigenvalues which can in turn be used to probe the microstructure in a particular voxel. For example, the major principal eigenvector $\lambda1$, which indicates the direction of the greatest apparent diffusivity $\lambda1$,

is thus thought to be parallel to tract orientation (Moseley et al., 1990) and it called axial diffusivity (AD). The mean of the two smaller eigenvalues $\lambda2$ and $\lambda3$ is called 'radial diffusivities' (RD). The mean amount of diffusion across all eigenvectors (i.e. $\lambda1$, $\lambda2$, and $\lambda3$) is called 'mean diffusion' (MD). All these diffusivities are measured in $\mu m^2/ms$. Additionally, fractional anisotropy (FA) is a summary measure of microstructural integrity that is highly sensitive to neuroplastic change. It describes the asymmetry in diffusion along the major axis ($\lambda1$) relative to the other two axes ($\lambda2$, and $\lambda3$) ranging from 0 in voxels with equal (perfectly isotropic) diffusion in all three major directions, to a maximum of 1 (infinitely anisotropic) where diffusion is only possible in the AD direction. In summary, it is a unitless measure of the normalised variance of the three eigenvalues ranging from 0 (perfectly isotropic) to 1 (infinitely anisotropic). However, in the brain, minimal FA values (approx. 0.1) are normally measured in the ventricles and maximal FA values (approx. 0.85) in the splenium of the corpus callosum (Pierpaoli &Basser, 1996).

## Water self-diffusion in the brain

### A. Isotropic

### B. Anisotropic

$\lambda 1$

$\lambda 2$

$\lambda 3$

$\lambda_1$ = longitudinal (axial) diffusivity(AD)

$(\lambda_2 + \lambda_3)/2$ = radial diffusivity (RD)

$(\lambda_1 + \lambda_2 + \lambda_3)/3$ = mean diffusivity (MD)

$\sqrt{\frac{1}{2}} \dfrac{\sqrt{(\lambda_1 - \lambda_2)^2 + (\lambda_1 - \lambda_3)^2 + (\lambda_2 - \lambda_3)^2}}{\sqrt{(\lambda_1^2 + \lambda_2^2 + \lambda_3^2)}}$ = fractional anisotropy (FA)
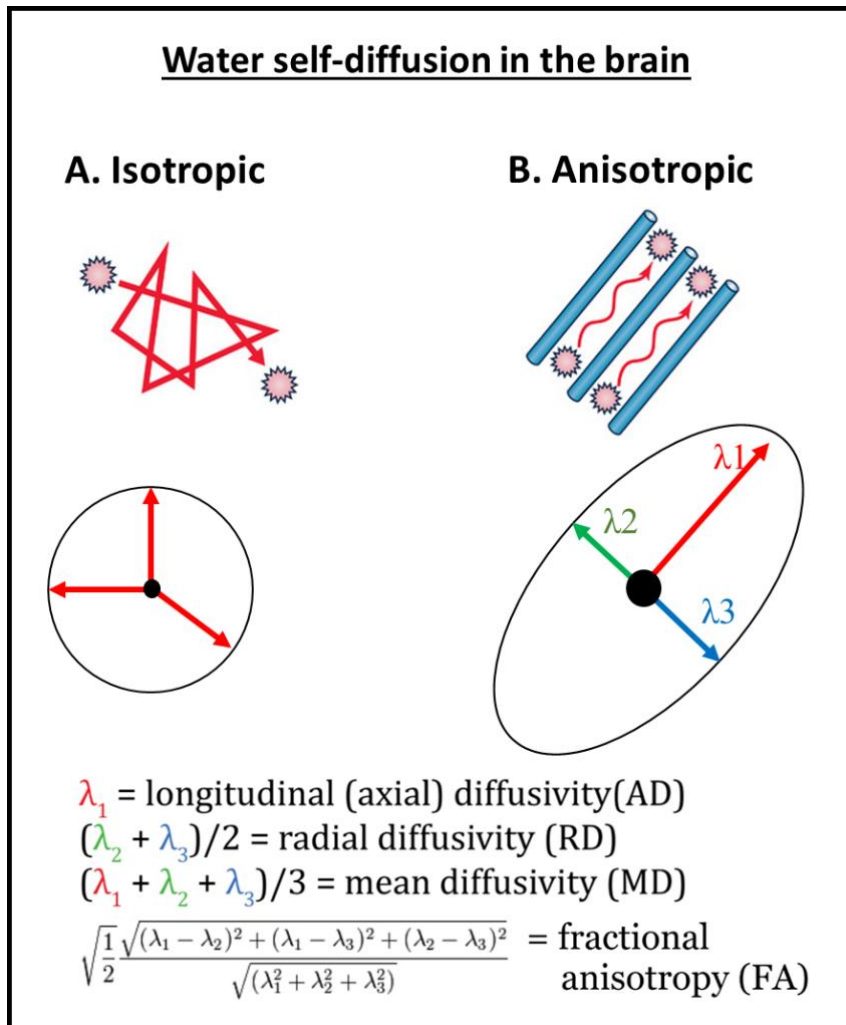
Figure 5. Water diffusion by Brownian motion. (A) Water molecules are free to travel in all directions following Brownian motion (isotropic). (B) In the presence of a restrictive boundary, water will travel with higher probability in set direction(s) (an-isotropic).

A common inference that is made in many DTI papers is that alterations in diffusivity mirror changes to the degree of myelination. For example, it has been claimed that FA is sensitive to detecting WM alterations, such as degeneration or plastic remodelling (Pierpaoli and Basser, 1996; Pierpaoli et al. 1996). Decreasing FA values are usually associated with ageing and loss of cognitive functions, whereas learning and rehabilitation are accompanied by increased FA values (Bengtsson et al. 2005; Engvig et al. 2012; Landi et al. 2011; Lebel et al. 2012;

Lindenberg et al. 2010). A decrease or increase in FA value is usually explained by decreased or increased diffusivity (respectively) perpendicular to the principal diffusion direction. FA value is thought to reflect decreased/increased fibre organisation or myelination on a microstructural level. The ever-growing number of DTI-based studies, applied and methodological, demonstrate the large degree of consensus within the neuroscientific community as to the great potential and veracity of the method. DTI has been applied to an incredible variety of neuroscientific studies (see reviews in Assaf et al., 2017; Lebel, et al., 2017; O' Donnell &Westin, 2011). Diffusion tensor imaging provides anatomical information with high specificity, making it an invaluable tool for measuring structural brain differences and changes in cross-sectional and longitudinal studies respectively.

## 1.10 Aim of this project

The main aim of this project is to quantify structural and functional changes resulting from musical training, using functional, anatomical, and diffusion MRI over six months of a drumming course. Diffusion tensor imaging (DTI), and voxel-based morphometry (VBM) were used to measure the anatomical changes. Task-based functional MRI (fMRI) was used to map the brain functional activation changes with the musical training.

# Chapter 2    Drumming task

This chapter aimed to answer the following questions: 1) why the drumming task was chosen for this project? 2) How the training task was designed? 3) What are the assessment methods that used to evaluate individual performance? 4) Do the participants show any drumming ability progression with training?

## 2.1  Drumming

Drumming is an ancient nonverbal form of communication that has been used across the world throughout history, with some of the earliest drums dating back to 5500–2350 BCE in China. Drumming is a unique activity that challenges the brain to synchronise multiple limbs within the constraints of timing, tempo, precision and volume.

The drumming intervention was chosen for this project because it targets cognitive and motor functions known to shape several cognitive and perceptual abilities (e.g., Petrini et al., 2009a,b, 2010a; Lee and Noppeney, 2011; Lee and Noppeney, 2014), as well as emotional processing from purely rhythmic music. More specifically, it is a coordinative exercise combining musicality, body coordination, cardiovascular exercise, bilateral arm and leg movements, and sensorimotor integration processes (De La Rue et al. 2013). It requires learners to use their arms and legs independently, or simultaneously, while keeping in time with the music. The training in this project focused on the learning of novel motor sequences and their rhythm and timing. This included focused attention (e.g. paying attention to the drumming sequence), multi-tasking attention (e.g., listening and simultaneous movement execution), movement-switching (e.g., switching between the dominant and non-dominant hand) and response speed.

Recent studies have shown that multiple areas in the frontal, occipital, and cerebellar lobes, together with the temporal lobes, integrate to facilitate memory and music perception, control sensorimotor function, and subsequently capture accurate timing; all of these elements are actively used when drumming (Dahl, 2011; Fujisawa & Miura, 2010).

**Why drumming?**

In the present study, we chose to use drumming training, firstly because it was considered to be an interesting experience that would be more likely to keep the subjects involved in the study over the full six-months course. Secondly, it is easily learned and reproduced from an early age with tangible consequences on perceptual and cognitive abilities (Gerson et al., 2015). In addition, playing the drums is more evident and less restricted to upper body movements compared to playing other instruments (Petrini et al., 2010b). Also, it is considered a co-ordinating exercise that combines musicality, body coordination, cardiovascular exercise, 'bilateral' arm and leg movements, and processes of sensorimotor integration (De La Rue et al., 2013). To the best of our knowledge, this is the first study characterising the functional properties of the effects of a six months drumming training course.

Furthermore, playing the drums could be a very effective means of therapy (Overy, 2003; Zentner & Eerola, 2010; Wan et al., 2011; Gerson et al., 2015). It has potential implications for music therapy and clinical practise, and theory of emotion inducement from music. It has been shown that music may be beneficial in relation to a number of symptoms in several kinds of impairment, such as epilepsy, Alzheimer's disease, Parkinson's disease and senile dementia (see Särkämö & Sihvonen, 2018 for an overview). Hence, it is possible to conceive of dealing with music in educational, clinical and therapeutic terms.

## 2.2 Subjects

Fifteen university staff and students (mean age: 38.6 y, range: 20y – 57y, 9 men, 6 women) with no prior drumming experience were recruited for this study. All recruits gave written informed consent prior to participation and the project was approved by the Committee on Research Ethics at the University of Liverpool (https://www.liverpool.ac.uk/governance/university-committees/committee-on-research-ethics/). All participants were right-handed, as assessed by Edinburgh Handedness Inventory Short Form (EHI). A radiologist examined all participants to ensure they demonstrated normal brain anatomy. The inclusion and exclusion criteria for healthy volunteers are summarised in the appendix Table 22.

| Subject ID | Sex | Age (years) |
|---|---|---|
| D1 | Male | 29 |
| D2 | Male | 30 |
| D3 | Female | 50 |
| D4 | Male | 50 |
| D5 | Male | 58 |
| D6 | Male | 57 |
| D7 | Male | 24 |
| D8 | Female | 30 |
| D9 | Female | 20 |
| D10 | Male | 37 |
| D11 | Female | 38 |
| D12 | Female | 42 |
| D13 | Female | 35 |
| D14 | Male | 31 |
| D15 | Male | 49 |

Table 3. Demographic details of study participants' sex and age. Abbreviations: D short of drummer/participant.

## 2.1    Task design

The participants took part in a 45-minute individual drumming session each week for 21 weeks. In addition, all participants had access to a drum kit for private practise and were encouraged to practise for at least 30 minutes a day. Each session was delivered by a professional drumming tutor. For the first lesson, participants worked on how to hold the drumsticks and how to use the sticks to hit the drums in a manner which produced audibly high-quality beats. Next, they started to perform a simple rudimentary exercise, such as single strokes, double strokes, paradiddle and triplets for five to fifteen minutes. During the later sessions, they worked on learning to read drum notation and how to execute it on the drum kit using their hands and feet. Once participants became skilled in reading and executing drum notation, the learning sessions incorporated a metronome to teach participants how to play in time. Once the aforementioned training was complete, they began to learn the songs from the book wrote by 'Various', 2012 *('Rockschool Drums - Debut ' . Rockschool Drums - Grade 4 (2012-2018) by Various (3-May-2012); Publisher: Rockschool Publications (3 May 2012) (1600)).* The complexity of drumming training was increased on a weekly basis in line with participants' drumming progression. Since some participants were able to read music and others were complete beginners, learning to read drum notation was easier for those with an existing musical background. Therefore, the remaining time after the rudimentary exercises was split according to each subject's needs.

## 2.2    Assessment methods

### 2.2.1 Teacher Assessment Scores

The  participants were assessed via the Teacher Assessment Scores marking criteria following the ABSRM exam structure. ABRSM is one of the largest music education bodies in the UK, the UK's largest music publisher and the world's leading provider of music exams. ABSRM marking criteria cover the different aspects of playing or singing under five areas: pitch, time, tone, shape and performance. These can be applied to all instruments, including voice, and all types of piece or song.

- Pitch – accuracy, clarity, reliability of notes and/or intonation.
- Time – suitability of tempo, stability of pulse, sense of rhythm.
- Tone – control and projection of sound, sensitivity and awareness in use of tonal qualities.
- Shape – effectiveness and clarity of musical shaping and detailing.
- Performance – overall command of the instrument or voice, involvement with the music, musical communication.

For this, the music teacher was asked to evaluate the participants' performance at each session and compare their performance to the last training session. These weekly assessments were reported on a 10-point scale, whereby 0 represented a very poor performance and 10 represented an excellent performance, as shown in the example of one of the participants (D7) in Table.4. During learning sessions, participants had to play the same song twice, once with a 'click track' (an audible pulse given during performance), and once without the click track. The songs were in the format of a play-along (music minus drums) from the Rockschool Grade Book series. The grade used for this was 'Debut', which is the grade below ABSRM grade 1. The songs in this grade are relatively easy to learn, but require already basic co-ordination skills and a basic ability to read musical notation.

| Date of lesson | Level of Performance | Weekly assessments |
|:---:|:---:|:---:|
| 19/07/2016 | 0 - 1.5 | n/a |
| 28/07/2016 | 2.0 | 7 |
| 16/08/2016 | 2.8 | 8 |
| 23/08/2016 | 3.0 | 3 |
| 30/08/2016 | 3.2 | 4 |
| 19/09/2016 | 3.4 | 4 |
| 26/09/2016 | 3.6 | 4 |
| 03/10/2016 | 3.7 | 3 |
| 13/10/2016 | 4.0 | 5 |
| 20/10/2016 | 4.1 | 2 |
| 27/10/2016 | 4.2 | 2 |
| 03/11/2016 | 4.4 | 4 |
| 10/11/2016 | 4.5 | 3 |
| 17/11/2016 | 4.7 | 4 |
| 24/11/2016 | 4.7 | 1 |
| 01/12/2016 | 4.9 | 3 |
| 08/12/2016 | 5.2 | 4 |

Table 4.  Example Assessments Scores sheet for participant (D7). Level of performance and weekly assessments scores are out of 10.

### 2.2.2 **Reading and timing test**

The formal test was divided into two parts: reading and timing. The reading aspect of the test was to measure the participants' ability to read the musical notations accurately and relate the notation to movement with hands and feet. The timing part was to measure the participants' ability to perform 'in time' with the play along track. Moreover, the test measured their ability to relate to a pulse, even if the play along track had no audible 'click', but rather only musical instruments. Furthermore, on the day of the test the participants had to play the song without having the chance to practise it beforehand. Due to the fact that some participants were completely new to music and musical notation, whereas others had previous knowledge and experience, the songs used for the test were not the same for everybody and differed according to each participant's current level of musical ability. The outcome formal test scores ranged from 0 to 10, as shown in Table 5.

### 2.2.3 **Advanced Measures of Music Audiation (AMMA)**

The Advanced Measures of Music Audiation (AMMA; Gordon, 1989) was performed in order to assess the participants' baseline drumming ability and prior musical experience. The AMMA is a twenty-minute-long musical aptitude test. For this, participants were asked to determine whether the two melodies that were played in sequence were identical or not. Additionally, they had to state whether these melodies differed in pitch content or in rhythm content. The participants' scores are shown in Table 5.

| Subject ID | AMMA | Number of attended drumming sessions | Performance scores Pre mid post training sessions | | | Reading Test score | Timing Test score |
|---|---|---|---|---|---|---|---|
| D1 | 46 | 21 | 1.5 | 4.3 | 5 | 10 | 6 |
| D2 | 57 | 21 | 1.8 | 3.8 | 4.6 | 7 | 9 |
| D3 | 64 | 20 | 1.4 | 3.1 | 4 | 7 | 6 |
| D4 | 54 | 20 | 1.2 | 2.3 | 3 | 9 | 7 |
| D5 | 63 | 16 | 1.2 | 3 | 5.3 | 9 | 8 |
| D6 | 54 | 20 | 1.4 | 3.8 | 5.3 | 9 | 8 |
| D7 | 54 | 18 | 2 | 4.4 | 5.2 | 9 | 9 |
| D8 | 42 | 20 | 1 | 1.9 | 2 | 4 | 2 |
| D9 | 55 | 20 | 1.4 | 3.1 | 3.1 | 7 | 6 |
| D10 | 58 | 15 | 1.2 | 4 | 4 | 8 | 9 |
| D11 | 48 | 16 | 1.2 | 3.1 | 3.1 | 7 | 6 |
| D12* | 55 | 16 | 1 | 2 | * | 8 | 9 |
| D13 | 62 | 10 | 1.2 | 4 | 5 | 8 | 9 |
| D14 | 48 | 20 | 1.5 | 3 | 3 | 8 | 9 |
| D15 | 46 | 13 | 1.2 | 2 | 2 | 3 | 5 |

Table 5. Participants' performance measures including the scores on the AMMA musicality test. A pre-training (baseline) assessment was administered before the first lesson for all participants. The mid-training assessmen was computed at the mid-point of all sessions attended by the participants, and the post-training assessment was computed at the last training session. The assessments scores are out of 10.**Please note that participant D12 was excluded from the study.

Figure 6. The indivual performances of the fiftteen particpants at each learning session, presented with the line fitting method.

| Subject ID | Slope Value | t-Value | P value |
|------------|-------------|---------|---------|
| D1 | 0.18961 | 7.81 | P<.001 |
| D2 | 0.16241 | 7.46 | P<.001 |
| D3 | 0.13684 | 7.18 | P<.001 |
| D4 | 0.18676 | 8.0 | P<.001 |
| D5 | 0.1985 | 8.86 | P<.001 |
| D6 | 0.24355 | 8.49 | P<.001 |
| D7 | 0.18421 | 5.82 | P<.001 |
| D8 | 0.03835 | 3.34 | .003 |
| D9 | 0.11429 | 2.89 | .013 |
| D10 | 0.16324 | 7.30 | P<.001 |
| D11 | 0.09265 | 4.02 | P<.001 |
| D12* | 0.24242 | 7.18 | P<.001 |
| D13 | 0.17293 | 13.0 | P<.001 |
| D14 | 0.09341 | 2.53 | .021 |
| D15 | 0.08333 | 3.97 | P<.001 |

Table 6. Results of line fitting methods with Individual Performance scores for all participants at each learning session. *Please note that D12 was excluded from the study.

## 2.3    Participants and Drum Progression

Based on the teacher assessment scores, all participants made good progress during the leaning course. Task performance differed significantly between the pre and the post-training imaging session. A paired t-test ($t = -8.67$, $df = 13$) revealed a significant improvement in drumming task performance ($p < .001$). Moreover, there was a gradual change in drumming performance task (see Fig.5; it presents the participants' performance score at each session).

Further statistical tests revealed that there was a significant positive correlation between the behavioural measurements. The mean score for drumming performance including the three (pre, mid, and post) sessions was positively correlated to the reading test score ($r_{(14)} = 0.74$, $p = .0024$), the AMMA test score ($r_{(14)} = 0.62$, $p = .017$), and to the timing test score ($r_{(14)} = 0.59$, $p = .028$) (see Fig.6; it presents the correlation between the mean performance score and the other behaviour measurements). Moreover, there was a positive correlation between AMMA and timing test scores ($r_{(14)} = 0.58$, $p = .03$), and a positive correlation (not significant) between AMMA and the Reading score ($r_{(14)} = 0.4$, $p = .15$). Also, there was a positive correlation between the Reading and Timing tests scores ($r_{(14)} = 0.64$, $p = .013$) (see Fig.9; it presents the correlation between the AMMA score and (reading and timing measurements).
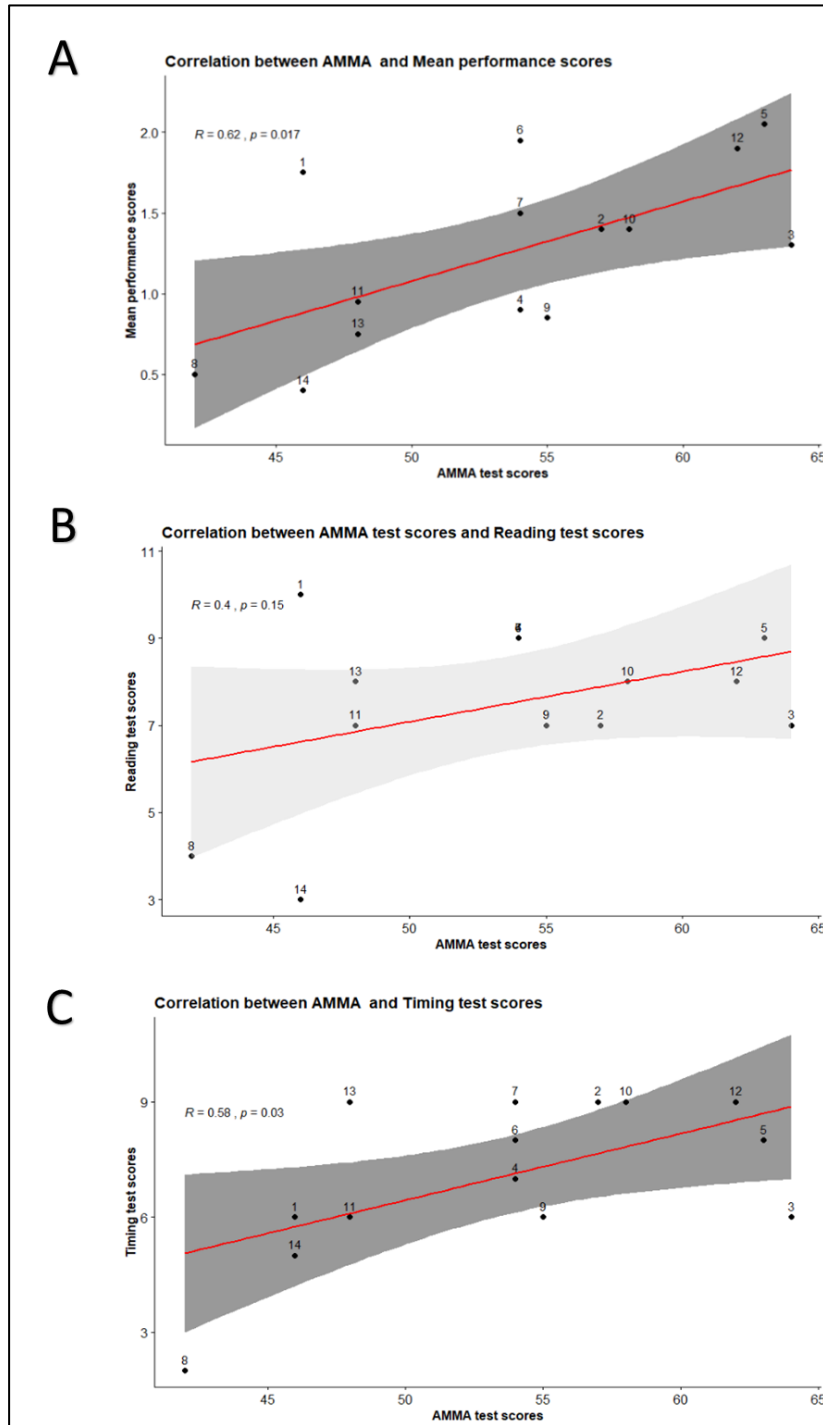
Figure 7. The scatterplot showed correlation between A. AMMA and mean performance score, B. AMMA and Timing test scores, and C. AMMA and Reading test scores.
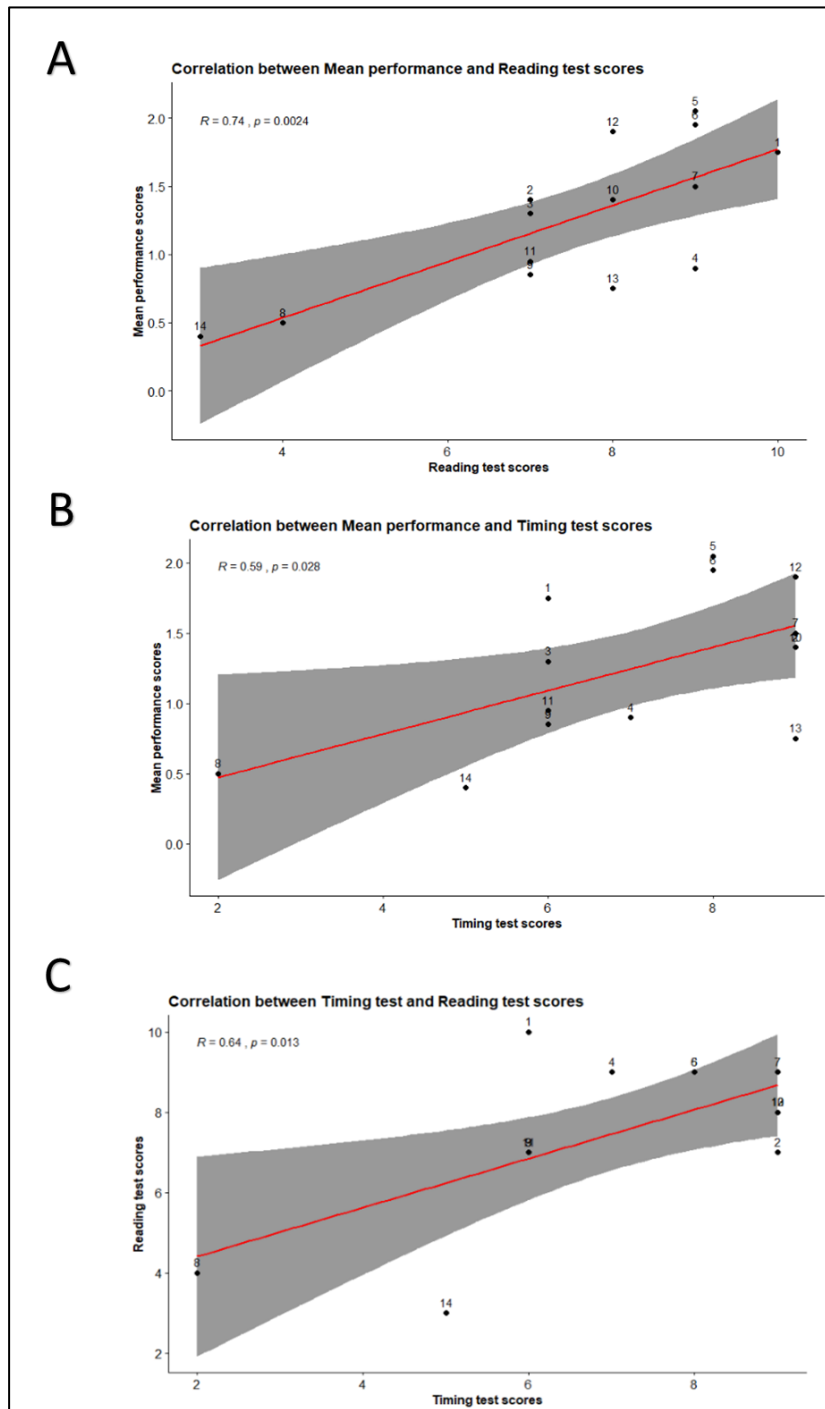
Figure 8. The scatterplots show correlations between A. The mean score for drumming performance and Reading test score, B. The mean score for drumming performance and Timing test score, and C. Reading test score and Timing test score.

## 2.3 Limitation

One of the limitations of the performance assessment is that all performance was subjectively assessed by the drumming tutor. This assessment included weekly performance and improvement scores as well as a 'mock' grade (i.e. reading and timing) exams. Recent work has shown that functional brain activity is more closely related to activity carried out in the scanner than in other environments (Aloufi et al., 2021). It would therefore have been beneficial to directly correlate functional and structural data with objective performance measures, and for functional data it would have been preferrable to collect functional activation data and performance measures at the same time in the scanner. A second potential limitation is while participants were evaluated weekly at their lessons, the amount of daily home practise was not recorded. An automatic system to provide this data would have provided potentially important insights int the link between practise time and functional and structural brain changes.

# Chapter 3    Drumming as a Tool for Promoting functional Brain Plasticity: Functional Magnetic Resonance Imaging study.

## 3.1 Introduction

Practicing a musical instrument has a profound impact on the structure and function of the human brain. It can induce substantial neuroplastic changes in cortical and subcortical regions (Li et al., 2018), and neurological changes can occur in a beginner training to play sequences on a piano keyboard (Lahav et al., 2007; Chen et al., 2012; Herholz et al., 2015), or learning to listen to and imitate different auditory rhythms (Chen et al., 2007), as well as learning to drum (Muriel et al.,2020; Amad et al., 2017; Petrini et al., 2011).

Functional imaging studies comparing adult musicians with matched non-musicians have revealed differences in musically relevant brain regions, such as increased activations of auditory areas (Gaab and Schlaug, 2003; Bermudez and Zatorre, 2005; Lappe et al., 2008) and motor areas whilst listening to music (Grahn and Brett, 2007; Bengtsson et al., 2009; Grahn and Rowe, 2009), as well as differences in the cerebellum. In 2001, Schlaug reported that a significantly higher mean relative cerebellar volume was observed in male musicians compared to male non-musicians. As well as, Schmithorst and Wilke (2002) observed greater white matter volume in musicians in central aspects of the cerebellum. Furthermore, these findings have been linked to subjects' performance. In 2001 Schlaug found that a positive trend between life time and daily practice and relative cerebellar volume. In 2003 Gaser and Schlaug noticed a positive correlation between practice hours and gray matter volume in the left cerebellum. This suggests that the amount of practice influences grey matter volumes in somatosensory areas.

In addition, differences between musicians vs non-musicians in sensorimotor brain areas, researchers reported that a positive correlation between somatosensory areas and musical experience. In 2003 Gaser and Schlaug reported that grey matter volume was highest in professional musicians, moderate in amateurs and lowest in non-musicians. This suggests that the amount of practice influences grey matter volumes in somatosensory areas. As well as

Broca's area (a classical language area in the brain including the posterior inferior frontal gyrus) during music perception tasks (e.g., Koelsch et al., 2002; Tillmann et al., 2003), active music tasks such as singing (e.g., Ozdemir et al., 2006), and imagining playing an instrument (e.g., Baumann et al., 2007; Meister et al., 2004) have also been identified.

Functional connectivity researchers found increased connectivity between prefrontal, temporal, inferior-parietal and premotor areas in musicians when compared to non-musicians (Klein et al., 2016). Similarly, it has been demonstrated that the posterior superior temporal gyrus is connected to a region within the middle temporal gyrus, which has been associated in musicians with absolute pitch (Loui et al., 2010).

These data from neuroimaging studies suggest that playing a musical instrument depends on a strong coupling of perception and action, mediated by sensory, motor, and multimodal integration regions distributed throughout the brain (e.g., Schlaug et al., 2010a; Zatorre et al., 2007). Despite the heterogeneity of the fMRI tasks used, an area that was commonly activated in many of the musical training studies was the posterior superior temporal gyrus, a region which is important for sound processing (Ellis et al., 2013; Pantev et al., 1998; Koelsch et al., 1999; Rüsseler et al., 2001; Li, Qiongling, et al., 2018), as well as the planum temporale (Vikene, K., et al., 2019). The next most common findings are in the primary motor cortex, supplementary motor area, dorsal and ventral pre-motor areas, premotor and parietal regions such as SMG in response to musical training (Amounts et al., 1997; Gaser & Schlaug, 2003; Han et al., 2009).

Most previous studies comparing musicians and non-musicians typically focus on groups of highly trained musicians with many years of experience. These cross-sectional designs have two shortcomings. Firstly, musicians and non-musicians are self-selected and any differences in cognitive processing could be pre-existing and not due to training. In other words, with cross-sectional studies it is impossible to determine which came first, the structural

differences or the musical training experience (May, 2011). Secondly, these studies typically select musicians with many years of training (often, in the case of older musicians, most of their lifetime), therefore, the time course of changes in regions of brain activation cannot be established.

**The Present Study**

The main goal of this project was to quantify functional and structural neuroplastic changes in response to learning a new musical motor task, in this case drumming. The main purpose of this fMRI study was to examine how BOLD activation changes over time in brain regions involved in musical training. The second goal was to shed light on brain processes involved in drumming action execution, as well as a passive observation drumming task, and their overlap.

We hypothesise that one or more regions previously identified as being involved in musicality, as listed in Table 2 of the introduction chapter, (page14 -15) will present significant BOLD changes over six months of drumming training. To investigate this hypothesis, two fMRI tasks were used, one being a passive Observation of a drumming video, and the other an Execution of musical notes task using hands during fMRI scanning. Then, the fMRI Execution experiment was applied to mapping those regions showing an increase in BOLD activation, and analyses of regions of interest were performed. These regions of interest analyses were used to extract the mean beta value from the three Observation fMRI tasks (i.e. pre, mid and post-training sessions, see Fig.9 and Fig.10). Next, a line fitting method was implemented to characterise the mean beta value changes over the six months drumming course. Finally, a linear correlation test was used to explore the relationship between the brain activation changes and the performance measurements.
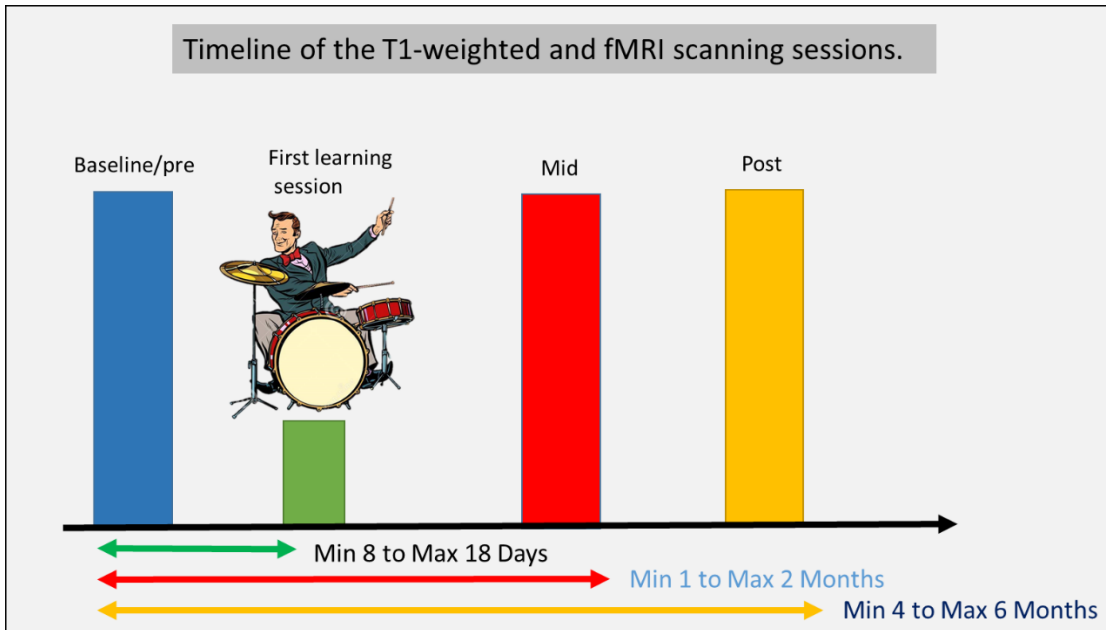
Figure 9. Timeline for the fMRI Experiment, the participants were scanned before, mid and after the drumming course.
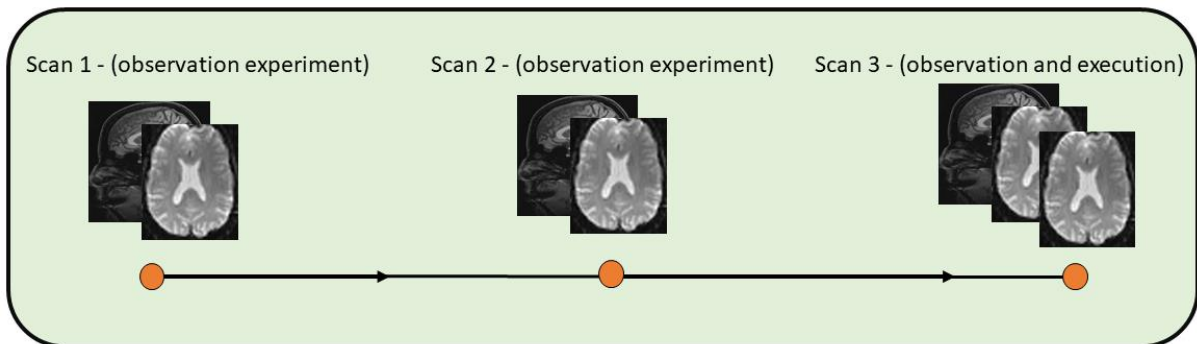


Figure 10. The three functional MRI sessions. The first and second sessions used the observation task only, whereas, the last session included both (i.e. observation and execution) fMRI tasks.

## 3.2 Methods

### 3.2.1 Subjects

Fifteen university staff and students (mean age: 38.6y, range: 20y – 57y, 9 men, 6 women) with no prior drumming experience were recruited for this study. One female was excluded due to abnormalities found upon neurological examination. More information concerning those recruited for the study can be found in the previous chapter (chapter 2, section 2.2, page 33).

**The fMRI study designs**

All participants attended each of the three functional scanning sessions. At the first and second scanning sessions, the observation sequence alone was used, whereas both observation and execution sequences were included in the third session once participants were adequately trained in execution, as shown in Fig. 10.

### 3.2.2 Data acquisition

The fMRI scanning of the participants was conducted at Liverpool Magnetic Resonance Imaging Centre (LiMRIC) using a 3T Siemens Trio MRI system with an eight channel receiver head coil. A high resolution T1-weighted imaging ($1mm^3$ isotropic resolution; 176 axial slices perpendicular to AC-PC line) and functional T2* weighted ($3.0 \times 3.0 \times 2.5$ mm) scans were performed. Data for two fMRI experiments (Observation and Execution) was acquired using the following parameters: T2* weighted with echo planar imaging (EPI) sequence, repetition time (TR) and an echo time (TE) of 3000 and 30ms respectively. Using the acquisition orientation axial, aligned with the AC-PC axis, the whole brain volume was covered with an interleaved order of slices. Each acquired volume consisted of 46 slices, with a slice thickness of 2.5mm and a 0.45mm gap between the slices. A flip angle of 90 degrees was also used. The field of view (FOV) was $192mm^2$, and the matrix size was $64 \times 64mm^2$. A

total of 310 volumes were acquired for the Observation experiment, whereas 230 volumes were acquired for the Execution experiment.

## The Observation Task

The Observation task consisted of 28 blocks comprising 14 blocks of drumming task video scenes and 14 blocks of fixation (Fig. 11A). The professional drumming tutor wrote out blocks consisting of 4 parts (bars) and 3 gaps each. Each block lasted for 16.5 seconds and had a tempo of 80 beats per minute, examples of which can be seen in Fig. 11B. There were two different kinds of blocks: (A) 'grooves' (3 voices, these being bass drum, snare drum and hi hat), or (B) 'fill-ins' (only 1 voice at a time, but 4 different pitches, these being snare drum, high tom, mid tom and floor tom). Both kinds of blocks ('grooves' and 'fill-ins') were subdivided into 3 categories: non-repeat blocks, blocks consisting of 1 repeat only and blocks consisting of 2 repeats. Participants were instructed to press the button with their thumb only if there were two identical consecutive blocks (two in a row), as shown in Fig. 11B. This is known as a 'one-back' paradigm – it is used extensively because it forces participants to encode and keep in memory the relevant sequences.
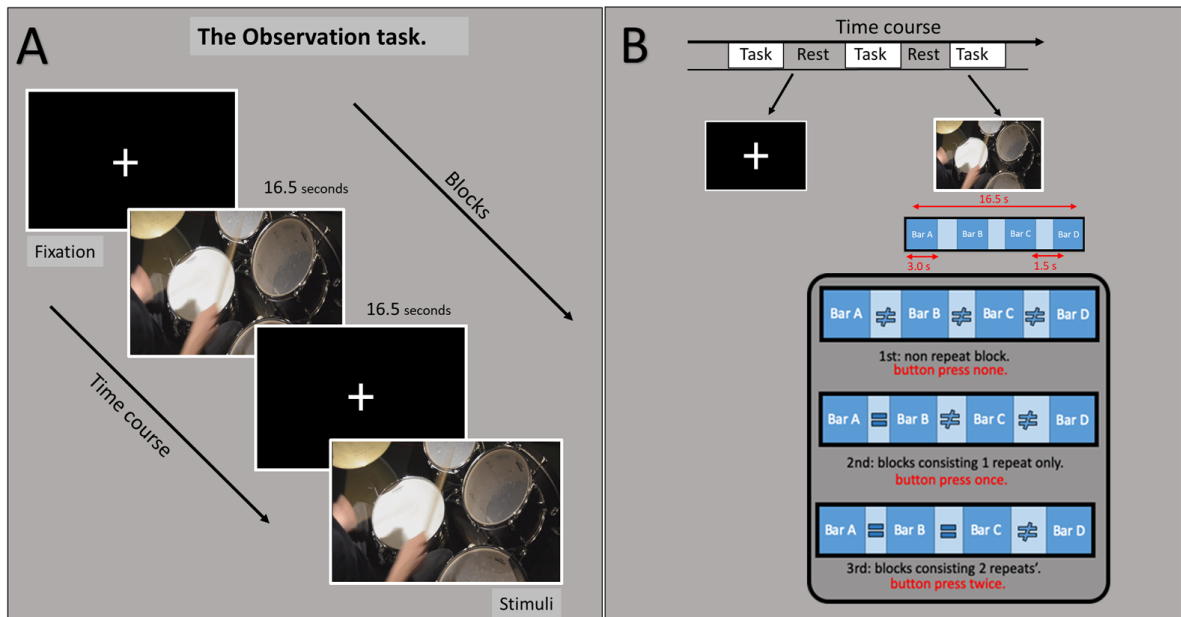
Figure 11. A) Schematic representation of the stimulus sequence: 28 blocks comprising 14 blocks of drumming task video scenes and 14 blocks of fixation, 16.5s long rest periods and drumming observation videos alternated for a total time of 462 seconds. B) Schematic diagram of the blocks design used in the observation task: each block consisted of four distinct video clips (consisting of 4 beat bars). Each block could contain zero, one or two repeated clips. Participants were asked to press a response button when they detected an immediate repetition of block.

## The Execution Task

The Execution task consisted of 20 blocks of video scenes and 20 blocks of fixation, as per the examples shown in Fig. 12. Participants were instructed to execute the musical notation that was shown on the screen as accurately as possible using their hands to play the musical note, which was a common beat (metronomes on an electronic drum) written by the tutor. Initially, task complexity was simple, but became gradually more complex as the task progressed (i.e. they had to use either their right or left hand *with* audio track during the earlier slides, then for the latter slides they had to use both hands following the common beat (metronome), as shown in Fig. 12). This task was only carried out at the post-training phase

because beforehand participants lacked the musical knowledge necessary for completion of the task.
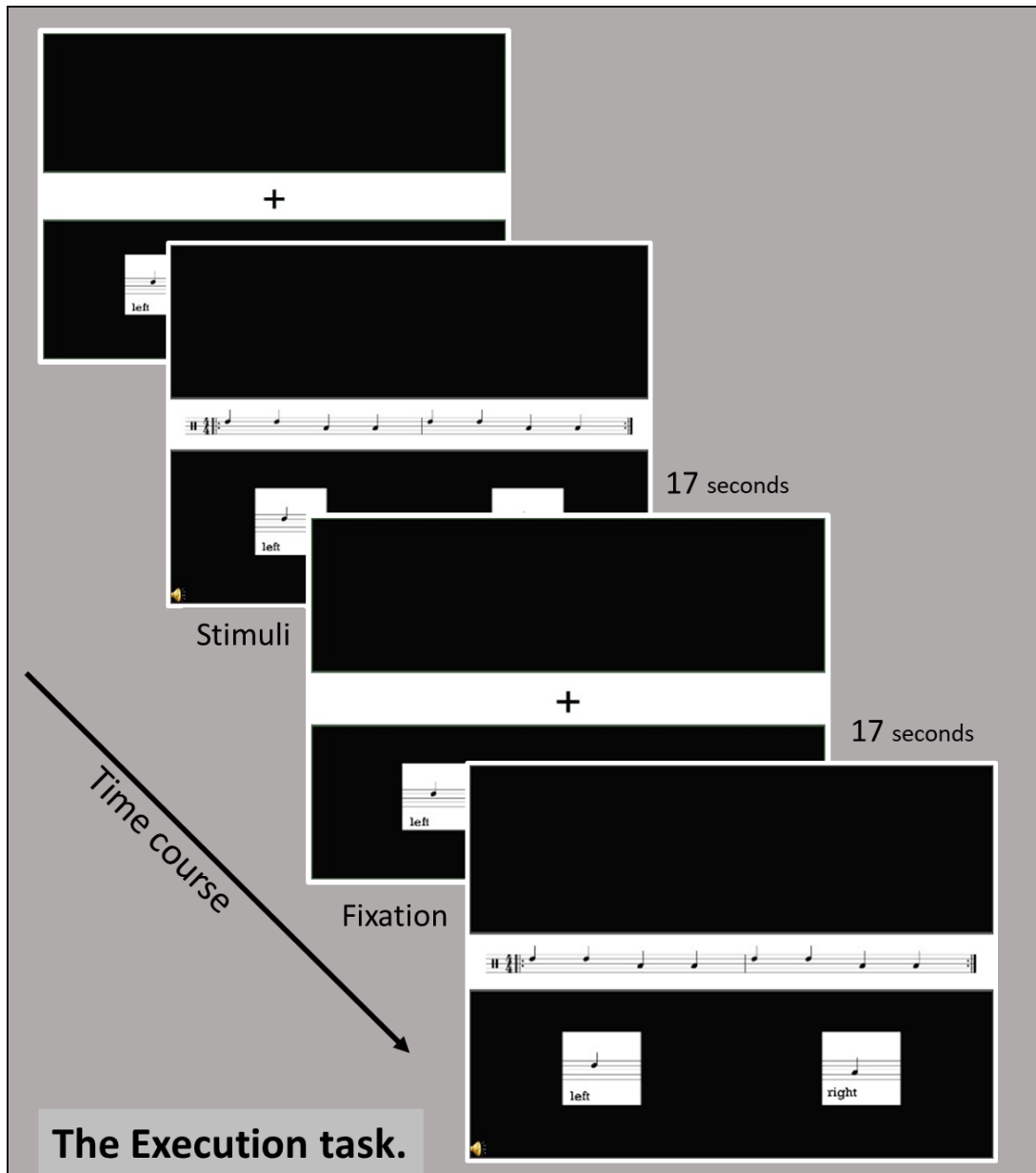


Figure 12. Schematic diagram representing the execution task: Participants were asked to 'tap' the pattern represented by the musical notation in time to a metronome sound that was delivered via headphones in the scanner. Taps were recorded by a custom-built optical sensor. Task execution and rest blocks alternated for 680 seconds.

**Visual and auditory stimulation**

Videos were displayed using a Panasonic PT-L785U projector which projected visual input from the back of the scanner to be observed by the participant via the appropriate screen and head coil mounted mirror. Auditory stimulation was provided by an MR Confon auditory stimulator. This device was connected to the laptop headphone socket, providing the stimuli via an MRI-compatible headphone (MR Confon GmbH, Magdeburg, Germany, see Fig.13.)
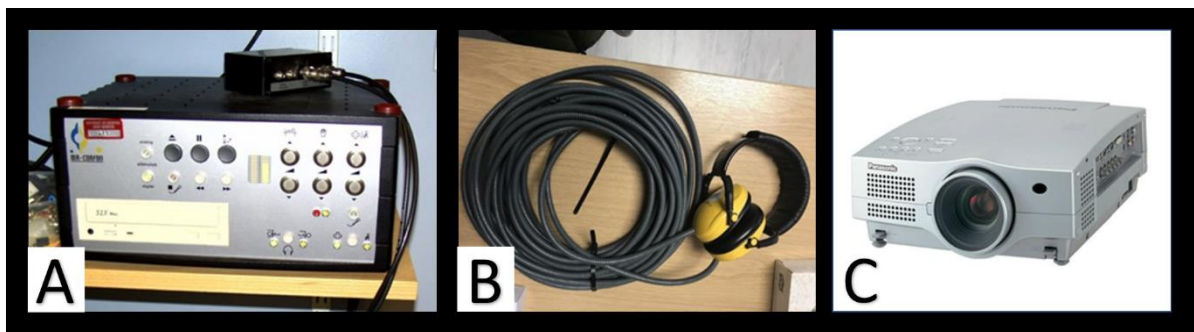


Figure 13. fMRI Stimulus Presentation Equipment: A) MR Confon headphone B) Auditory stimulator C) Panasonic PT-L785U projector.

### 3.2.3 **Data analysis**

#### I.    **Pre-processing**

Functional MRI data was pre-processed in MATLAB R2018a and in SPM12 (v7219) software packages ([http://www.fil.ion.ucl.ac.uk/spm/software/spm12/](http://www.fil.ion.ucl.ac.uk/spm/software/spm12/)) with standard parameters.

The order of pre-processing operations was that of 1) Slice Timing, 2) Realign & Unwarp, 3) Segment, and 4) Co-register: Estimate, Normalise, and Smooth.

- ***Slice timing correction:*** This was applied to Execution and the three Observation fMRI sessions, and the slice order was ascending with the reference slice as the first one.

- ***Realign and unwarp:*** fMRI sessions were first realigned to each other (rigid body) by aligning the first scan from each of the latter sessions to the first scan from the first session. Then, scans from each session were aligned to the first scan of the session that is aligned to the average model of the first session of each of the three scans. The estimation options and their values were Quality (0.9), Separation (4.0mm), Smoothing (5.0mm), and Interpolation (2$^{nd}$ Degree B-spine).

- ***Segment:*** The anatomical image (T1) was segmented into WM, GM and CSF.

- ***Co-register:*** fMRI images data were co-registered to the corrected anatomical image by manipulating the mean image from the first fMRI session (rigid body).

- ***Normalise:*** All T1 images were spatially normalised to the Montreal Neurological Institute (MNI 125) template 1mm$^3$, and the same transformation was applied to all of the fMRI sessions.

- ***Smooth:*** The aligned fMRI images were resliced to 1mm$^3$ resolution, and 5mm isotropic full width at half maximum (FWHM) Gaussian kernel was applied. Finally, a high-pass filter with a 128s cut-off was applied to remove low-frequency fluctuations in the BOLD response.

## II. Whole Brain Statistical analysis

### *Single-Subject (First level)*

For each subject and for each time period separately (pre, mid and post-training), the onsets and stimuli durations were entered into the design matrix and modelled in a general linear model. For the Observation task, there were mapping contrast images (Active vs. Rest) for each of the pre, mid and post-training sessions. For the Execution task, only one mapping contrast image (Active vs. Rest) was of interest during the post-training session.

### *Group (Second level)*

First, to test the impact of training, the paired t-test was used to examine differences in functional brain data between the pre and post-training sessions using the Observation task. Second, to test the impact of task, the factorial t-test was used to examine the differences between the Observation and Execution tasks at the post-training session.

### *The Contrast Manager*

In order to determine brain regions that are more active when subjects observe the drumming task, compared to when the subjects executed the drumming task, the T - contrasts were defined in three ways. Firstly, the conjunction was analysed in order to identify brain regions which were active in both contexts (Observation [POST] and Execution) of the drumming tasks. Secondly, the Execution > Observation [POST] and thirdly, the Execution < Observation [POST] comparisons were made to find the activations that were greater for the Execution than the Observation task, and vice versa.

# III.    Regions of Interest analysis: ROI(s)

ROI(s) analysis was used to examine task-related brain activity in each individual subject for each of the pre, mid and post-training conditions maps. For this analysis:

1)    The clusters that were active during the drumming performance fMRI task (the execution task) were used to create binary masks. A 'p' threshold (p ≤ 0.001) was used to extract the voxels that were considered activated in the task. There was no restriction for the maximum cluster size.

2)    The fMRI clusters were large enough to cross anatomical boundaries, therefore, for the cerebral cortex, a Brodmann's areas atlas was used to aid identification of regions of activation (https://people.cas.sc.edu/rorden/mricron/index.html). The binary masks from the fMRI task were multiplied by individual Brodmann's areas (BA) using Image Calculator batch tool in SPM12. Only BAs which have consistently been linked to musical expertise in previous studies, as listed in Table 2 in the introduction chapter, were included in this analysis.

3)    The output files from the previous step were used as ROIs to extract the mean beta values across the pre, mid and post-training conditions maps using REX tool, which is available as part of the BIT toolbox. REX is normally used to extract values from the selected data files at the specified ROI(s) (https://www.nitrc.org/projects/rex/).

4)    The extracted data was normalised to the average value of the three sessions, and the mean and standard error were calculated.

5)    Then, a linear regression was applied using across the pre, mid and post-training statistical parametric maps, this workflow is presented in Fig.14.
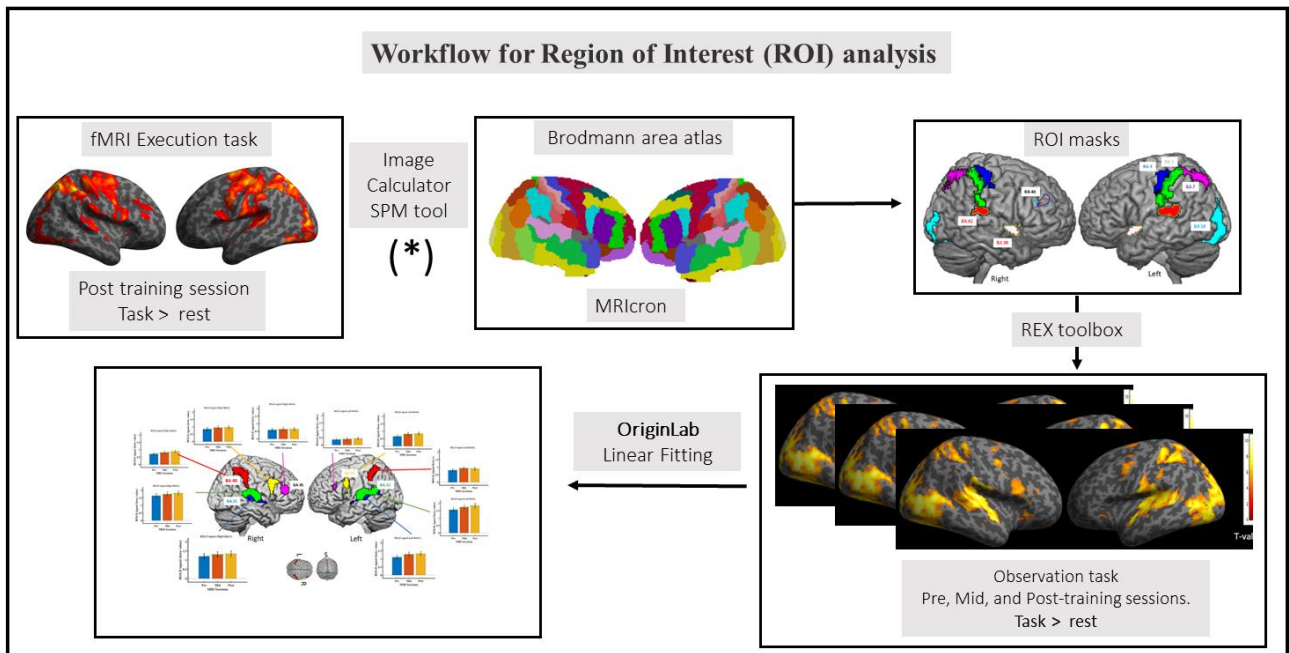
Figure 14. The workflow for ROI analysis show that 1) the anatomical masks were extracted from a probabilistic atlas of Brodmann's areas from MRIcron Toolbox using SPM12, 2) the masks were then used to extract the data from the three session of the observation task.

## 3.3 Results

The results section has been divided into three main parts: 1) The impact of drumming training A) using whole-brain analysis with a one-sample t-test (task > rest) for the pre, mid and post-observation task, B) paired t-test (post > pre) statistical parametric maps to compare brain activations before and after training as a result of acquiring drumming expertise. 2) The impact of and differences between the observation and execution fMRI tasks, and their overlapping brain activations, including the conjunction contrast map. 3) The correlational nature of these brain activation changes and the performance measurements.

### 3.3.1 **Impact of drumming training**

A) In order to determine changes in brain activation as a result of acquiring drumming expertise, the statistical parametric maps (task > rest) for the pre, mid and post-training observation tasks were analysed in SPM12 using a one-sample t-test with familywise error correction (FWE) applied. A few regions did show a significantly increased brain activation ( $p < .05$) following training, such as the primary auditory cortex, primary visual cortex, cerebellum and insula regions (see Fig. 15 and Fig. 16).
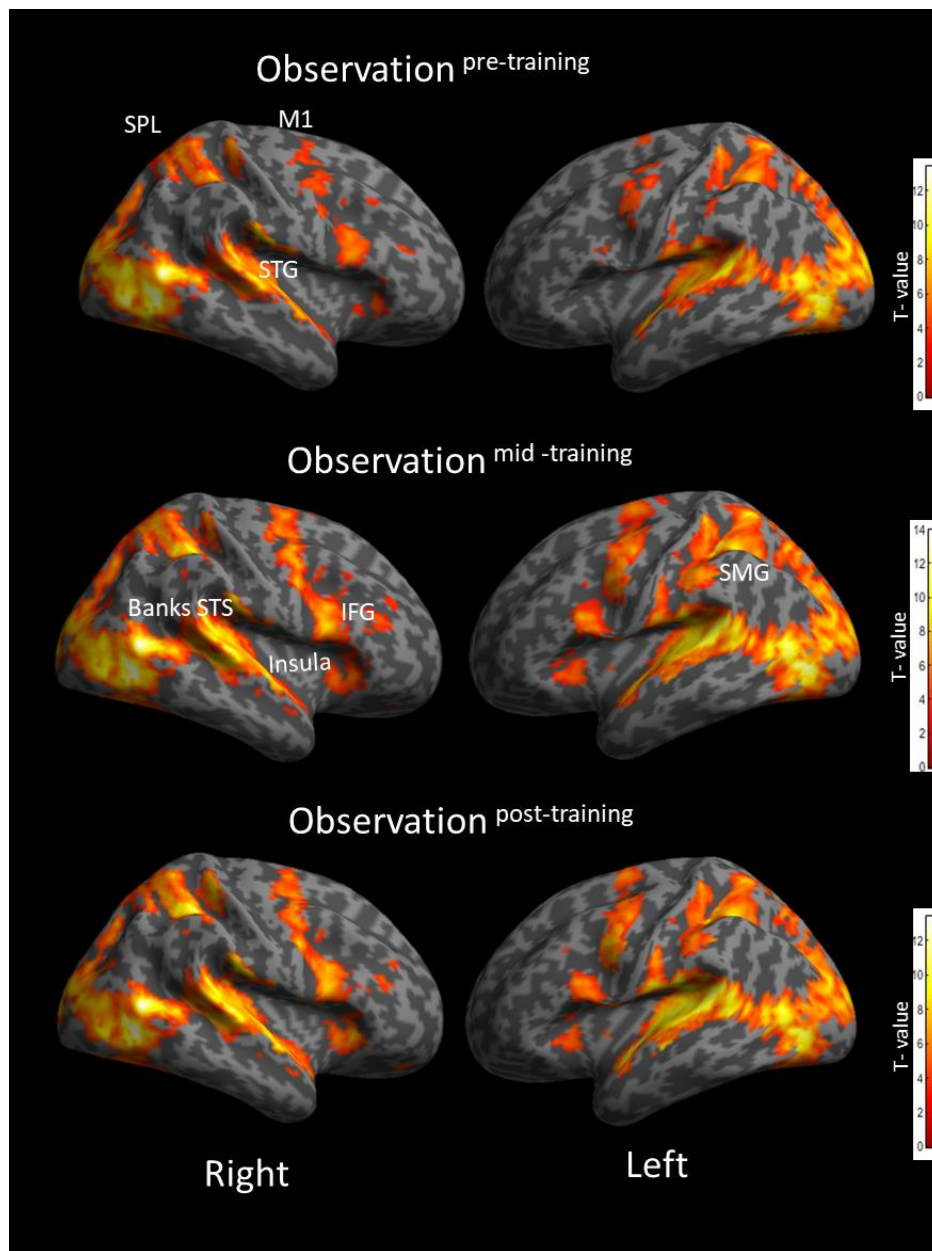
Figure 15. **fMRI results.** Areas of the brain greater activated by Observation tasks (task> rest, corrected SPMs, threshold of p < .05), with contrast mapping rendered as an inflated brain (SPM12). Abbreviations: SPL= Superior Parietal Lobe, STG= Superior Temporal Gyrus, M1= Primary Motor Area, SOG= Superior Occipital Gyrus, IOG= Inferior Occipital Gyrus. Details of the clusters are summarised in Table 8.
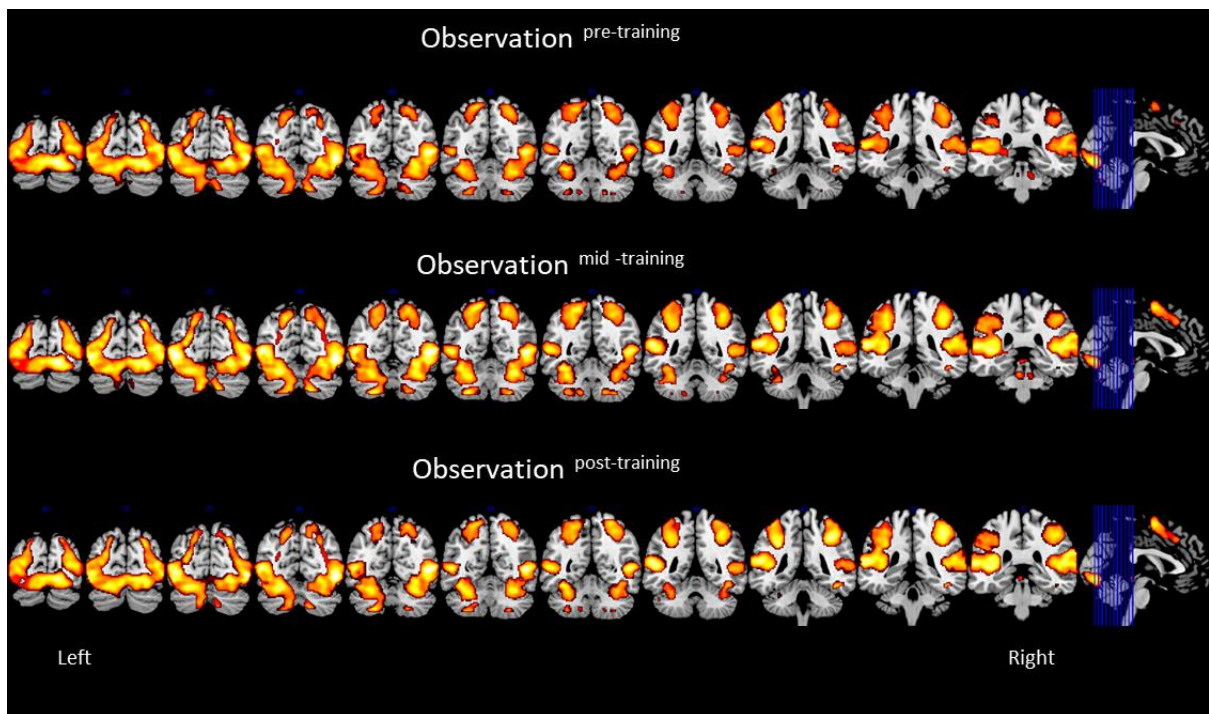
Figure 16. **fMRI results.** Areas of the brain greater activated by Observation tasks (task> rest, corrected SPMs, threshold of p = 0.05), with contrast mapping present on the single brain (MRIcron).

B) In addition, the paired t-test for drumming training was used (i.e. (post> pre) contract mapping) were applied. There were no survive voxels with a with familywise error correction (FWE) applied (p <.05). Therefore, (uncorrected for multiple comparisons; cluster-forming voxel threshold: p <.001) were presented here. The main finding was increased activations in bilateral supramarginal gyrus (BA40), part of the Inferior Parietal Lobule (IPL). Analyses also showed increased activity in the middle temporal gyrus (MTG) bilaterally, areas are known as BA21 and BA22, respectively, in response to training. The cluster details (size, p and t values) are presented in Fig. 17 and Table 7.
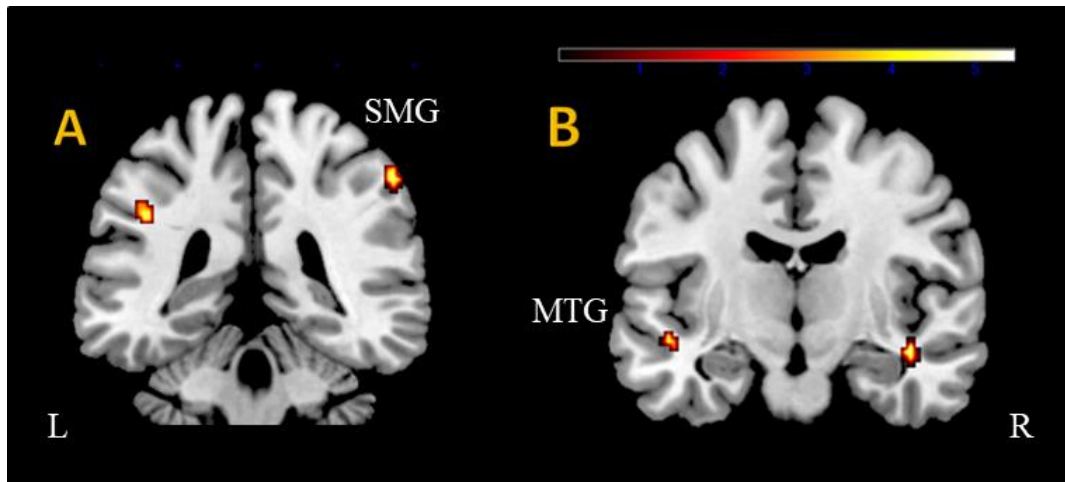
Figure 17. fMRI results. Areas of the brain greater activated by Observation tasks (post > pre, uncorrected SPMs, a threshold of p <.001), with contrast mapping present on the single brain (MRIcron).

| Anatomical region | Talairach coordinate | | | Number of voxels | BA | Z value |
|---|---|---|---|---|---|---|
| | x | y | z | | | |
| Left SMG | -54 | -34 | 36 | 16 | 40 | 3.79 |
| Right SMG | 56 | -36 | 48 | 21 | 40 | 3.44 |
| Left MTG | -48 | -14 | -10 | 39 | 21 | 3.71 |
| Right MTG | 68 | -30 | 32 | 15 | 21 | 3.74 |

Table 7. fMRI results. Whole-brain analysis with .paired t-test (post > pre-training) contrast (uncorrected SPMs, threshold of p <.001).

### 3.3.2 **Impact of Observation and Execution fMRI tasks.**

In addition, we investigated the observation and execution fMRI tasks and their overlap of brain activation. This section was divided into three parts: A. Observation [Post] > Execution condition, B. Execution > Observation [Post], and C. Conjunction analysis condition.

## I.    Whole-brain analysis

In both tasks, the BOLD signal was significantly greater than baseline (i.e. task vs. rest) contrast maps with uncorrected for multiple comparisons (p <.001). The main reason for showing uncorrected results in this section because these maps will be used later as binary masks to extract the mean beta values, and gray volume measures (VBM chapter 4) from the three MRI sessions (i.e. pre, mid and post-training sessions).  However, the binary mask may contain false-positive errors, but further analysis will be carried out using diffusion data to confirm the final results.

For the Observation task, most clusters produced robust patterns of brain activation in the primary visual, audio, and motor brain areas. Whereas, for the Execution task, the main clusters were in the pre and postcentral and supplementary motor cortex (see Fig. 18). Details of the clusters identified for each condition are separately summarised in Table 8.
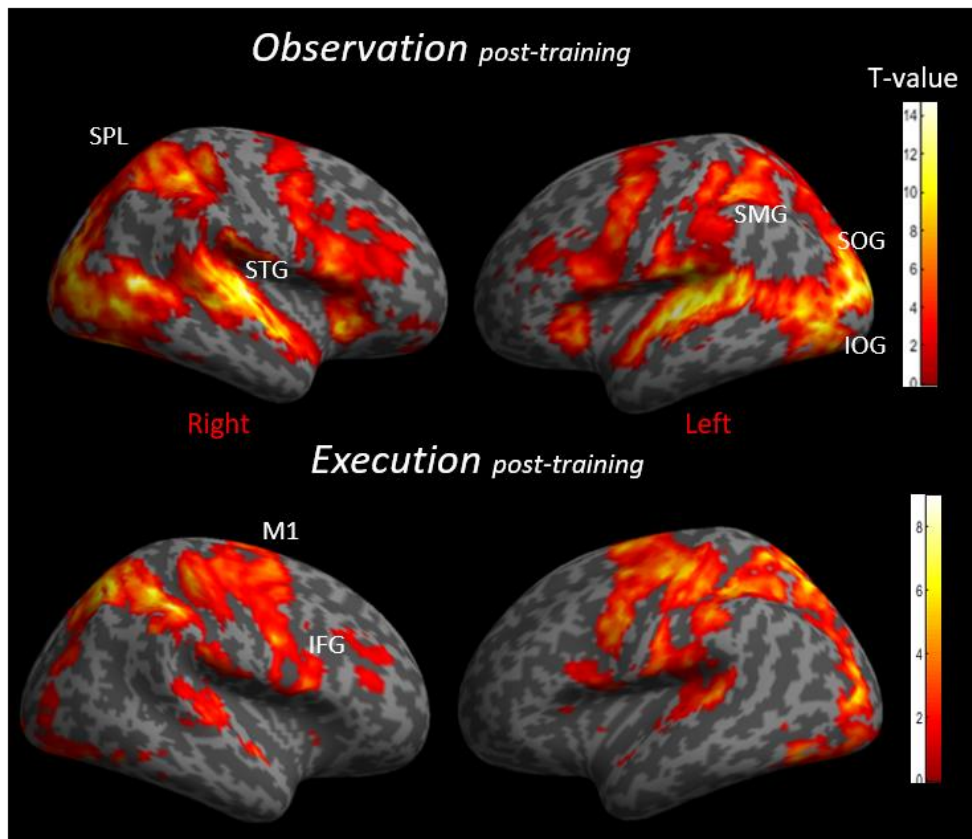
Figure 18 . fMRI results. Areas of the brain greater activated by Execution and Observation tasks (task> rest, uncorrected SPMs, threshold of p < .001), with contrast mapping rendered as an inflated brain (SPM12). Abbreviations: SPL= Superior Parietal Lobe, STG= Superior Temporal Gyrus, M1= Primary Motor Area, SOG= Superior Occipital Gyrus, IOG= Inferior Occipital Gyrus, SMG = Supramarginal Gyrus.

## A. *Activity for Observation* [Post] *> Execution condition*

The activated areas covered a large part of the cortex bilaterally, including the superior and middle occipital gyri (BA17: primary visual cortex (V1), BA18: secondary visual cortex (V2), and BA19: associative visual cortex (V3, V4, V5)). Additionally, the posterior of superior and middle temporal gyrus (BA21: Wernicke's area (left), and (BA38: planum temporale (PT)) also demonstrated increased activations.

Correspondingly, a large part of the middle and inferior temporal gyrus (BA41/42: primary audio cortex) was activated when observing rather than executing drumming patterns. Similarly, the anterior insula and the middle orbital gyrus, or anterior part of Broca's area (BA47: pars orbitalis of the IFG), as well as the left side of the cerebellum (VI, VII, IX), all demonstrated changes in function (see Fig. 19a and Table 8).

### B. *Activity for Execution > Observation* [Post] *condition*

The main activations were located bilaterally in the frontal cortex (BA6: supplementary motor area), the anterior precentral gyrus (BA4: primary motor cortex), and part of the posterior precentral gyrus gyrus (BA1/2: primary somatosensory cortex). Additionally, part of IPL (BA40: supramarginal gyrus), and calcarine gyrus (BA23: posterior cingulate gyrus), just superior to the splenium of the corpus callosum were activated. Visual areas within the inferior and middle occipital gyrus and cuneus (BA17: primary visual cortex (V1), BA39: angular gyrus), as well as IPL (BA7: precuneus), and cerebellum showed some activations (see Fig. 19b and Table 8).
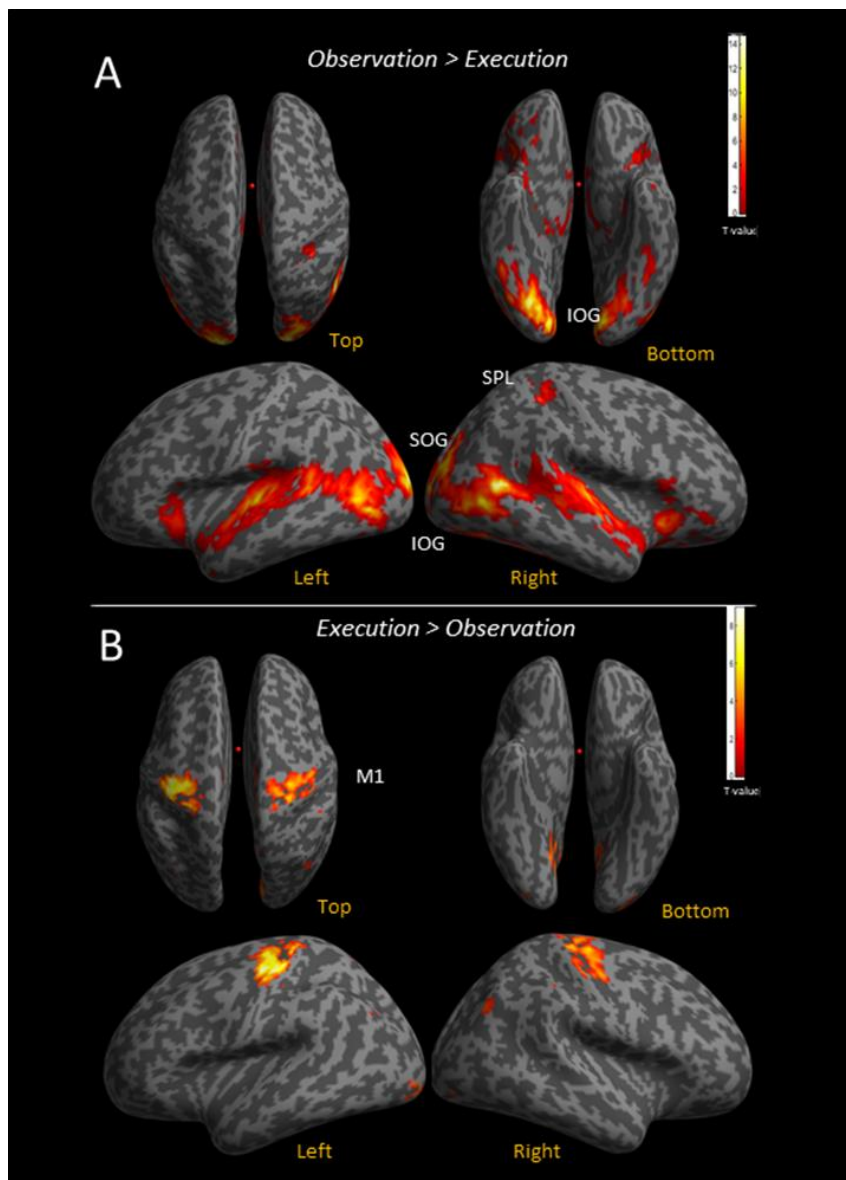
Figure 19. **fMRI results**. Activation of the group-level found in the whole-brain analysis (task> rest, uncorrected SPMs, threshold of p < .001) with contrast mapping represented on a render view (SPM12). Abbreviations: SPL= Superior Parietal Lobe, M1= Primary Motor Area, SOG= Superior Occipital Gyrus, IOG= Inferior Occipital Gyrus.

## C. Activity for Conjunction analysis condition

To identify overlapping areas of activations between observation and execution drumming tasks, a conjunction analysis was performed. There was a significant activation of clusters within the human mirror system specifically inferior parietal lobule (BA7/40), and inferior frontal gyrus (BA 45 and BA44), which is considered to be part of Broca's area, as well as a region within the audio cortex (BA 21 and BA 22). The mirror neurons transform visual observation into knowledge. Studies on humans during action observation have shown activation of the IFG, the IPL and a region within the STS. Furthermore, (fusiform gyrus; BA37), and the cerebellum, were also activated in response to drumming training as shown in Fig.20. Each of the aforementioned regions have a specific role in motor action performance, such as that which is necessary for playing a drum kit (see discussion section).
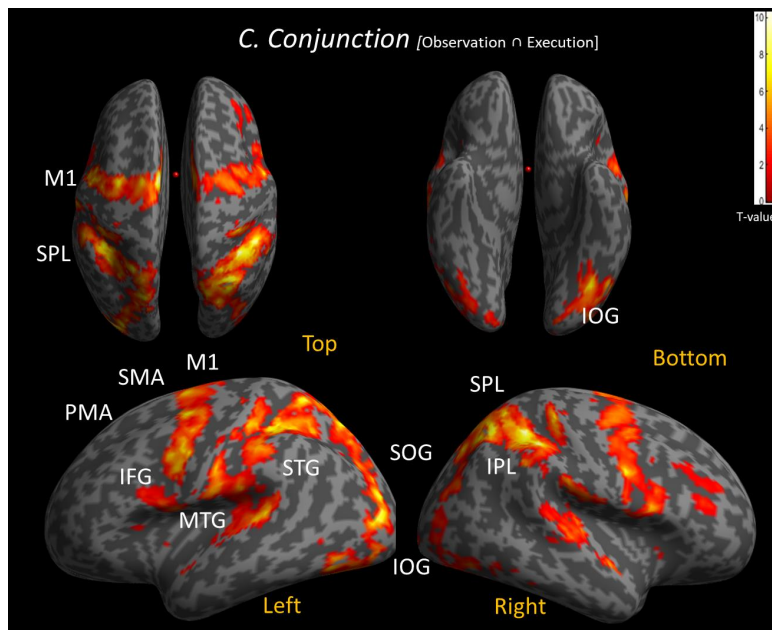


Figure 20. **fMRI results**: Statistical parametric maps (t values) for the conjunction is – Observation ∩ Execution, contrast mapping represented on a render view (SPM12). Activation of the group-level found in the whole-brain analysis (uncorrected SPMs, threshold of p <.001). Abbreviations: SPL= Superior Parietal Lobe, M1= Primary Motor Area, SOG= Superior Occipital Gyrus, IOG= Inferior Occipital Gyrus.

Contrasting Execution and Observation conditions directly across the entire brain, the pre-SMA and cingulate motor areas, as well the angular gyrus, were significantly more active for Execution than Observation of the drumming task. The cerebellum also showed an increased BOLD response in the anterior lobe in response to the drumming execution. On the other hand, the visual and audio brain regions showed higher activations in response to Observation compared to the Execution, as shown in Fig. 19c. and Fig.21.
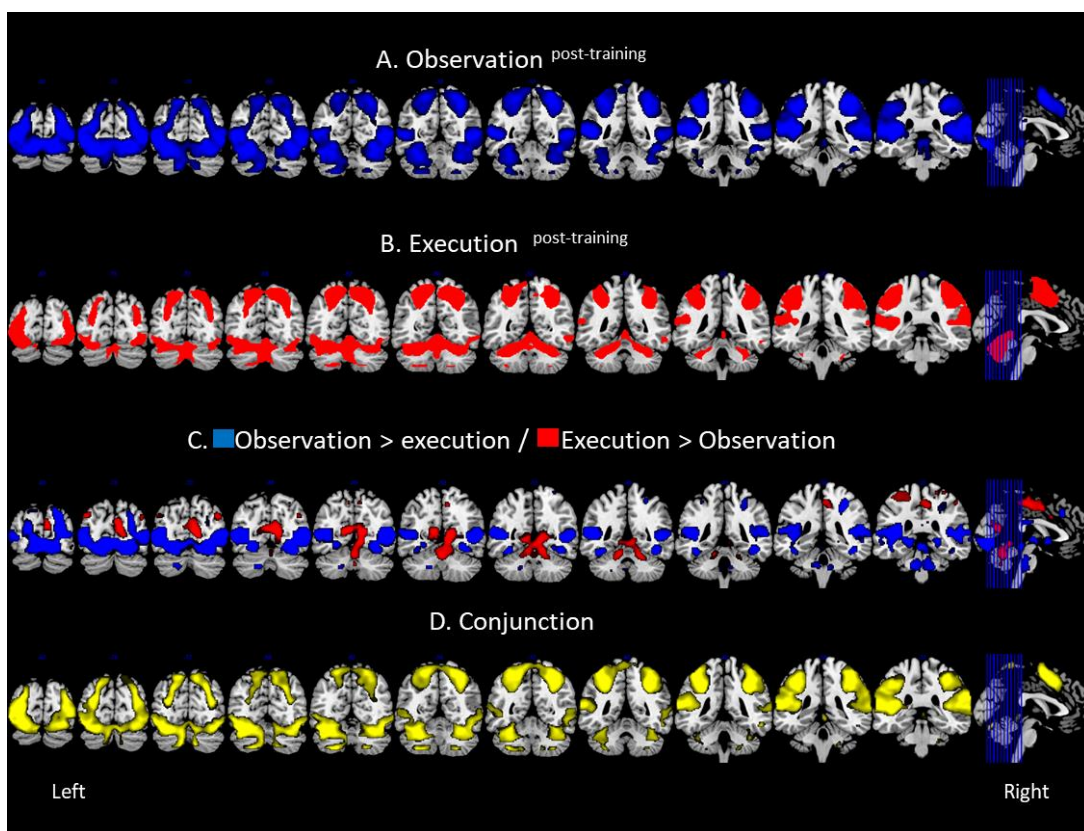


Figure 21. Activation at the group-level found in the whole-brain analysis (task> rest, uncorrected SPMs, threshold of p <.001), with contrast mapping represented on a render view (SPM12).

| Brain region | Hemisphere | Number of voxels | Z | MNI coordinaste | | | BA |
|---|---|---|---|---|---|---|---|
| | | | | x | y | z | |
| 1. Execution condition | | | | | | | |
| Inferior parietal lobule | Right | 1830 | 6.91 | 46 | -36 | 54 | 40 |
| Superior parietal lobule | Right | | 6.57 | 28 | -64 | 52 | 7 |
| Precuneus | Right | | 5.94 | 12 | -66 | 54 | 7 |
| Supplementary motor area | Left | 989 | 6.67 | 0 | -4 | 58 | * |
| Superior parietal lobule | Left | 2188 | 6.42 | -18 | -70 | 52 | 7 |
| Inferior parietal lobule | Left | | 6.02 | -38 | -40 | 44 | 40 |
| Superior parietal lobule | Left | | 5.93 | -22 | -60 | 60 | 7 |
| Occipital_Mid | Left | 216 | 6.2 | -36 | -86 | 6 | 18/19 |
| Fusiform gyrus | Left | 564 | 5.83 | -42 | -66 | -20 | 37 |
| Cerebellum | Left | | 5.56 | -28 | -64 | -22 | * |
| Precentral gyrus | Left | 328 | 5.81 | -46 | 0 | 34 | 6 |
| Precentral gyrus | Right | 64 | 5.74 | 54 | 10 | 38 | 6 |
| Superior temporal gyrus | Left | 93 | 5.48 | -56 | -30 | 12 | 22 |
| Cerebellum | Right | 116 | 5.44 | 30 | -56 | -26 | * |
| Temporal_Pole | Left | 144 | 5.43 | -60 | 6 | -2 | 22 |
| Temporal_Pole | Right | 60 | 5.31 | 60 | 6 | -2 | 22 |
| Superior Frontal lobule | Right | 233 | 5.31 | 26 | -2 | 62 | 6 |
| 2. Observation POST | | | | | | | |
| Superior temporal gyrus | Left | 23645 | 7.83 | -46 | -22 | 6 | * |
| Middle temporal gyrus | Right | | 7.79 | 46 | -62 | 4 | * |
| Heschl gyrus | Right | | 6.89 | 48 | -20 | 6 | 21/22 |
| Supplementary motor area | Left | 1136 | 5.78 | -4 | 2 | 60 | 6 |
| Supplementary motor area | Right | | 5.26 | 4 | 20 | 46 | 32 |
| Inferior parietal lobule | Right | 1970 | 6.31 | 36 | -40 | 50 | * |
| Superior parietal lobule | Right | | 5.73 | 28 | -62 | 50 | * |

| | | | | | | | |
|---|---|---|---|---|---|---|---|
| Cerebellum | Left | 114 | 5.47 | -24 | -64 | -50 | * |
| Cerebellum | Right | 29 | 5.55 | 22 | -64 | -50 | * |
| Superior Frontal lobule | Right | 13 | 4.98 | 24 | 46 | -12 | * |
| Middle Frontal lobule | Right | 21 | 4.73 | 44 | 38 | 20 | 46 |
| Superior Frontal lobule | Right | 4 | 4.72 | 26 | -4 | 62 | 6 |
| 3.   *Observation* [POST] *> Execution* **condition** | | | | | | | |
| Middle occipital gyrus | Left | 22517 | 7.59 | -18 | -98 | 10 | 18 |
| Superior occipital gyrus | Right | | 7.38 | 16 | -100 | 16 | 18 |
| Middle temporal gyrus | Right | | 7.29 | 46 | -62 | 4 | 19 |
| Postcentral gyrus | Right | 232 | 5.14 | 32 | -38 | 52 | 1 |
| Superior parietal lobule | Right | | 3.30 | 26 | -48 | 58 | 7/40 |
| Cerebellum (VI) | Left | 112 | 3.82 | -16 | -70 | -38 | * |
| Cerebellum (VII) | Left | | 3.52 | -20 | -56 | -38 | * |
| Cerebellum (IX) | Left | | 3.25 | -22 | -48 | -44 | * |
| Inferior frontal gyrus | Left | 23 | 3.61 | -46 | 14 | 18 | 44 |
| Cingulate gyrus | Right | 147 | 3.59 | 12 | -22 | 28 | * |
| Cingulate gyrus | Left | | 3.28 | -4 | -18 | 28 | * |
| Superior medial gyrus | Right | 197 | 3.54 | 4 | 24 | 42 | 8 |
| Cingulate gyrus | Left | | 3.48 | -10 | 22 | 36 | 32 |
| Superior medial gyrus | Left | | 3.34 | -4 | 28 | 36 | 8 |
| Inferior temporal gyrus | Left | 31 | 3.47 | -44 | 8 | -34 | 38/21 |
| Middle orbital gyrus | Right | 23 | 3.43 | 26 | 42 | -12 | 47 |
| 4.   *Execution > Observation* [POST] *condition* | | | | | | | |
| Postcentral gyrus | Left | 1526 | 6.00 | -38 | -22 | 48 | 1 |
| Precentral gyrus | Right | 1230 | 4.99 | 28 | -26 | 66 | |
| Calcarine gyrus | Right | 2537 | 4.16 | 8 | -68 | 18 | 17 |
| Cuneus | Right | | 3.99 | 10 | -80 | 18 | 18 |
| Inferior occipital gyrus | Left | 112 | 3.78 | -28 | -94 | -10 | 18 |

| Region | Side | Size | Value | x | y | z | BA |
|---|---|---|---|---|---|---|---|
| Supplementary motor area | Right | 702 | 3.52 | 2 | -22 | 52 | 6/4a |
| Supplementary motor area | Left | | 3.44 | -4 | -16 | 52 | 6 |
| Middle occipital gyrus | Left | 62 | 3.25 | -40 | -78 | 36 | 39 |
| Inferior occipital gyrus | Right | 36 | 3.17 | 38 | -90 | -6 | 18 |
| Middle occipital gyrus | Right | 104 | 5.61 | 42 | -76 | 34 | 39 |
| Precuneus | Right | 11 | 4.74 | 8 | -58 | 52 | 7 |
| **5. Conjunction condition** | | | | | | | |
| Supplementary motor area | Left | 575 | 6.49 | -4 | 0 | 60 | 6 |
| Supplementary motor area | Left | | 5.01 | -2 | 8 | 44 | 32 |
| Postcentral gyrus | Right | 1096 | 6.49 | 44 | -38 | 52 | 40 |
| SupraMarginal gyrus | Right | | 5.93 | 42 | -38 | 40 | 40 |
| Superior parietal lobule | Right | | 5.92 | 28 | -62 | 50 | 7 |
| Middle occipital gyrus | Left | 216 | 6.20 | -36 | -86 | 6 | 18/19 |
| Inferior parietal lobule | Left | 723 | 6.01 | -38 | -40 | 44 | 40 |
| Superior parietal lobule | Left | | 5.92 | -22 | -60 | 60 | 7 |
| Cerebellum (VI) | Left | | 5.91 | -18 | -72 | 52 | 7 |
| Fusiform gyrus | Left | 474 | 5.83 | -42 | -66 | -20 | 37 |
| Cerebellum (VI) | Left | | 5.47 | -34 | -72 | -20 | * |
| Precentral gyrus | Left | 313 | 5.80 | -46 | 0 | 34 | 6 |
| Middle frontal gyrus | Left | 181 | 5.64 | -30 | -6 | 52 | 6 |
| Superior frontal gyrus | Left | | 5.54 | -26 | -4 | 62 | 6 |
| Superior temporal gyrus | Left | | 4.82 | -44 | -10 | 56 | * |
| Superior occipital gyrus | Right | 35 | 5.51 | 26 | -68 | 40 | 7 |
| Precentral gyrus | Left | 93 | 5.47 | -56 | -30 | 12 | 22 |
| Precuneus | Left | | 5.4 | -62 | -38 | 14 | 22 |

Table 8. Regions showing significant increases in activation as a result of each condition, (uncorrected SPMs, threshold of p <.001).

## II.    Region of Interest Analysis

In addition to the whole brain univariate approach, we further explored how BOLD activation changed within each session. To advance understanding of neuroplasticity in response to musical training, or more specifically drumming training, insights may be derived by observe the signal in areas of interest plotted for each condition (i.e. pre, mid and post-training sessions). The ROIs details are presented in Fig. 22, Fig. 23 and Table 9.
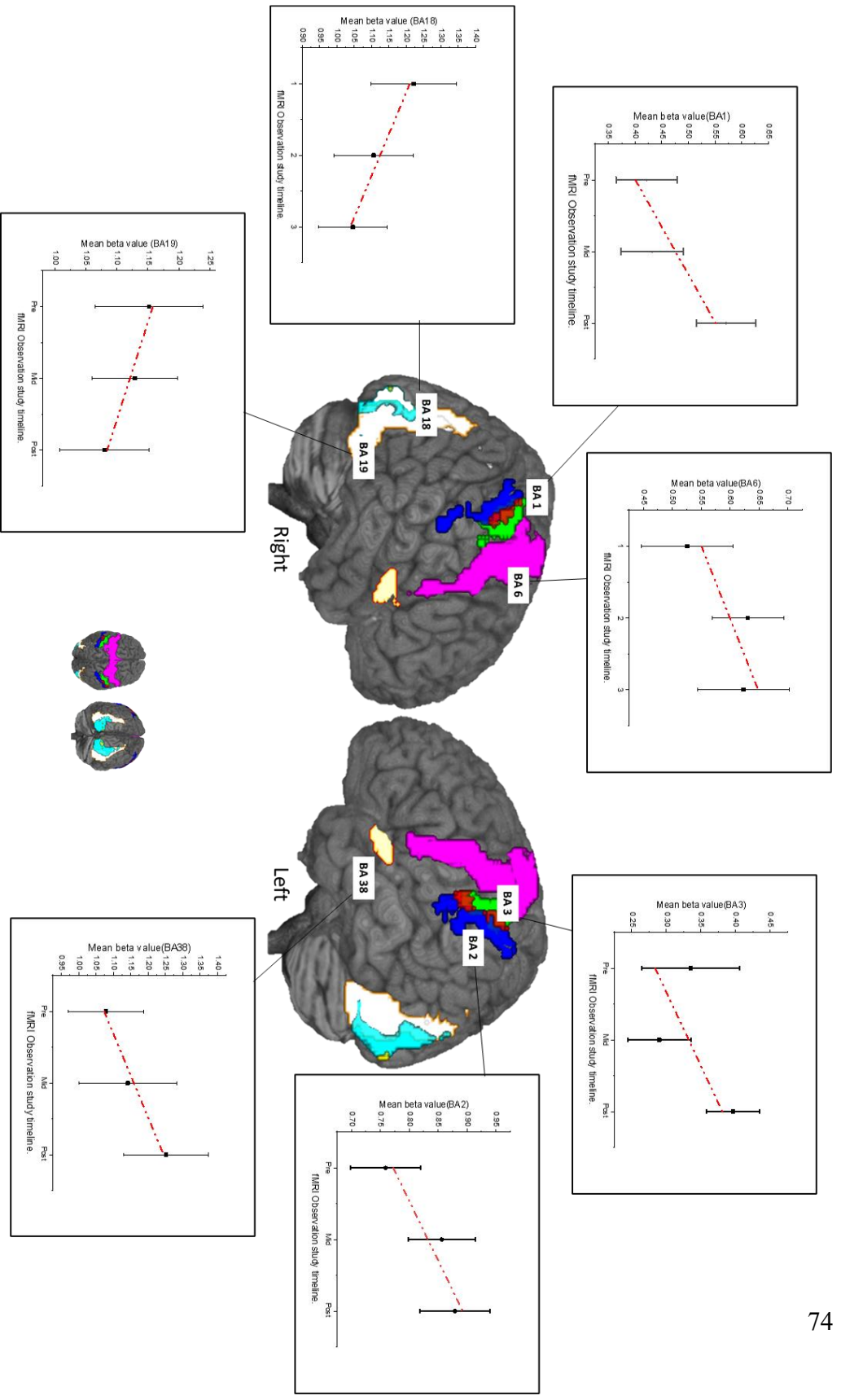
Figure 22. fMRI (ROIs) results. Brain surface projection of activated Brodmann areas of (1, 2, 3, 6, 18, 19 and 38) bilaterally during Execution task. BA = Brodmann area.
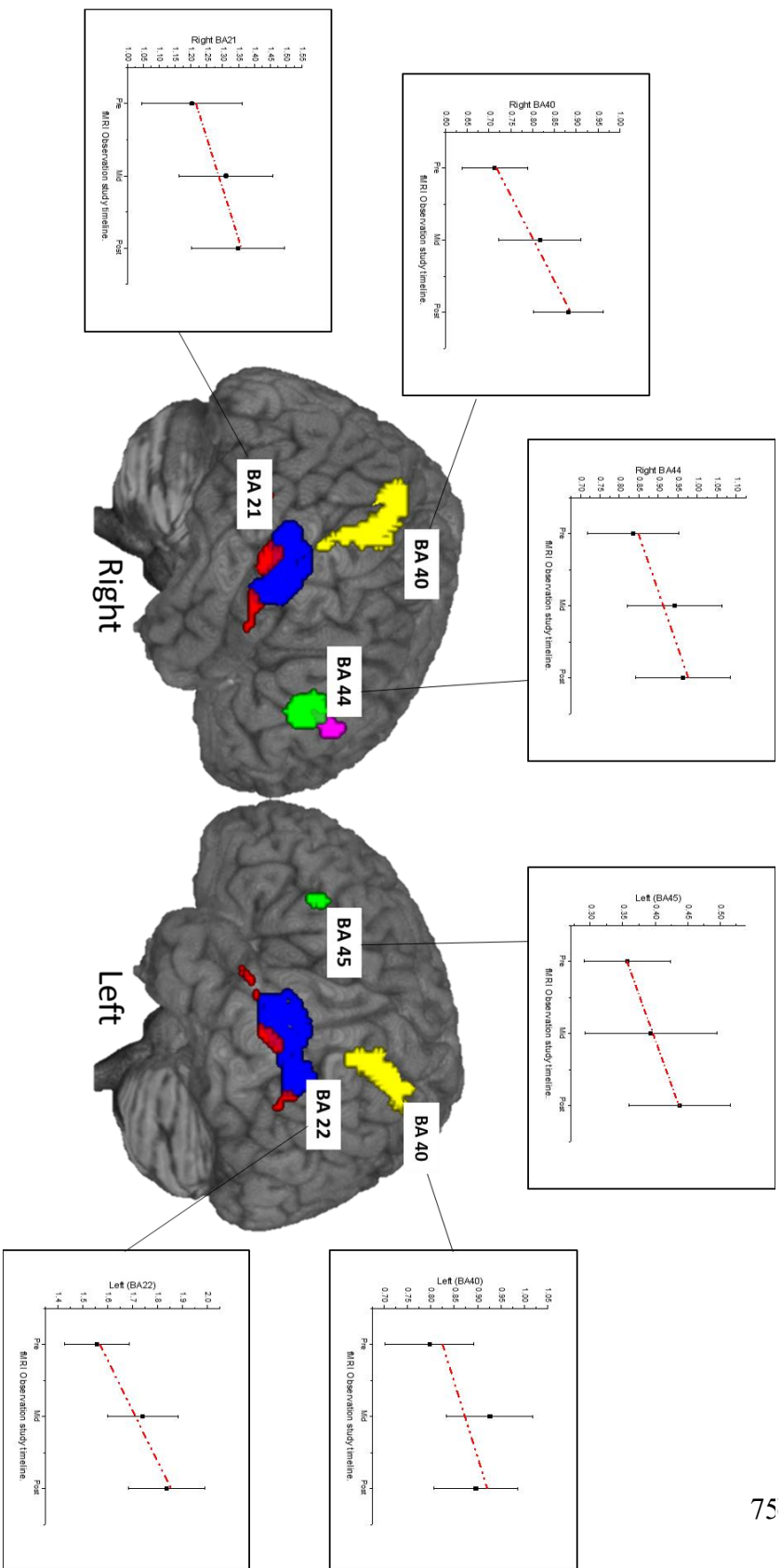
Figure 23 . **fMRI (ROIs) results**. Brain surface projection of activated Brodmann areas of (21, 22, 40, 44, and 45) left and right sides during Execution task.

BA = Brodmann area.

75

| BA | Hemisphere | ROI size (voxels) | Slope value | Slope statistics |
|---|---|---|---|---|
| 1 | Bilateral | 93 voxels | +0.0744 | p=.038 t(13)=2.30 |
| 2 | Bilateral | 1030 voxels | +0.0603 | p=.048 t(13)=2.17 |
| 3 | Bilateral | 1285 voxels | +0.0306 | p=.205 t(13)=1.33 |
| 6 | Bilateral | 6590 voxels | +0.0488 | p=.123 t(13)=1.647 |
| 18 | Bilateral | 1984 voxels | -0.0878 | p=.140 t(13)=-1.57 |
| 19 | Bilateral | 3670 voxels | -0.0360 | p=.415 t(13)=-0.841 |
| 38 | Bilateral | 255 voxels | +0.0864 | p=.088 t(13)=1.84 |
| 21 | (Right) | 95 voxels | + 0.0726 | p=.140 t(13)=1.56 |
|  | (Left) | 72 voxels | + 0.1127 | p=.010 t(13)=2.73 |
| 22 | (Right) | 607 voxels | + 0.0897 | p=.180 t(13)=1.38 |
|  | (Left) | 549 voxels | + 0.1401 | p=.060 t(13)=2.01 |
| 40 | (Right) | 1330 voxels | + 0.0845 | p=.040 t(13)=2.27 |
|  | (Left) | 1027 voxels | + 0.0495 | p=.096 t(13)=1.79 |
| 44 | (Right) | 629 voxels | + 0.0636 | p=.049 t(13)=2.16 |
|  | (Left) | 338 voxels | + 0.0964 | p=.005 t(13)=3.39 |
| 45 | (Right) | 439 voxels | + 0.0253 | p=.460 t(13)=0.75 |
|  | (Left) | 84 voxels | + 0.0401 | p=.280 t(13)=1.12 |

Table 9. fMRI (ROIs) results. Brain surface projection of activated Brodmann areas (21, 22, 40, 44, and 45) left and right sides during Execution task.

### 3.3.3 The correlation relationship between the brain activation changes and the performance measurements.

Surprisingly, there was no significant correlation between the amount of activation change, as indicated by the BOLD response, and the performance measures that were used to evaluate the individual performance improvement process for the participants.

## 3.4 Discussion

The main goal of this study was to determine the time course of fMRI activation for healthy participants engaging in drum training. A concurrent goal was to shed light on the brain processes involved in a) action execution, and b) passive action observation fMRI tasks, as well as their overlap. For this study, participants completed the Observation task at all three time points, i.e. the pre, mid and post-training fMRI sessions, and also completed the Execution task during the post-training session once they had acquired the relevant training necessary to do so'.

### 3.4.1 Impact of drumming training (Observation task)

In terms of functional brain plasticity with learning, the paired t-test (i.e. Post > Pre-training) of the whole brain showed increased activation in both sides of the supramarginal gyrus (SMG), which is a portion of the parietal lobe known as BA40. This is consistent with the findings of Meister et al. (2004) and Miendlarzewska et al. (2014), as both of these studies implicated BA40 in the control of movement via visuospatial information processing and/or performing creative tasks, such as drumming. Along with the above, we successfully located an increase activation patterns change in both sides of the superior temporal gyrus (STG) and middle temporal gyrus (MTG), known as BA22 & BA21, respectively. This result is also

consistent with previous experiments regarding learning to play a melody on a piano keyboard (Chen et al., 2012), hammering or clapping (Lewis et al., 2005; Galati et al., 2008), as well as the activations of expert drummers (Tsai et al., 2012), which showed that the STG and MTG were selectively responsible for action-related sounds. In accordance with the present results, most authors concluded that the posterior part of the superior/lateral temporal cortex, from Wernicke's language area to Brodmann areas 21 and 22, is involved in complex language ( i.e. plays a much larger role in speech production) and auditory processing (James, 2014). Wernicke area (commonly known as Wernicke's area) unequivocally as "the area where a lesion will cause language comprehension deficit." (Bogen & Bogen, 1976).  It is easy to define Wernicke's area which corresponds to the language auditory processing area in the left hemisphere.

Overall, our results are directly in line with previous findings that showed higher activation in certain areas in response to musical training. These findings may help us to understand more about the function of the brain regions involved in drumming training. For example, Tsai et al. (2012) found the posterior temporal lobes to be essential for audio-motor processing,  and Petrini et al. (2011) demonstrated that expert drummers present a reduced activation bilaterally during an audio-visual task in both the cerebellum and the left parahippocampal gyrus, areas involved in the action–sound representation and audio-visual integration, respectively. This may reflect the more automated nature of drumming execution in experts, whereby conscious and focussed attention on the task is no longer of primary importance, as it is with beginners.

## 3.4.2  Impact of Observation and Execution fMRI tasks

The second goal of this project was to explore the different activation patterns between passive observation and execution of the drumming task. The whole-brain analysis clearly showed differences in activation between the observation and execution tasks.

A. **Observation** [post] **> Execution**: The mean increases in activity for all subjects during the passive observation were located in the primary and secondary audio cortex, heschl gyrus (BA 21and BA22), and the primary and secondary visual cortex (BA 17 , BA 18 ,and BA19), as well as planum temporale (PT). The PT plays a role in the analysis and processing of incoming complex sounds (i.e. musical temporal patterns) at different scales and is sensitive to patterns and metrical complexity (Vikene K, et al., 2019).

B. **Observation** [post] **< Execution:** Most activation clusters from execution drumming were located at the primary motor cortex (M1), and the Supplementary Motor Area (SMA). The primary motor cortex (M1) is usually activated when subjects perform a sequence, and it has also been found active during the execution of simple movements. SMA, however, has been strongly implicated as being involved in 'higher-order' aspects of motor behaviour (Tanji, 1994 & 2001). For example, the SMA was reported to be the only region of the brain activated when subjects imagined that they were performing a complex sequence of finger movements (Roland et al., 1980). In contrast, during simple movements, activation was present in M1, but not the SMA. These and other observations lead to the suggestion that the SMA was a supra-motor area specifically involved in the internal generation of complex movements (Orgogozo and Larsen, 1979; Roland et al., 1980; Goldberg, 1985).

C. **The Conjunction of the Observation and Execution**

The main changes in BOLD response during both the Observation and Execution conjunction condition were located in parts of mirror neuron system (MNs), such as inferior frontal gyrus (IFG; BA44/45), and inferior parietal lobule (IPL). Pars opercularis and Pars triangularis

regions of the inferior frontal gyrus, as well as part of Broca's area, usually activate with the observation of distal hand and mouth actions, whereas the activation of the premotor cortex reflects proximal arm.

IPL regions BA40 & BA39 are involved in representing rhythmic auditory phrases (Michael et al., 2014), and so an increase in activity in this area in response to musical training would also be expected. The angular gyrus (BA39) has an important role in various functions, such as language processing, attention, self-processing, semantic information processing, emotion regulation, and mentalising. Since these functions are required in music performance according to the recent study carried by (Shoji & Eiji, 2019), one would also expect to find increased activity in the angular gyrus in response to musical training. In the present study, a significant gradual increase in activation of BA39 was found over the course of drumming training.

### 3.4.3 Regions of Interest analysis

According to the line fitting method used in this study, the primary somatosensory cortex and middle temporal gyrus showed a significant increase of BOLD activation from the pre, to the mid and post-training fMRI sessions, which was positively correlated with the amount of training received. The second most interesting find was that the Brodmann regions involved in sensory, motor and audio functions showed a gradual change over the six months drumming course. In particular, the primary somatosensory cortex (BA1, BA2 and BA3) and primary motor cortex (BA6) showed gradually increasing BOLD responses and activations over the six months drumming course. On other hand, the secondary visual areas (BA18 and BA19) showed a gradually decreasing BOLD response over the learning course.

## 3.5  Limitation

Functional imaging measures metabolic changes during task execution. There are a number of possible limitations in this approach. It is well known that functional imaging data reflects aspects such as task difficulty (Gould et la., 2003) and attention (Ress et al., Nature 2000). This explains why data that link functional activation changes to learning provide contradictory outcomes: Some studies show a reduction in functional activity (Erickson et al., 2007) with learning, some show increases (Kelly & Garavan, 2005) yet others show non-monotonic behaviour. Differential metabolic demands while participants learn new tasks offer good explanation why these different functional activity changes are seen: efficiency gains during learning would predict a reduction in activity while participants learn to execute learnt tasks more effectively (Fitts & Posner ,1967) in direct opposition to this is the expected neural activation patterns when brain regions become active during the learning of novel tasks (Dehaene-Lambertz et al.,2018).  For example, demonstrate increased activity in the visual word form area when children learn to read.  The competing effects of efficiency gains in existing areas and the exaptation of brain areas for novel tasks explains possible non-monotonic behaviour.

A further limitation to this study that should be acknowledged, is that a low statistical significance threshold was used to identify areas of functional plasticity change over the training course. The reasoning behind the choice of ($p<0.001$, uncorrected) as statistical threshold is in line with existing literature (Patel et al., 2013) but may result in false positive results. These results, therefore, should be interpreted with caution. They indicate regions that are likely to be involved in learning drumming and further analyses using VBM (chapter 4), and DTI (chapter 5) show data that is consistent with these findings.   Future studies, replicating these results would add support to the findings.

## 3.6  Conclusion

To sum up, this study successfully showed that the inferior frontal gyrus (Broca's area) and STG (Wernicke's area) are actively involved with learning new motor complex tasks, such as drumming. Broca's and Wernicke's areas are important for speech fluency. More precisely, these areas enable the ordering of words to form complete and sensical sentences. With ongoing repetition, language processing can enhance the efficiency of rehabilitation centres, helping to form new and strengthen existing neuronal connections. The fact that the adult brain can undergo continual modifications throughout the lifetime highlights the potential of rehabilitation treatments designed to induce plastic changes to overcome impairments due to brain injury, such as stroke.

# Chapter 4 Drumming Induces Plasticity in Gray and White Matter volumes: Morphometric Magnetic Resonance Imaging Study Applying CAT12 toolbox.

## 4.1 Introduction

The human brain has been found to achieve diverse neuroplastic outcomes, which vary depending upon factors such as experience and behaviour. That is, outcomes are likely to be task-dependent and also dependent upon the amount of task-experience of the individual performing the task. Therefore, neuroplastic outcomes should differ according to task and level of experience, such as minimal versus prolonged experience of a juggling task (Scholz et al., 2009), a whole -body balancing task (Taubert et al., 2010), a working memory task (Takeuchi et al., 2010; Salminen et al., 2016), motor tasks (Tracy et al., 2003; Jolles et al., 2007 and Arima et al., 2011) and musical training (Kim et al., 2004; Oechslin et al., 2010; Steele et al., 2013). Several investigations have demonstrated that continuous and consistent skill learning results in increased GMV, WMV or cortical thickness in certain regions of the adult human brain, regions which are involved in the task at hand.

Since musical instrumental training is multimodal, involving the development of motor skills, including balance and bimanual coordination, together with audio–motor integration, and also cognitive processes such as memory, attention and executive functions (Schmithorst and Wilke, 2002; Zatorre et al., 2007; for a review see Koelsch, 2010), learning to play and practice a musical instrument over a long period has become a popular paradigm in the study of whole-brain human neuroplasticity. In the last decade, several studies have investigated the neuroplastic changes induced by long-term musical training.

In cross-sectional studies, structural differences in musicians' brains vs those of non-musicians have been reported in multiple research papers. For example, the GMVs in primary motor, somatosensory, premotor and visuospatial cerebral areas were found to be greater in musicians than in non-musicians (Amunts et al., 1997; Gaser and Schlaug, 2003; Han et al., 2009). Moreover, the cerebellar volume was also found to be larger in musicians (Schlaug et al., 1995a; Han et al., 2009). Greater GMV in the left hemisphere of male musicians (sup.

temporal gyrus (HG), planum, inf. pre & postcentral gyrus, caudate and occipital pole) has also been reported (Luders et al., 2004), together with GMV increases in the right fusiform gyrus, right mid. orbital gyrus, left inf. frontal gyrus, left intraparietal sulcus, bilateral cerebellar Crus II & left HG (James et al., 2014). A summary of the findings of some previous voxel-based morphometric studies using cross-sectional designs to compare musicians to non-musicians is presented in Table 10.

Together, these studies demonstrate the malleability of the mature brain, as intensive skill learning in adulthood can induce structural alterations, as well as regional cerebral blood flow and metabolic (functional) changes. However, most previous cross-sectional studies focused on the differences between the neural system of musicians with a higher level of expertise (acquired after long periods of training) and non-musicians. Therefore, it is difficult to conclude from these particular studies whether the observed human brain structural differences were due to sample-selection based on genetic predispositions, or to specific musical experiences. Moreover, the specific time course of human brain structural changes (e.g. GMV increase) due to musical training remains largely unknown.

| Authors/years | Subjects | Results |
| --- | --- | --- |

| | | |
|---|---|---|
| **Gaser and Schlaug (2003)** | Professional musicians (n = 20), amateur musicians (n = 20) & non-musicians (n = 40) | GM uppermost in professional musicians in the following areas: primary motor (BA4), premotor (BA6) and somatosentory areas (BA1/2/3), ant. sup. parietal (BA40), inf.temporal gyrus, left cerebellum, left HG, and left inf. and right medial frontal gyrus. GM intermediate in amateur musicians and lowest in controls. |
| **Luders et al. (2004)** | Musicians: non-absolute pitch (n = 40) & with absolute pitch (n = 20) | More GM in musicians with absolute pitch in the left hemisphere: sup. temporal gyrus (HG), planum, inf. pre- & postcentral gyrus, caudate and occipital pole (BA17/18/19). |
| **Bermudez et al. (2009)** | Musicians (n = 71) vs. non-musicians (n = 64) | Greater GM and thickness in superior temporal (more on the right), greater cortical thickness in inferior frontal gyrus (BA44/45) and orbital area (BA47) and greater GM and thickness in sup. central sulcus in musicians. |
| **Han et al. (2009)** | Musicians-pianists (n = 18) vs. non-musicians (n = 21) | Higher GM in left sensorimotor cortex (BA6) and right cerebellum in musicians. |
| **James et al. (2014)** | Professional pianists (n = 20), amateur pianists (n = 20) & non-musicians (n = 19). | GM greater in right fusiform gyrus, right mid orbital gyrus, left inf. frontal gyrus, left intraparietal sulcus, bilateral cerebellar Crus II & left HG in musicians. |

Table 10. Overview of previous MRI–VBM cross-sectional studies with adult musicians. Participants and results are summarised. Abbreviations: GM: grey matter, HG: Heschl's gyrus, SMA: somatosensory, BA: Brodmann's area, sup.: superior, inf.: inferior, mid.: middle, ant.: anterior, post.: posterior.

This thesis aimed to reveal structural and functional brain changes occurring over a six-month drumming training course. In this chapter, a voxel-based morphometric (VBM) technique was

used alongside fMRI (previous chapter), to discover whether brain regions with increased functional activation will show structural alterations with drumming learning. The relationship between practise-induced GMV and WMV changes and neural activations was then investigated using this combined longitudinal functional and morphometric magnetic resonance imaging (MRI) study technique.

Morphometry is the study of the size and shape of the brain and its structures. VBM is an objective approach that enables a voxel-wise estimation of the local amount of a specific tissue. The default workflow of VBM comprises three basic pre-processing steps: (1) Tissue classification into grey matter (GM), white matter (WM) and cerebrospinal fluid (CSF) after removing the skull bones (Ashburner & Friston, 2000, and Kurth et al., 2015). (2) Spatial normalisation of all the images to the same stereotactic space. This is achieved by registering each of the images to the same template image, by minimising the residual sum of squared differences between them. Specifically, each image is matched to the template image by estimating the optimum 12-parameter affine transformation (Ashburner et al., 1997). It should be noted that the spatial normalisation does not attempt to match every cortical feature exactly, but merely corrects for global brain shape differences. If the spatial normalisation was perfectly exact, then all the segmented images would appear identical and no significant differences would be detected, so VBM tries to detect differences in the regional concentration at a local scale having discounted global shape differences. (3) Smoothing, and finally performing a statistical analysis to localise, and make inferences about, the differences found.

Statistical analysis using the general linear model (GLM) is used to identify regions that are significantly related to the particular effects under study (Fristonet al.,1995b). GLM is a flexible framework that allows many different tests to be applied, ranging from group comparisons and identifying regions that are related to specified covariates, such as learning or age effects. That is, if we know exactly what tissue can be found at a specific

voxel, we can quantify and analyse it. Most commonly, VBM is directed at examining GM, but it can also be used to examine WM. The output from the method is a statistical parametric map showing regions where GM concentration differs significantly between groups or after the training.

**The Present Study**

There are two main questions to be answered in this chapter. Firstly, whether six months of drumming learning leads to significant changes in GMV and WMV. Secondly, whether any correlation between the induced GMV and WMV changes and observed neural activations can be found

To answer these questions, three T1-weighted images 1) pre, 2) mid, and 3) post-training sessions recordings were acquired over a six-month drumming learning course. Then, voxel-based morphometry (VBM) using the Computational Anatomy Toolbox (CAT12) was applied to investigate the whole-brain GMV and WMV changes. Secondly, the regions that showed elevated BOLD signal activation in response to the execution functional MRI task design were used to identify ROIs here. The reason for this was to enable investigation of the relationship between practise-induced GMV changes and neural activation. We hypothesised that the regions which showed learning-related changes in functional activation would also exhibit changes in GMV over the study timeline.

## 4.2  Methods

### 4.2.1  Subjects

Fifteen university staff and students (mean age: 38.6y, range: 20y – 57y, 9 men, 6 women) with no prior drumming experience were recruited for this study. One female was excluded due to abnormalities found upon neurological examination. More information regarding participants can be found in (chapter 2, section 2.2, page 33).

**The VBM study designs**

Participants took part in a 45-minute individual drumming session each week for 17 - 21 weeks. Each session was delivered by a professional drumming tutor. All volunteers agreed to three T1-weighted MRI scans. A pre (baseline) scan was performed at the start of the study. The second scan was performed in the middle of the drumming course after 3/4 months, whereas, the third scan was carried out 5/6 months after study commencement when the course was completed, as shown in Fig. 24.
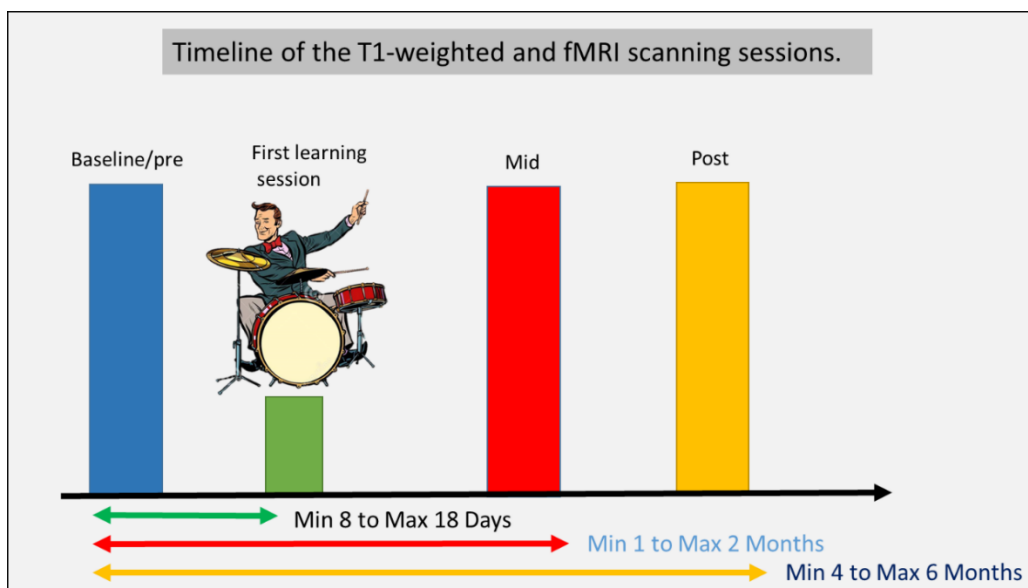


Figure 24. Timeline for the Experiments pre, mid and post drumming course.

## 4.2.2 Data acquisition

The brain scanning of participants was conducted at Liverpool Magnetic Resonance Imaging Centre (LiMRIC) using a 3T Siemens Trio MRI system with an eight-channel receiver head coil to perform a high-resolution, and T1-weighted imaging (axial slices perpendicular to AC-PC line), and analysis of brain matter was applied. Using the acquisition orientation axial, aligned with the AC-PC axis, the whole brain volume was covered with an ascending order of slices. Each acquired volume consisted of 176 slices, with a slice thickness of 1mm and no gap between slices. A repetition time: 2040ms; echo time: 5.57ms; flip angle: 8°; was also used. The field of view (FOV) was 256mm$^2$ and an acquisition time of 7:38 min was also applied.

### 4.2.3 Data analysis

#### I. Pre-processing

The VBM analyses were conducted using the Computational Anatomy Toolbox (CAT12, http://dbm.neuro.uni-jena.de/cat/), which is an extension toolbox of Statistical Parametric Mapping software (SPM12, http://www.fil.ion.ucl.ac.uk/spm/software/spm12), by applying the default settings described in detail in the CAT12 toolbox manual (http://dbm.neuro.uni-jena.de/cat12/CAT12-Manual.pdf). Firstly, the T1 images were spatially registered to the Montreal Neurological Institute (MNI) template. Then, the whole brain structural data were segmented into WM, GM and CSF. Following this segmentation procedure, probability maps of GM and WM were 'modulated' to account for the effect of spatial normalisation by multiplying the probability value of each voxel by its relative volume in native space before and after warping. Bias correction was performed to remove intensity non-uniformities. Finally, modulated images were smoothed with an 8mm full width half maximum (FWHM) Gaussian kernel, in line with other VBM studies (Ilg, Rüdiger, et al., 2008) This smoothing

kernel was applied prior to statistical analyses to reduce signal noise and to correct for image variability.

## II.     Whole brain analysis

The pre and post individual normalised and smoothed GM and WM segmentation were entered into a second-level analysis within the general linear model. To detect the structural changes between the pre and post drumming course, a paired t-test was calculated with post > pre as a contrast condition.

## III.     Regions of Interest analysis ROI(s) Extraction

For this analysis:

1) The activation clusters that were active during drumming performance in the fMRI task (experiment 2 in the fMRI chapter), were used to create binary masks. A threshold of $p \leq 0.001$ was used to extract the voxels that were considered activated in the task. There was no restriction on the maximum cluster size.

2) The fMRI clusters were large enough to cross anatomical boundaries, therefore, for the cerebral cortex, a Brodmann's areas atlas (https://people.cas.sc.edu/rorden/mricron/index.html) was used to help identify specific brain regions. The binary masks from the fMRI task were multiplied by individual Brodmann's areas (BAs) using the Image Calculator batch tool in SPM12. Only BAs which have consistently been linked to musical expertise in previous studies were included in this analysis, as listed in Table 2. For the cerebellum cortex, a probabilistic MR Atlas of the human cerebellum was used (Diedrichsen J. et al., (2009). A probabilistic MR Atlas of the human cerebellum. Neuroimage.)

3) The output files from the previous step were used as ROIs to extract the mean beta values across the pre, mid and post-training conditions maps using REX tool, which is available as part of the BIT toolbox. REX is normally used to extract values from the selected data files at the specified ROI(s) (https://www.nitrc.org/projects/rex/).

4) The extracted data was normalised to the average value of the three sessions, and the mean and standard error were calculated.

5) Then, a linear regression was applied across the pre, mid and post-training sessions using statistical parametric maps (see Fig. 25).

6) Finally, the BA21, BA22, BA44 and BA45 areas, which are believed to be involved with Broca's and Wernicke's areas, were divided into right and left sides to enable a more accurate monitoring of GMV changes over the pre, mid and post-training sessions.
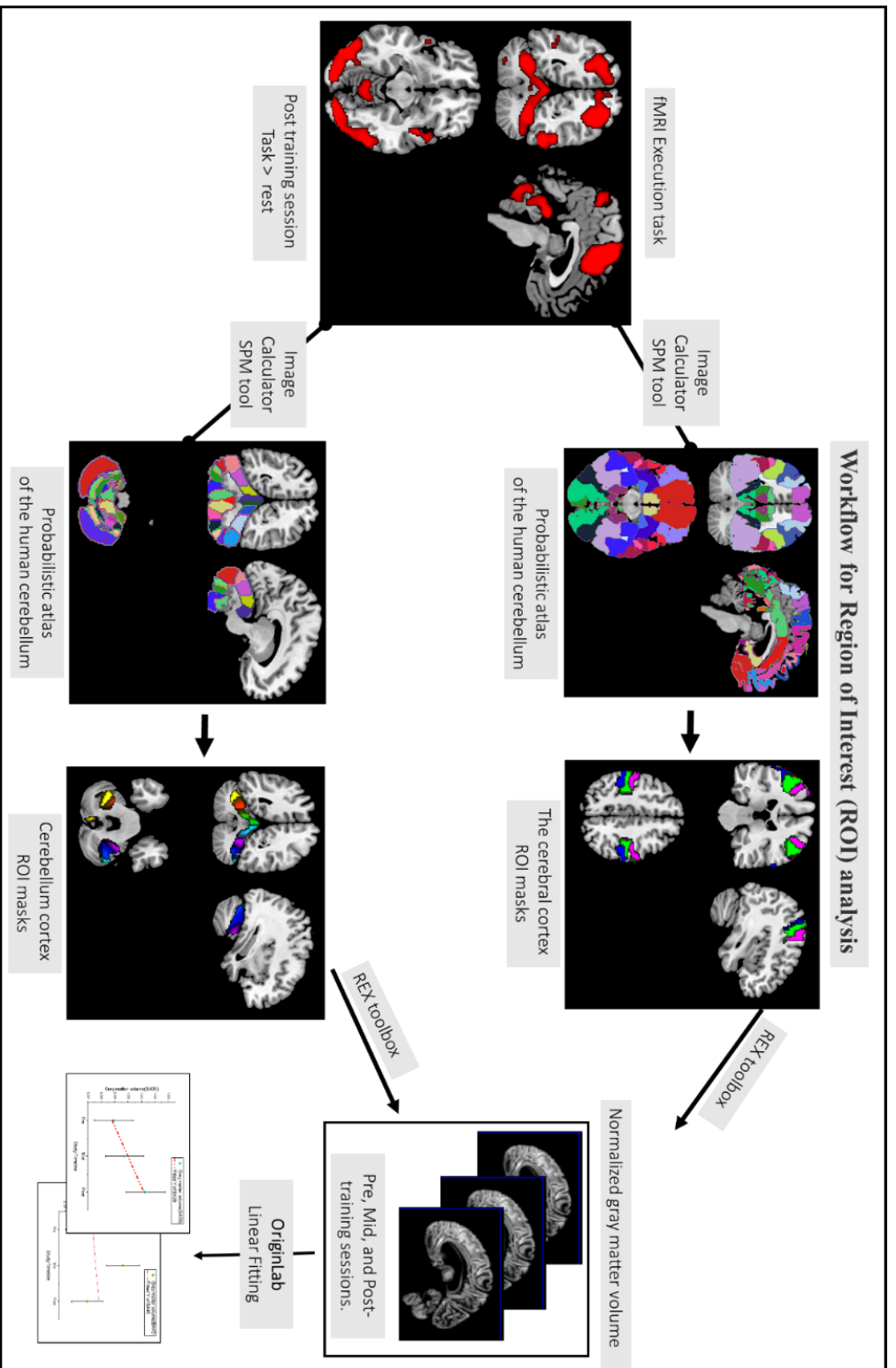
Figure 25. Workflow for the cerebral and cerebellum cortices analysis. These steps involved defining the ROI(s) using the fMRI clusters and MR Atlas of the human Cerebral and Cerebellum cortices; GMV values were extracted and a fit line was calculated using origin LAB software.

93

## IV.    Statistical data analysis

The statistical analysis of whole-brain data was conducted using SPM12 and the CAT12 extension. A paired t-test model was used to perform a post > pre contrast to identify areas of increased activation in response to drumming training. However, a comparison of changes in the cerebral and cerebellum cortices between the pre, mid and post-training time points was made using the linear regression method of analysis in Origin Lab.

# 4.3  Results

The results section has been divided into three main parts: 1) the whole-brain analysis, which discusses the GM and WM volume changes in response to the impact of a six-month drumming learning course, 2) the second part investigates the correlation between the BOLD signal changes and GMV over the three scanning sessions, and 3) the correlation analysis between the GMV changes and performance measurements.

## 4.3.1  Whole-Brain Analysis

**Gray matter volume (GMV)**

The longitudinal analysis (i.e. paired t-test) showed an increase in whole-brain GM, mostly on the right side of the brain. There were no survive voxels with a familywise error correction (FWE) applied (p <.05). Therefore, (uncorrected for multiple comparisons; cluster-forming voxel threshold: p <.001) were presented here. Specifically, following drumming training, GMV had increased in the superior and inferior parietal lobule (BA40), angular gyrus (BA39), superior temporal gyrus, postcentral gyrus (BA6), cuneus, precuneus, superior of the occipital lobe and right side of the insula. Also, there was an increase in GMV on the left side of the brain in putamen and the middle and inferior of the occipital lobule (BA18 and BA19). The clusters details summary can be found in Table 11, and see Fig. 26.
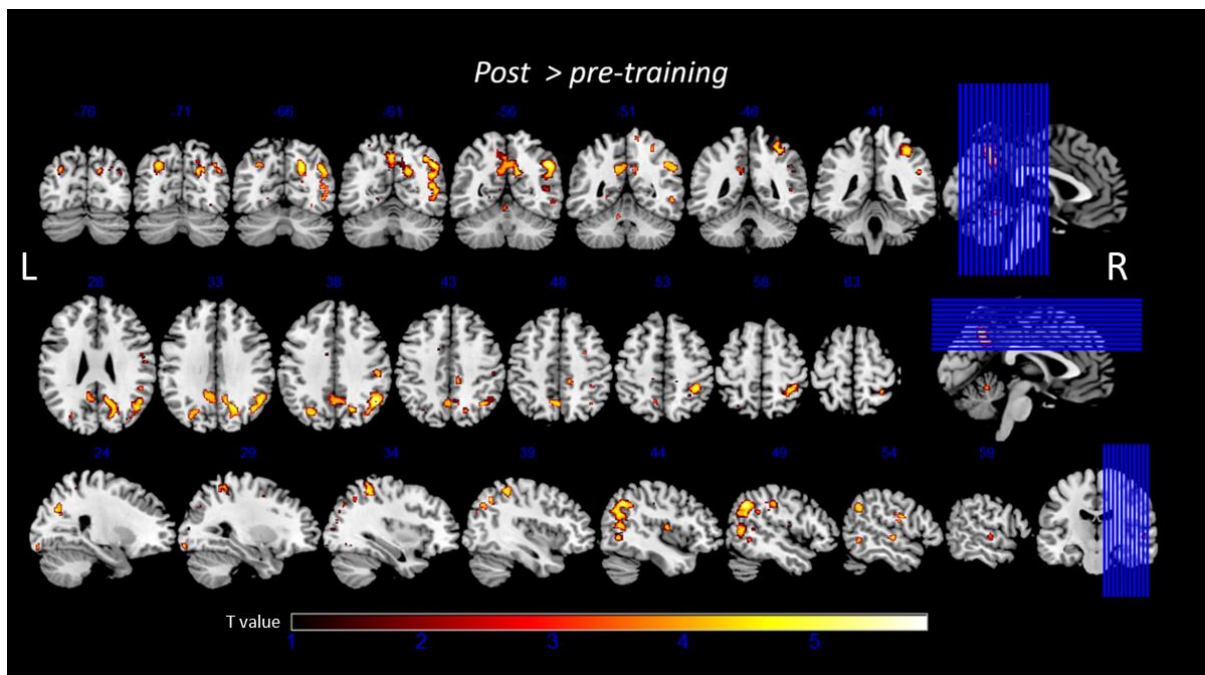
Figure 26. Areas of increased grey matter volume (GMV). GMV was quantified using voxel-based morphometry (VBM) and comparisons between the pre (baseline) and post-training sessions were made with a threshold of p < .001, uncorrected at whole-brain-level. Clusters are superimposed on a single-subject anatomical brain derived from MRIcron.

| Brain region | Hemisphere | ROI size (voxels) | Z | MNI coordinates | | | BA |
|---|---|---|---|---|---|---|---|
| | | | | x | y | z | |
| Angular gyrus | Right | 1369 | 4.78 | 48 | -58.5 | 37.5 | 39 |
| Cuneus | Right | 1342 | 4.20 | 19.5 | -66 | 34.5 | * |
| Precuneus | Right | | 3.97 | 12 | -57 | 28.5 | * |
| Occipital (sup) | Right | | 3.91 | 19.5 | -73.5 | 28.5 | * |
| Occipital (sup) | Left | 252 | 3.79 | -24 | -72 | 37.5 | * |
| Putamen | Left | 458 | 4.20 | -22.5 | 7.5 | 12 | * |
| Postcentral | Right | 61 | 4.08 | 51 | -3 | 25.5 | 6 |
| Calcarine | Right | 257 | 3.98 | 18 | -94.5 | -6 | * |
| Occipital (inf) | Right | | 3.57 | 27 | -93 | -12 | 18 |
| Occipital (inf) | Left | 79 | 3.53 | -15 | -100.5 | -7.5 | * |
| Parietal (inf) | Right | 361 | 3.93 | 36 | -42 | 52.5 | * |
| Parietal (sup) | Right | | 3.76 | 31.5 | -48 | 58.5 | * |
| Temporal (sup) | Right | 88 | 3.72 | 55.5 | -13.5 | 0 | * |
| Temporal (mid) | Right | 62 | 3.44 | 52.5 | -52.5 | -1.5 | 21 |
| Insula | Right | 57 | 3.58 | 43.5 | -9 | 10.5 | 13 |
| SupraMarginal | Right | 30 | 3.53 | 49.5 | -40.5 | 30 | 40 |
| Cingulum (mid) | Right | 62 | 3.46 | 10.5 | -34.5 | 45 | * |
| Occipital (mid) | Left | 21 | 3.44 | -30 | -82.5 | 10.5 | * |
| Vermis 4/5 (cerebellum) | Left | 19 | 4.01 | -1.5 | -55.5 | -12 | * |
| Culmen (cerebellum) | Left | 14 | 3.43 | -10.5 | -51 | -24 | * |

Table 11. GMV results: Differences in grey matter volume comparisons between the pre (baseline) and post-training sessions with a threshold of $p < 0.001$, uncorrected at whole-brain-level. For each cluster, its size in voxels and hemisphere are indicated first. For each of the subpeaks of the cluster, the cytoarchitectonic areas (based on the Xjview toolbox for SPM), followed by their MNI coordinates and t-value are reported. Abbreviations: BA: Brodmann's area, sup.: superior, inf.: inferior, mid.: middle, ant.: anterior, post.: posterior.

**White matter volume (WMV)**

The longitudinal analysis (paired t-test) showed a significant increase in WMV at the right side of paracentral lobule (BA4), left side of cuneus, and right side of extra-nuclear corpus collosum. Bilateral changes were observed in WM at the junction between cuneus, precuneus, and superior parietal lobule. The clusters details summary can be found in Table 12, and see Fig. 27.
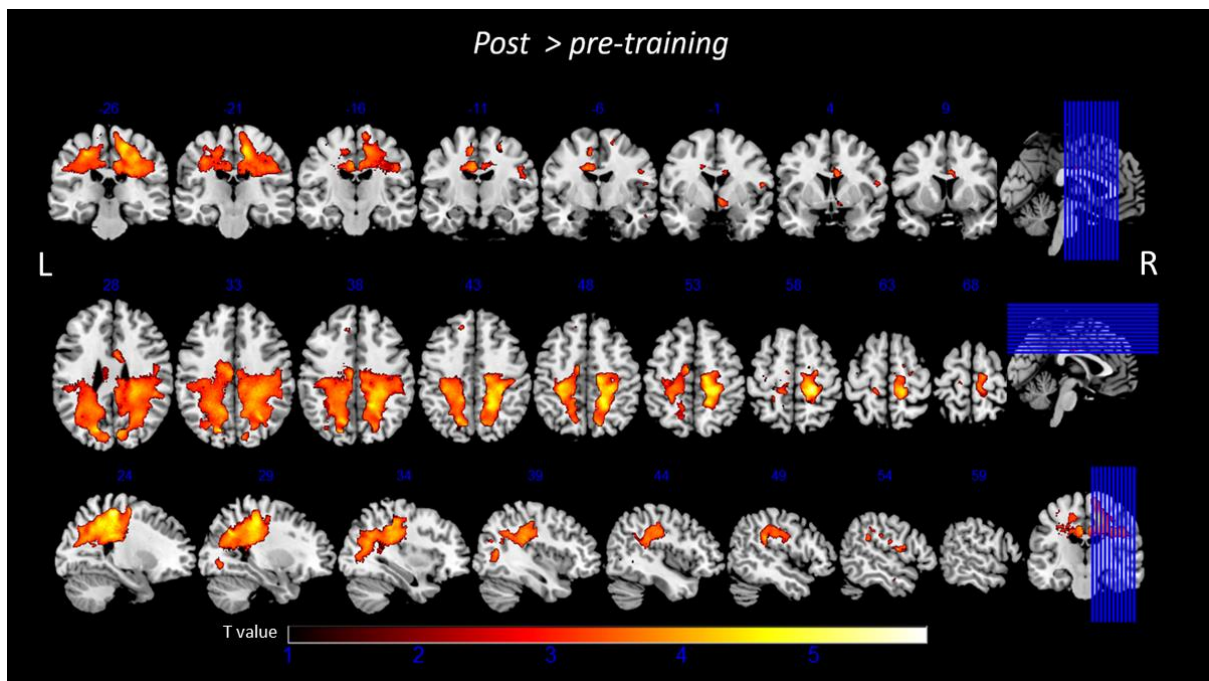


Figure 27. Areas of increased white matter volume (WMV). WMV was quantified using voxel-based morphometry (VBM) and comparisons between the pre (baseline) and post-training sessions were made with a threshold of p < .001, uncorrected at whole-brain-level. Clusters are superimposed on a single-subject anatomical brain derived from MRIcron.

| Brain region | Hemisphere | ROI size (voxels) | Z | MNI coordinates | | |
|---|---|---|---|---|---|---|
| | | | | x | y | z |
| Paracentral | Right | 31880 | 5.42 | 19.5 | -30 | 57 |
| Paracentral | Left | 15 | 3.32 | -12 | -24 | 69 |
| Cuneus | Left | | 4.94 | -15 | -75 | 33 |
| Extra-Nuclear | Right | 193 | 4.33 | 9 | 0 | 24 |
| Cingulum (ant) | Right | | 4.07 | 3 | 9 | 28.5 |
| Frontal (sup) | Left | 65 | 4.04 | -13.5 | 37.5 | 45 |
| Calcarine | Left | 103 | 3.97 | -10.5 | -46.5 | 6 |
| Precuneus | Left | | 3.19 | -7.5 | -46.5 | 13.5 |
| Rolandic_Oper | Right | 115 | 3.95 | 55.5 | -3 | 13.5 |
| Frontal (sup) | Right | 15 | 3.47 | 15 | -6 | 61.5 |

Table 12. WMV results: Differences in white matter volume comparisons between the pre (baseline) and post-training sessions were made with a threshold of p < 0.001, uncorrected at whole-brain-level. For each cluster, its size in voxels and hemisphere are indicated first. For each of the subpeaks of the cluster, the cytoarchitectonic areas (based on the Xjview toolbox for SPM), followed by their MNI coordinates and t-value are reported. Abbreviations: sup.: superior, inf.: inferior, mid.: middle, ant.: anterior, post.: posterior.

## 4.3.2 Regions of Interest analysis ROI(s)

Here, previously defined ROIs were investigated to discover whether there were any GMV changes in the regions activated by drumming execution in the fMRI task. The most interesting finding here is that both the right and left side of BA40 showed a significant increase in GMV. And, as expected, the somatosensory cortex (BA2 and BA3) showed a significant increase in GMV when using the line fitting method of analysis. Also, occipital visual areas (BA17 and BA18), as well as BA7 and BA 39 which are part of the parietal cortex in the human brain, showed a significant increase in GMV over the three scanning sessions. The ROIs details summary can be found in Table 13, and see Fig. 28 and Fig. 29.
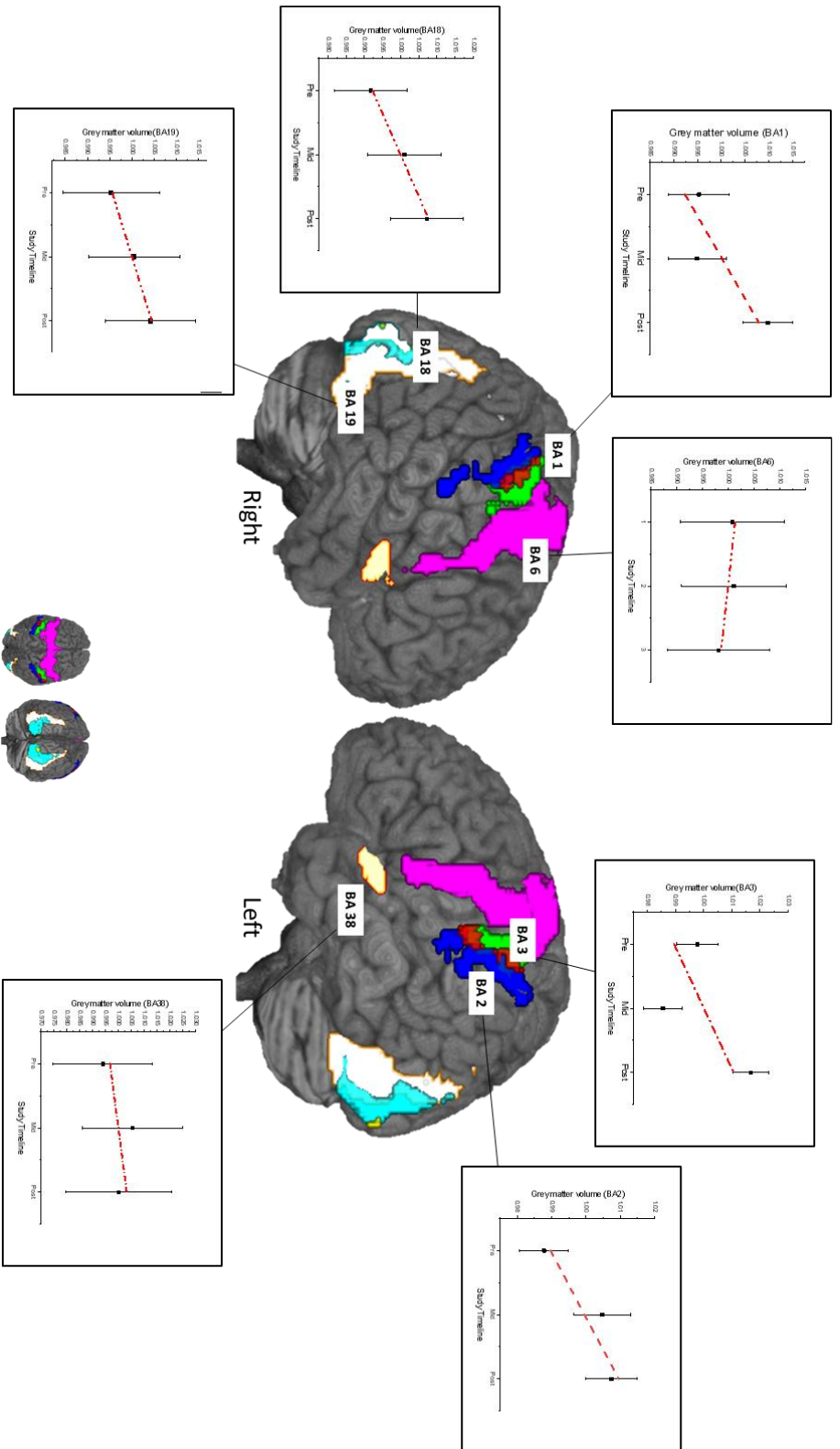
Figure 28. Brain areas in which grey matter (GM) changed with drumming training. It displays the ROIs masks within Brodmann Bilateral locations, combined with the results of the data extraction over the pre, mid and post-training sessions.
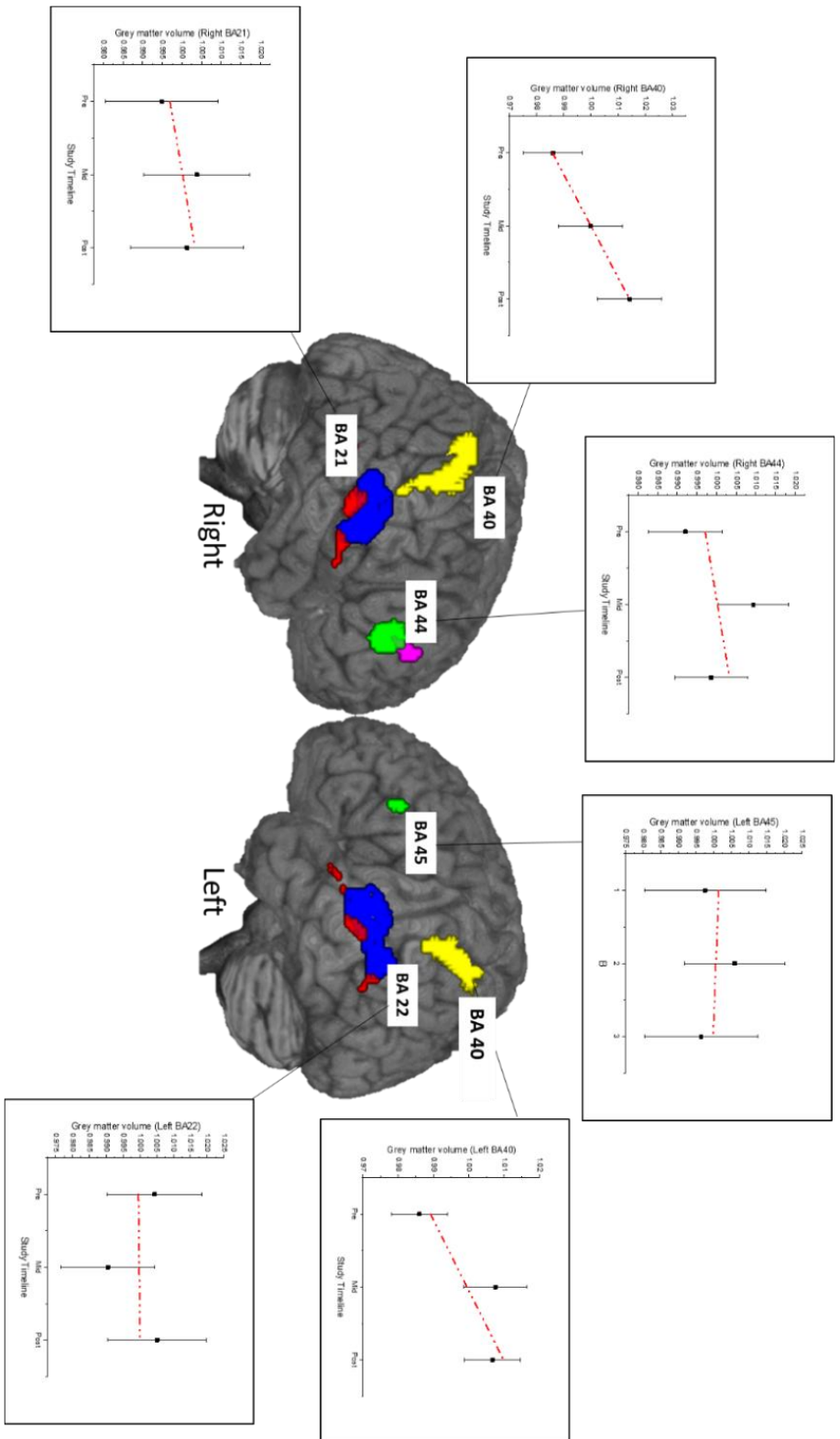
Figure 29. Brain areas in which grey matter changed with drumming training. It displays the ROIs masks within Brodmann Bilateral locations, combined with the results of the data extraction over the pre, mid and post-training sessions.

| BA | Hemisphere | ROI size (voxels) | Slope value | Slope statistics |
|---|---|---|---|---|
| 1 | Bilateral | 93 voxels | +0.00777 | p=.241 t(13)=1.22 |
| 2 | Bilateral | 1030 voxels | +0.00992 | p=.022 t(13)=2.57 |
| 3 | Bilateral | 1285 voxels | +0.01058 | p=.026 t(13)=2.51 |
| 6 | Bilateral | 1202 voxels | -0.00137 | p = .870 t(13) =-0.19 |
| 18 | Bilateral | 1984 voxels | +0.00771 | p=.016 t(13)=2.74 |
| 19 | Bilateral | 3670 voxels | +0.00442 | p=.104 t(13)=1.74 |
| 38 | Bilateral | 255 voxels | +0. 0032 | p=.209 t(13)=1.32 |
| 21 | (Right) (Left) | 95 voxels 72 voxels | +0.0027 +0.0007 | p=.317 t(13)=0.80 p=.080 t(13)=0.95 |
| 22 | (Right) (Left) | 607 voxels 549 voxels | +0.0012 +0.0003 | p=.710 t(13)=0.60 p=.010 t(13)=0.98 |
| 40 | (Right) (Left) | 1330 voxels 1027 voxels | +0.0052 +0.0037 | p=1.77 t(13)=0.33 p=1.84 t(13)=0.32 |
| 44 | (Right) (Left) | 629 voxels 338 voxels | +0.0013 +0.0006 | p=.465 t(13)=0.72 p=.193 t(13)=0.87 |
| 45 | (Right) (Left) | 439 voxels 84 voxels | +0.0013 - 0.0005 | p=.290 t(13)=0.81 p=.956 t(13)=-0.06 |

Table 13. Brodmann areas Bilateral in which grey matter changed with drumming training. The slope statistics are the results from the simple linear regression method, and the slope value is the average including all the participants, for both right and left sides of Brodmann areas in which grey matter changed with drumming training.
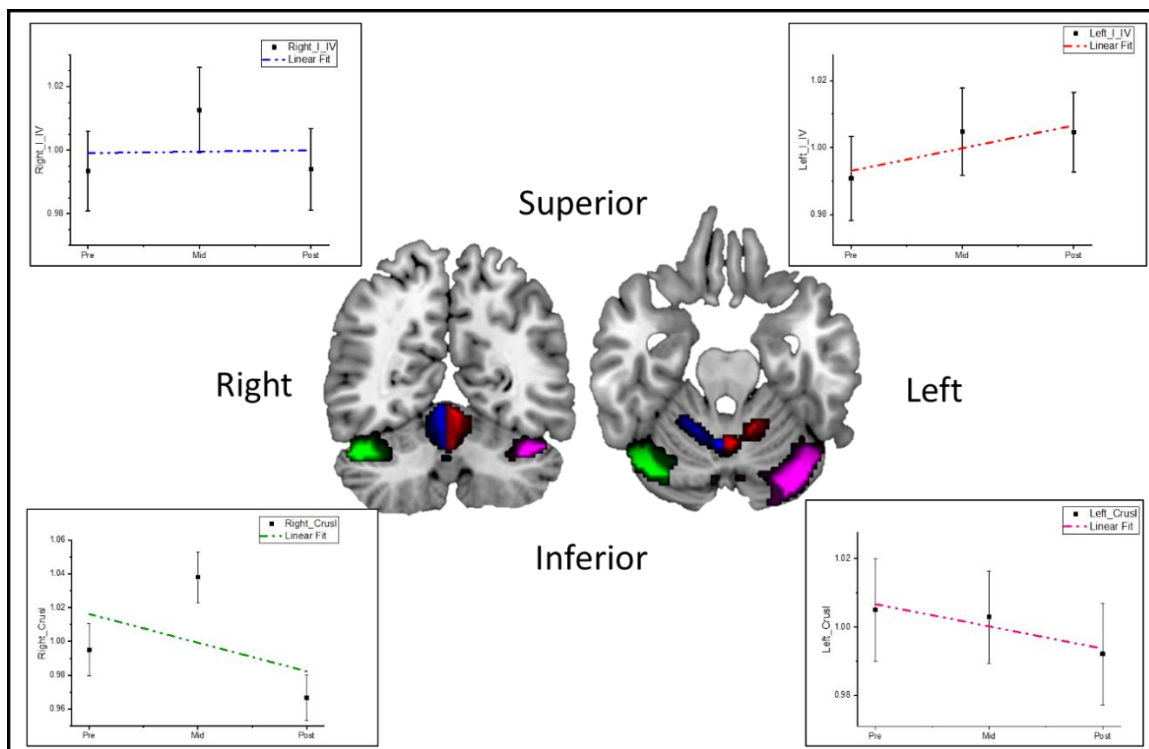
Figure 30. Grey matter volume change in the cerebullm over the six months drumming course. A) Right_I_IV, B) Left_I_IV, C) Right_CrusI, and D) Left_CrusI.

| Cerebullm regions | ROI size (voxels) | Slope value | Slope statistics |
|---|---|---|---|
| Left_I_IV | 419 voxels | +0.00676 | t(13)=1.738 p = .33 |
| Right_I_IV | 553 voxels | +0.000424 | t(13)= 0.040 p=.97 |
| Left_CrusI | 659 voxels | -0.00647 | t(13)=-2.40 p= 0.25 |
| Right_CrusI | 610 voxels | -0.00371 | t(13)=-0.52 p= .69 |

Table 14. The linear fitting method results, including the slope value and slope statistics for the cerebullum regions.

Contrary to expectation, there was no significant correlation between the degree of change in GMV and the performance measures that were used to evaluate the individual performance improvement process for participants over the drumming course.

## 4.4  Discussion

The present study addressed the effects of drumming training by scanning this non-musician cohort before, during, and after the six-month drumming learning course. An initial objective of the project was to examine the impact of learning a new complex task, such as drumming, on the adult human brain. The first goal was to determine whether GMV and WMV changes could be detected using the voxel-based morphometry (VBM) approach. The second was to identify whether there were any correlations between the induced GMV changes found in this study, and the BOLD activation response, as previously established in the fMRI study.

### 4.4.1  Whole-brain Analysis

The longitudinal analysis showed an increase in both WMV and GMV, mostly on the right side of the brain, which is in line with the findings of previous studies. A highly significant finding in neuroimaging studies (Zatorre, 1985; Samson and Zatorre, 1988; Liegeois- Chauvel et al., 1998; Samson et al., 2002) is that the right hemisphere is preferentially activated when listening to music, and that even imagining music activates areas on this side of the brain (Blood et al, 1999; Stewart et al, 2006). Thereof, our results are consistent with the right hemisphere dominance that has previously been described in the literature. Furthermore, in the present study there was an increase in the volume of the putamen on the left side of the brain. The putamen is one of the striatum's three sub-regions (caudate, putamen, and nucleus accumbens), and is most consistently implicated in the acquisition and execution of motor patterns, particularly for beat-based metrical motor coordination and perception (Bashwiner, and Bacon, 2020). Interestingly, there was also a significant increase in WMV on the right

side of the paracentral lobule (BA4). The paracentral lobule is located on the medial surface of the cerebral hemisphere, and includes parts of both the frontal and parietal lobes. It is the medial continuation of the precentral and postcentral gyri, and has motor and sensory functions related to the lower limb.

## 4.4.2 **Regions of Interest analysis ROI(s)**

To recap, here the clusters from experiment 2 (execution task) were defined as regions of interest (ROIs) and were used as masks in this chapter. This was to enable the investigation of GMV changes in the same clusters that showed an increase in BOLD activation during the fMRI execution task. Specifically, part of the primary somatosensory cortex (BA2 and BA3) showed a significant increase in GMV, as did the secondary visual area, BA18. The primary somatosensory cortex is responsible for movement organisation and voluntary hand/tongue movement (Luria, 1976; Mesulam, 2000; Brodmann and Garey, 2005; Clark et al., 2010; Trans Cranial Technologies Ltd., 2012). According to the literature, secondary visual areas are active in visual processing, working memory, and language (i.e. response to visual word forms; Trans Cranial Technologies Ltd., 2012). Furthermore, motor network areas, including ventral premotor and parietal areas, displayed GMV increases in response to drumming training. Specifically, GMV increases were found in the superior and inferior parietal lobule (BA40), as well as the angular gyrus (BA39). This finding is interesting, as it corresponds with the increased activity found in these areas in the fMRI study (previous chapter), and also with previously published study papers (Tanaka and Kirino, 2019). The supramarginal (BA40) and angular gyrus (BA39) are both located in the posterior part of the inferior parietal lobule (IPL), separated by the intraparietal sulcus. The angular gyrus (AG) is involved in various cognitive processes, including attention, spatial cognition, conceptual representation, semantic processing, language, reasoning, social cognition, and episodic memory (Vincent et al., 2006; Binder et al., 2009; Seghier et al., 2010; Seghier & Price, 2012; Bonner et al., 2013; Seghier, 2013; Price et al., 2015). Most of these cognitive functions are required when playing

a musical instrument, and so the AG likely plays a role in musical performance. The superior and middle temporal gyrus (BA22 and BA21), are included amongst brain areas involved in auditory data processing. The primary auditory cortex, located in Heschl's gyrus (HG), processes basic features of sound (Warrier et al., 2009; Brewer & Barton, 2016).

Finally, GMV changes also occurred in parts of the cerebellum (i.e. Right ,and Left_I_IV, Right and Left_CrusI). Right and left_I_IV showed an increase in GMV over the six-months drumming course, as shown in Fig. 30 and Table 14. Whereas, Right, and Left_CrusI presented a decrease in GMV with training. It is also interesting to note that the most prominent GMV changes could be seen at the mid-training phase, which may be because the main learning process had already occurred. Thereof, the functional networks which had developed may have already been sufficient for the new task, and so GMV could afford to begin returning to its original size. The major challenge for future research is to identify and compute the behavioural consequences and cellular mechanisms underlying training-induced neuroanatomic plasticity.

## 4.5 Limitation

The main limitation of this chapter is that the volumetric analysis assumes major changes to brain structure. This seems an unreasonable assumption for tasks where participants skills that – while being novel – complement an extensive set of existing skills. Drumming, for example, requires precise and well-synchronised motor action, but these skills are inherent in many other, everyday motor tasks (De La Rue et al., 2013). It may therefore be argued that large scale structural change may not be expected in tasks, even as extensive as the six-month drumming training that our participants underwent. Other techniques, for example, the DTI analysis discussed in the next chapter may offer more appropriate analysis techniques..

## 4.6 Conclusion

The presented research contributes to the understanding of the effect of long-term drumming training on the non-musician group. Long-term music training has been shown to affect several different cognitive and perceptual abilities (e.g., Petrini et al., 2009a, b, 2010a; Lee and Noppeney, 2011; Lee and Noppeney, 2014). We confirmed the results of previous work which demonstrated that skill learning could lead to increased GMV and WMV in some brain regions. Taken together, our results provide a detailed picture of changes in the brain related to musical training-induced brain plasticity, which might provide valuable information for further exploration of underlying neural mechanisms. This has potential implications for music therapy, and clinical practise.

# Chapter 5    Drumming Induces Plasticity in Gray and White Matter microstructural: Diffusion Tensor Imaging (DTI) Study.

## 5.1 Introduction

*Learning induced changes*

Human brain imaging studies show that the white matter (WM) of the brain continues maturation during later childhood and adolescence in response to both genetics and environmental conditions (Catherine and Sean.,2018; Stiles and Jernigan, 2010, Jancke 2009b; Schlaug 2001; Wan and Schlaug 2010; Schlaug 2015). WM is mainly composed of long-range myelinated axonal cells that connect cortical portions of the brain. The majority of the myelination process occurs during the first two years of life. This process then continues through childhood, adolescence and adulthood, reaching peak myelination in the second or third decade of life (Yakovlev and Lecours, 1967), and undergoing refinements throughout the lifespan thereafter. The primary function of myelination is to speed conduction of the electric impulse along an axon, allowing the action potential to travel long distances faster (reviewed in Freeman et al., 2016; Hartline and Colman, 2007).

It is known that genetics and environmental factors are not only responsible for WM plasticity, but similarly, plastic changes can be induced by learning or intense activity (Fields, 2008; Zatorre et al., 2012). Changes in WM have previously been observed following both short (minutes/hours) and long (weeks/years) episodes of training in activities, such as juggling (Scholz et al., 2009), playing music (Chen et al., 2012), training in specific laboratory-controlled tasks involving the whole body (Taubert et al., 2010).

Current studies of cortical thickness reveal that grey matter (GM) microstructures are modified during development and are sensitive to training. For example, in 2012 Yaniv Sagi reported significant microstructural changes (i.e., increased FA value) in the hippocampus and parahippocampus after only 2 hours of learning a spatial navigation task. As another example, Hofstetter et al. (2013) reported immediate decreases in mean diffusivity (MD) in the fornix, a WM pathway associated with the hippocampus, after just 2 hours of training in

a car racing game that required navigational skills. This observation was also found by Colom et al. (2012), who reported microstructural changes in the hippocampal region (i.e., that there was an increase in axial diffusivity (AD), after just 16 hours of playing a videogame). Furthermore, Takeuchi et al. (2010) found a significant increase of FA in the region adjacent to the intraparietal sulcus after 2 months of repeating a verbal and visuo-spatial training task. In addition, Landi et al. (2011) reported increased FA in the primary motor cortex after 5 hours of a visuo-motor adaptation task. Since then, Piervincenzi et al. (2017) identified an FA increase in tracts related to sensorimotor and cognitive functions following 6 weeks of daily Quadrato Motor Training.

This highlights a challenge in interpreting measures, in that the timescale of structural remodelling that accompanies functional neuroplasticity is largely unknown. Although structural remodelling of human brain tissue is known to occur following long-term (weeks) acquisition of a new skill, little is known as to what happens structurally when the brain needs to adopt new sequences of procedural rules, or memorise a cascade of events, within minutes or hours. It still remains unclear whether training-induced changes in DTI parameters could occur over longer periods, such as 6 or 12 months, or after a very short period of time such as 2 hours.

*Imaging*

Our understanding of training induced changes to grey matter volume (GMV) and white matter volume (WMV) draw on a range of different neuroimaging techniques, such as diffusion magnetic resonance imaging (dMRI). Its non-invasive techniques offer powerful approaches for characterising human WM microstructure in vivo (Alexander et al., 2017; Assaf &Pasternak, 2008; Basser et al., 1994; Basser and Pierpaoli, 1996), as well as changes in WM function in response to experience via diffusion analysis. Diffusion tensor imaging (DTI) is an extension of DWI and is sensitive to the diffusion of water molecules, the direction of which is dependent upon the presence or absence of barriers in neural tissue. If no barriers

are present, such as in the cerebrospinal fluid, water diffuses uniformly in all directions (i.e., isotropic diffusion). By contrast, if water movement is restricted in any direction, diffusion tends to follow the long axis of those barriers (i.e., anisotropic diffusion). Water diffusion in a voxel can be modeled as a 3D ellipsoid with a $3 \times 3$ matrix, multiple summary parameters can be obtained from the diffusion tensor represented by an ellipsoid see Fig.5. page 28 in the introduction chapter. For instance, the ellipsoid volume describes the mean diffusivity (MD), which is a measure of the overall mean displacement of water molecules, and ellipsoid eccentricity describes fractional anisotropy (FA), which characterizes the fraction of molecular displacements that can be attributed to the orientation of the axon fiber. FA values vary between 0 for (isotropic), and 1 (anisotropy) diffusion.

Neuroimaging studies have consistently identified FA reductions, and MD increases, with ageing. In contrast, FA has been found to increase, whilst MD decreases, in response to learning (Särkämö et al.,2018). FA measures the directionality of water diffusion and is a measure of the coherence of aligned fibres. The higher the FA value, the more aligned fibres are in a specific direction (Lauren J. O'Donnell, 2011). Higher FA values reflect better WM integrity as a result of greater intra-voxel coherence of fibre orientation, axon density and diameter, and/or myelination (Beaulieu et al., 1996; Sen and Basser, 2005; Caminiti et al., 2013). Reduced FA values cooccur with ageing, and also with psychiatric and neurological disorders (Taubert et al., 2012; Barysheva et al., 2013; Mayo et al., 2017). Axial diffusivity (AD) is a measure of water diffusion along the main direction of a tract and a measure of axonal integrity. Any alterations in AD have been associated with changes in axon morphology (Kumar et al., 2012), and lower AD values have generally been related to decrements of axonal density or calibre (Mac Donald et al., 2007). Furthermore, radial diffusivity (RD) is a measure of water diffusion perpendicular to the main direction of a tract or an indicator of myelination. RD has generally been associated with myelination (Song et al., 2002, 2005), whereby RD decrease has been thought to reflect increased myelination (Keller and Just, 2009; Bennett et al., 2010). The mean diffusivity (MD) and fractional

anisotropy (FA) are widely used as surrogate measures of microstructural properties of WM change during normal brain development and ageing, or during the onset and progression of neurological disorders and learning.

The main goal of this project was to quantify functional and structural brain plasticity in response to learning a new motor task, which was in this case drumming. The main purpose of this chapter is to map out the time course of alterations in different diffusion parameters (i.e. fractional anisotropy (FA), mean diffusivity (MD), axial diffusivity (AD), and radial diffusivity (RD) involved in musical training over a relatively long period of time (6 months). To examine these changes, diffusion imaging was used to capture WM and GM microstructure plasticity induced by the drumming training. Playing music has generally been associated with greater GMV and cortical thickness in auditory cortices (see Penhune, 2019; Schlaug, 2015, for reviews), as well as WMV increases, especially in the corpus callosum (CC). The corpus callosum (CC) is the largest commissural fibre in the brain and contains about 200 million axons (Aboitiz et al. 1992). It connects the left and right hemispheres and is responsible for most communication between these two sides of the brain. It plays an important role in the execution of complex bimanual motor sequences, such as those involved in musical training. The structure of the CC has been shown to adapt differently depending upon the specifics of the musical training. For example, the size of the anterior corpus callosum was found to be greater in musicians who had begun musical training before the age of 7y (Schlaug et al., 1995a), and this finding has been replicated by different research groups using different methodological approaches (Hyde et al., 2009; Lee et al., 2003; Oztürk et al., 2002). Furthermore, the mid-sagittal CC has been repeatedly reported to be larger in musicians compared to non-musicians (Oztürk et al., 2002; Lee et al., 2003; Steele et al., 2013).

**Present study**

The main purpose of this chapter is to map or model the time course of diffusion parameters (i.e., fractional anisotropy (FA), mean diffusivity (MD), axial diffusivity (AD), and radial diffusivity (RD)) changes in GM and WM microstructure in the brain regions involved in musical training over a 6 months period. The brain regions of interest in this chapter were chosen because they have previously been shown to be involved in musical performance (see Table 2 in the introduction chapter). A line fitting method was used to establish the trajectory of changes in diffusion parameters with learning in the superior and middle temporal gyrus, superior marginal gyrus, inferior frontal gyrus, and precentral gyrus.

It is hypothesised that GM and WM will undergo microstructural changes, and that FA will increase, whereas MD, AD and RD will decrease over the drumming training course. In particular, response modulations in at least one of the five sub regions of the corpus callosum are expected to be found.

## 5.2 Methods

### 5.2.1 Subjects

Fifteen university staff and students (mean age: 38.6y, range: 20y – 57y, 9 men, 6 women) with no prior drumming experience were recruited for this study. More information regarding participants can be found in section chapter 2 , section 2.2, page 33).

### 5.2.2 **Study design**

Participants took part in a 45-minute individual drumming lesson each week for 20 weeks. Each drumming lesson was delivered by a professional drumming tutor and the complexity of drumming training was increased every week in line with participants' improvement (for more information, see the drumming task chapter). All participants had access to a drum-kit and were encouraged to practise for at least 30 minutes daily. All participants were scanned twice before their first one-to-one drumming lesson to provide baseline measures. The next diffusion scan was performed on the day that followed the first learning session. After that, participants had multiple regular scans (e.g. on day 3 – day 7 and day 14, etc., see Fig. 31), and they had weekly learning sessions with the tutor until the course was completed.
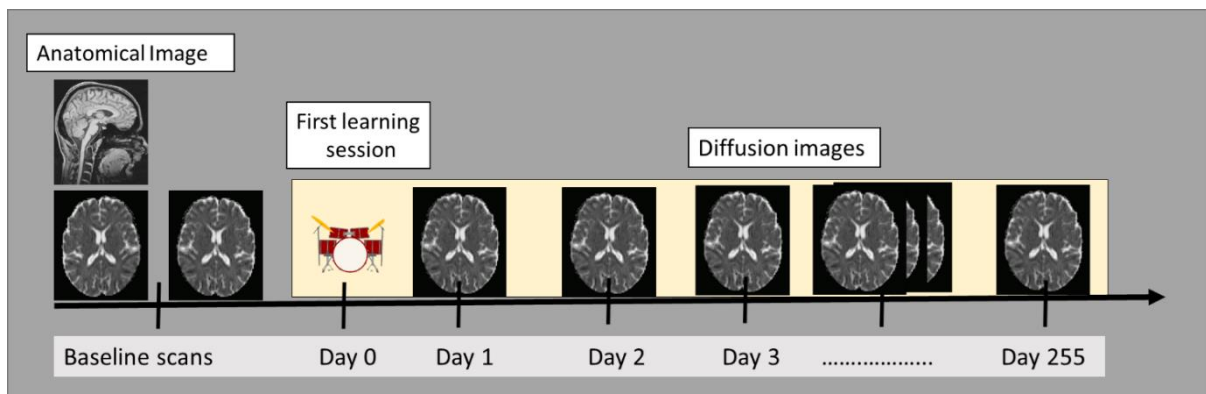


Figure 31. Timeline of the study. Illustration of the different time points of DWI scanning sessions.

### 5.2.3 **Data acquisition**

**Anatomical Image**

First, for each participant a T1-weighted high-resolution anatomical image (axial slices perpendicular to AC-PC line) was acquired using a 3T Siemens Trio MRI system with an eight-channel receiver head coil. Using an axial acquisition orientation, aligned with the AC-PC axis, the whole brain volume was covered with an ascending order of slices. Each acquired volume consisted of 176 slices, with a slice thickness of 1mm and no gap between slices. A repetition time: 2040ms; echo time: 5.57ms; flip angle: 8°; was also used. The field of view (FOV) was 256mm$^2$ and an acquisition time of 7:38 minutes was also applied.

**Diffusion-Weighted Images**

A diffusion-weighted image was acquired using a spin-echo EPI sequence consisting of 60 diffusion-weighted volumes each (b: 1000, and 2000s/mm$^2$). In addition, five volumes with no diffusion weighting (b: 0 s/mm$^2$) were acquired for motion correction. The other parameters were repetition time: 5700 ms; echo time: 104 ms; flip angle: 90°; slices matrix size: 222 × 222; and resolution: 3.1×3.1×3.1 mm (direction of acquisition: AP); along 60 directions. Total acquisition time of the diffusion-weighted images was 12 minutes.

5.2.4 **Data analysis**

     **I.    Pre-processing**

**Anatomical Image**

The anatomical images were processed with the FreeSurfer software (http://surfer.nmr.mgh.harvard.edu/, version 6.0) using the "recon-all" processing stream with default parameters to create a 3-dimensional cortical surface model for each individual subject. The automatic reconstruction steps included skull stripping, grey and white matter segmentation, and reconstruction. Hemispheres were separated and the cerebellum and brain stem were excluded. The results of the segmentation procedure were controlled slice by slice. For each individual image, the atlas-based automatic parcellation was applied within the individual T1 native space.

The surface model was anatomically parcellated using the Desikan-Killiany atlas and standard FreeSurfer tools (Fischl et al., 2004; Desikan et al., 2006). Subcortical structures were similarly identified by volume segmentation (Fischl et al., 2002). In the automatic subcortical segmentation, each voxel in the normalised brain volume is assigned one of about 37 labels, including 11 bilateral structures (accumbens area, amygdala, caudate, hippocampus, pallidum, putamen, thalamus, cerebral white matter, cerebral cortex, cerebellum white matter, cerebellum cortex) and cerebrospinal fluid. The corpus callosum (CC) was automatically segmented into five sub regions, from genu to splenium, those being the anterior ($CC_A$), mid-anterior ($CC_{MA}$), central ($CC_C$), mid-posterior ($CC_{MP}$), and posterior ($CC_P$) sections. The technical details of these procedures have previously been described in scientific literature (Fischl B, et al., 2000 and Fischl B, et al., 2002). This algorithm is implemented in FreeSurfer and can be used after tissue segmentation.

**Diffusion-Weighted Images**

Pre-processing of diffusion-weighted images included a correction for eddy currents and head motion, as well as a volume-wise correction of the gradient direction using the rotation parameters from head motion. Secondly, the Brain Extraction Tool (BET) performed a brain extraction, with non-brain voxels excluded. Thirdly, the DTIFIT command of FMRIB Diffusion Toolbox (FDT) was used to fit the corrected diffusion-weighted maps at each voxel. The output of DTIFIT processing was the tensor-fitted voxel-wise maps (e.g. fractional anisotropy (FA), mean diffusivity (MD), radial diffusivity (RD), and axial diffusivity (AD)), and the scalar magnitudes of tensors (i.e. three eigenvalues, the principal (L1), secondary (L2), and tertiary (L3) were produced.

## II.    Co-registration and extraction

Before any analyses can be carried out, the different sessions need to be registered to each other. This step is to enable the co-registration of each of the four diffusion parameters (e.g. FA, MD, RD, and AD) to T1 (Anatomical Image) in the native space for each subject. Then, the data extraction step, including all the diffusion parameters maps, could be performed as shown in Fig. 32.

The co-registration of each of the four diffusion parameters to T1 (Anatomical Image) is a two-stage process. 1) The diffusion map with $b = 0$ was linearly registered (six degrees of freedom) to the individuals' anatomical space of reconstruction, since the study is within-subjects using the linear registration tool FLIRT (FMRIB's Linear Image Registration Tool from FSL (Centre of Functional Magnetic Resonance Imaging of the Brain, University of Oxford, Oxford, UK), (Jenkinson, M. et al., 2002 & 2001; Greve, D.N. & Fischl, B. 2009) see Fig.32.  The transformation matrix was applied to transform all four parameters, as shown in Figure 32. The second step in this stage is data extraction after the DTI maps have been transferred into the anatomical space. Diffusion parameters values were extracted from each

brain region (i.e. the five sub-regions of corpus callosum) using an in-house, purpose-written script for MATLAB.
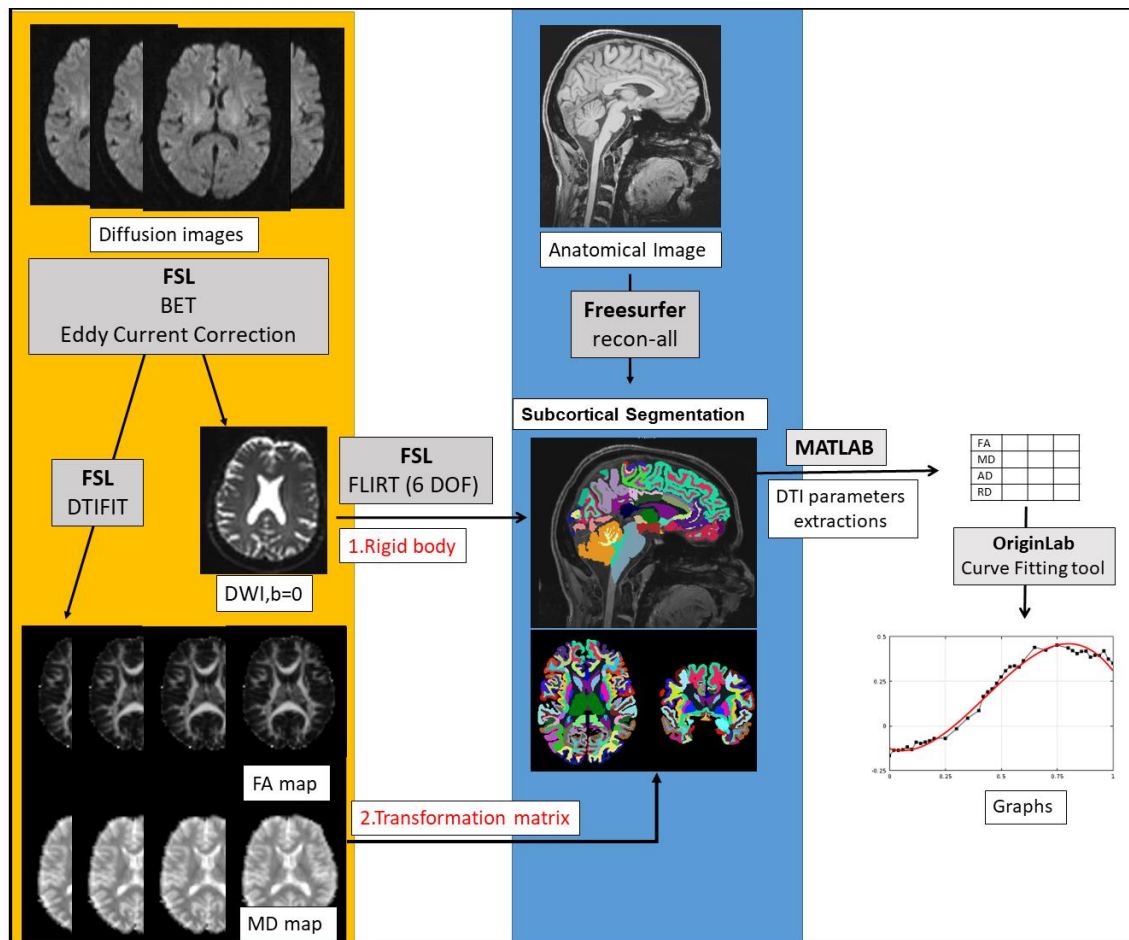


Figure 32. Illustration of the DTI and T1 processing pipeline for each subject, which included multiple steps (as indicated by the black arrows) and made use of several different software packages (shown in grey). After the DTI pre-processing, which included the motion correcting and skull-stripped stages, DTIFIT was performed and DTI maps were transformed into T1 native space using the FLIRT tool. Then, DTI parameters were extracted from the subcortical regions using MATLAB. Lastly, the curve was fitted by using Origin Lab.

## The impact of in-scanner head motion

Multiple studies have shown that artifacts caused by head motion, as well as magnetic susceptibility, can negatively impact diffusion model fitting and subsequent microstructural measures (for more, see Baum et al., 2018). For this reason, and to exclude any changes in measurements due to the participants' head motions in the scanner, the "total head movement" (the most common measure of average motion between all successive volumes) was calculated at each scanning session. Basically, this file is a summary of the total head movement in each volume of the DWI and is created by calculating the displacement of each voxel and then averaging the squares of those displacements across all intracerebral voxels (as determined by brain mask), before finally taking the square root of that calculation. This file has two columns, in which the first contains the how much the subject moves relative to the first volume, and the second column the how much the subject move relative to the previous volume for each scanning session. Then, the mean value of the second column was calculated for each session. Following this, a correlation analysis was conducted to investigate whether there was any relationship between FA values changes and the average value of total head movement using three separate analyses.

Firstly, a simple correlation analysis was used to determine whether a correlation between the head motion parameters and FA values existed for each of the five CC regions at each scanning session. The idea behind this was that 'if motion distorts the results', then it would be expected to do so in the same way for all data. The simple correlation test, covering all sessions, found no significant correlation between FA values scores and head movement parameters scores ($r_{(14)}$ =-0.00123, p = .95). Secondly, a paired T-test was used to establish whether the difference in motion estimates values between the two sessions (baseline and day 1) might explain this odd jump in FA data. The differences between the two sessions for motion and FA for each participant were calculated. No significant difference was found between these two sessions ($t_{(14)}$ = -0.51, p = 0.61).

Thirdly, a simple correlation analysis was used to assess if the difference in values of the motion estimates and FA changes for day0 and day1 were correlated. No significant correlation was found between the FA and head movements in the five sub-regions of the CC for day0 and day1 data. The results of the correlational analysis are shown in Table 15.

| regions of corpus callosum | Slope Value | R-Square |
|---|---|---|
| CC$_P$ | -0.04344 | -0.03377 |
| CC$_{MP}$ | 0.04755 | -0.06019 |
| CC$_C$ | 0.05134 | -0.05517 |
| CC$_{MA}$ | 0.05613 | -0.04955 |
| CC$_A$ | -0.04084 | -0.05352 |

Table 15. Results of regression analysis examining the changing of FA values and the movement measurement for each visit.

Taken together, these results show that there is no association between head motion, either overall or between the session's day0 and day1, and the changes in FA and MD data. Therefore, these unexpected FA & MD data value changes appear to be unaffected by head movement measurement values.

## The impact of in-scanner Headphones artefact

In this project, there were a few DWI sessions where the participants were required to wear headphones during DWI scanning. In order to investigate if there was any impact of the headphones on the DWI parameters measures, the paired t-test was applied to compare parameter values between DWI sessions with headphones and the sessions without headphones. The p value was significant (p=.039), and so the DWI sessions with the headphones were excluded from the analysis. The individual timeline and scanning sessions are labelled in Table 23 in the appendix.

### III.  Normalisation and Grouping the data

The data was normalised due to the fact that there is considerable variation in raw diffusivity measures between individuals as shown in Fig.33 and Fig.34. We therefore express changes proportional to the individual diffusion average data over all scans, as shown in Figure 32. The average over all scans, rather than a single baseline scan, was chosen because of the apparent variability of the DIT data between scans. So, to ensure that noise in a single scan does not unduly affect all subsequent measures, the diffusion data were normalised to the mean value for each of the brain regions.
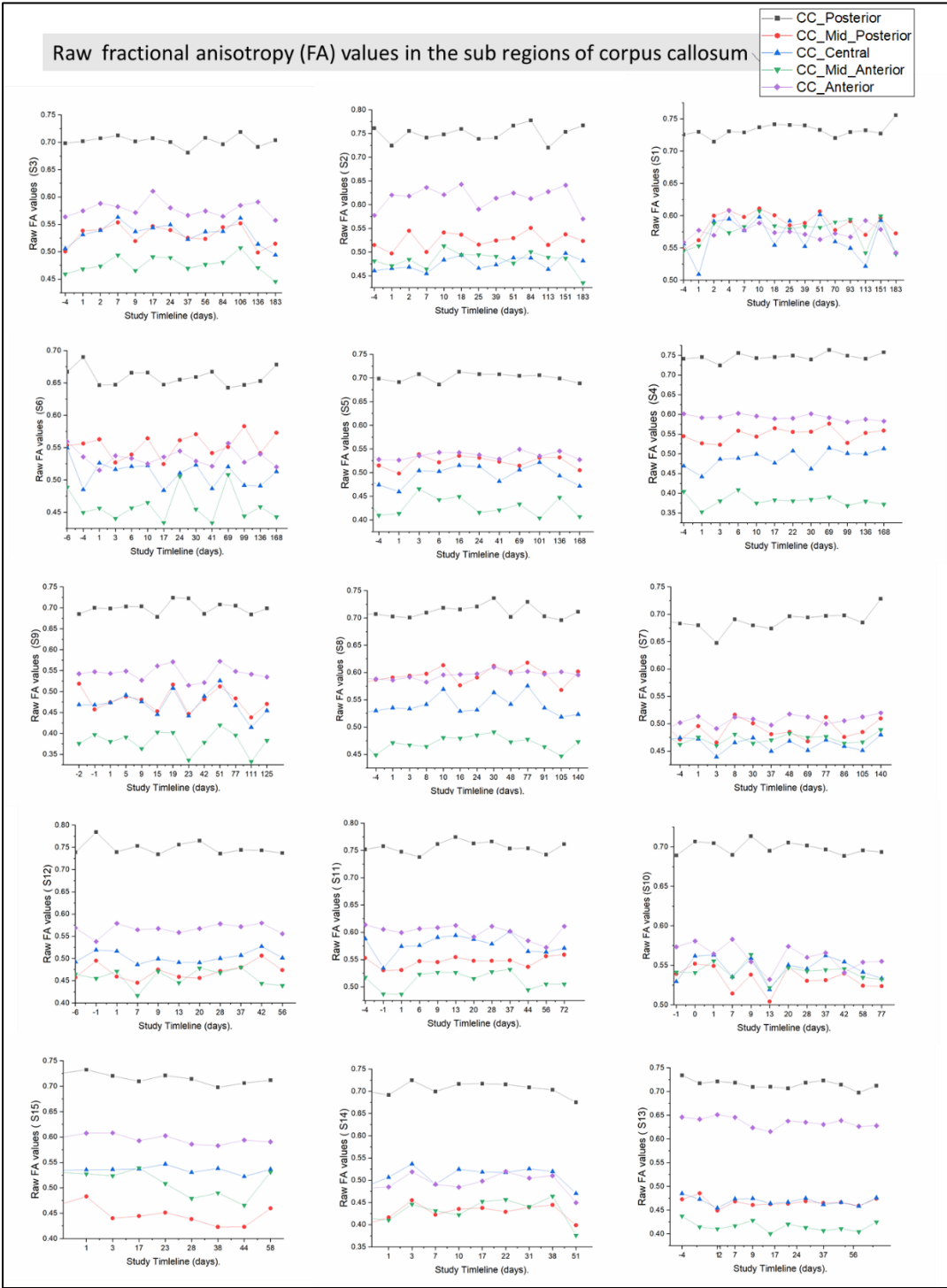
Figure 33 . Shows how the original (FA) values of the five regions of CC vary over the study timeline.
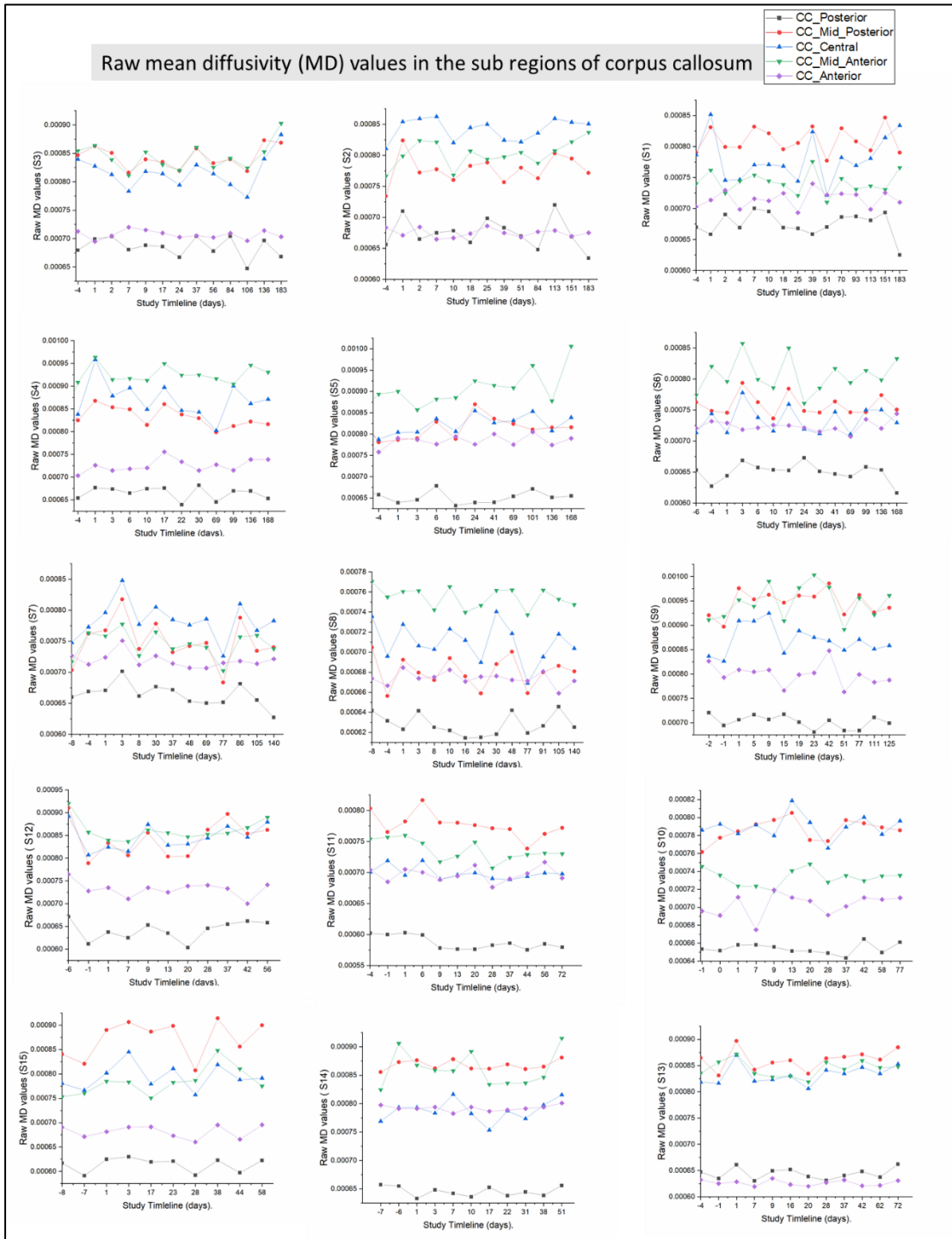
Figure 34. Shows how the original (MD) values of the five regions of CC vary over the study timeline incilding all the particpants.

Due to the fact that it was not possible to scan all participants after exactly the same duration following training onset, the scans were arranged to become less frequent over time, as described in the introduction section. For presentation and curve fitting, the data for all participants was binned into time slots that followed a log2 duration pattern, using the following equation:

$$b = 0; \text{ for all } d < 0$$

$$b = \log_2(d)$$

$$b = f(d) = \begin{cases} 0, & x < 0 \\ \lfloor log_2(\text{d}) \rfloor, & x \geq 0 \end{cases}$$

$$b = f(d) = \begin{cases} 1, & x < 0 \\ \lfloor log_2(\text{d}) \rfloor + 1, & x \geq 0 \end{cases}$$

Where $b$ = the corresponding bins data and $d$ = the interval ranges of scanning days. This ensured that all bins contained comparable numbers of measurements.

| Bins corresponds | Interval range | Scanning sessions |
|---|---|---|
| 0 | Pre-training days | Included the two baseline sessions. |
| 1 | Day 1 | Included data recorded the day after the first learning session only. |
| 2 | Day 3 | Included data recorded on either day 2 or 3 after the first learning session. |
| 3 | Day 7 | Included data recorded between day 4 and day 7. |
| 4 | Day 15 | Included data recorded between day 8 and day 15. |
| 5 | Day 31 | Included data recorded between day 16 and day 31. |
| 6 | Day 63 | Included data recorded between day 32 and day 63. |
| 7 | Day 127 | Included data recorded between day 64 and day 127. |
| 8 | Day 255 | Included data recorded between day 128 and day 255. |

Table 16.Time periods used in the analysis including the corresponding bins data and the ranges of scanning days.

## IV.   Model Fitting

A linear fitting method was applied to create the model using OriginLab version 2018b (https://www.originlab.com/2018b).

## 5.3  Results

The main purpose of this chapter was to map the diffusion parameters changes in the brain regions involved in musical training over the 6-months training period. The second aim was to model the diffusion parameters changes within the five sub-regions of the corpus callosum. A linear fitting method was used to illustrate the trajectory of changes in diffusion parameters

values in the sub regions of the corpus callosum, superior and middle temporal gyrus, superior marginal gyrus, (pars triangularis: BA44) part of IFG, and the primary motor area located in precentral gyrus, in response to drumming learning.

# I.        Linear fitting five regions of corpus callosum

The most surprising and unexpected aspect of the corpus callosum data output was that there was an initial decrease, not increase, in fractional anisotropy data, whereas there was an initial increase, not decrease, in mean and axial diffusivity data, as shown in Fig.35.

One possible explanation for these unexpected results may be the influence of head motion during the image acquisition under the MRI scanner. Therefore, to establish whether head movement parameters were accountable for creating this early drop in the FA data, multiple statistical tests were conducted, as previously covered in the method section. The final results showed that there was no association between head motion, either overall or between the session's day0 and day1, and the changes in FA and MD data. Therefore, these unexpected FA and MD data value changes appear to have been unaffected by head movement measurement values.
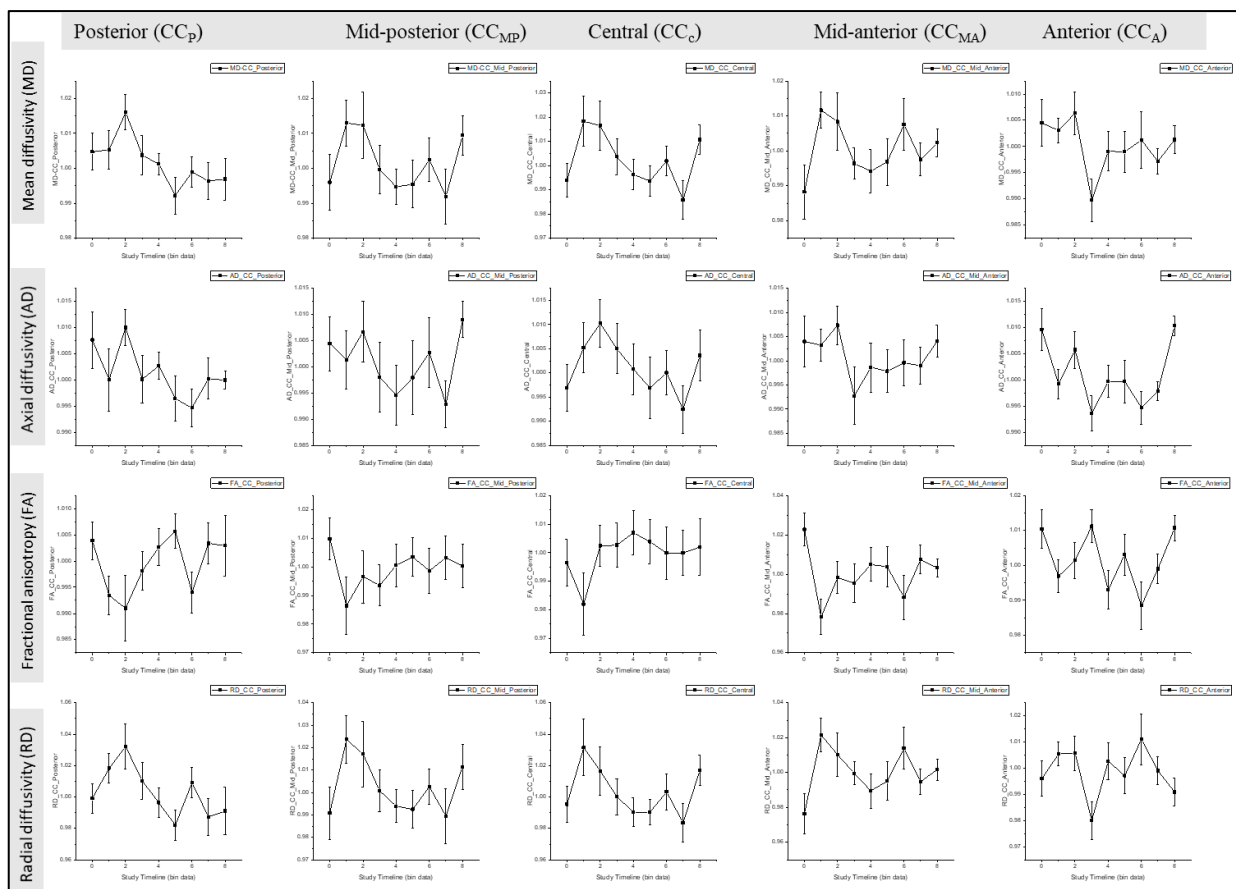
Figure 35. Presents an overview of the normalised diffusion changing within five sub regions of CC. The rows represent the diffusion parameters, and the columns show the five sub regions of CC.

The second possible explanation for this data distortion was the potential effect of wearing headphones, as there were some DWI scans which combined the task-based functional MRI in the same session. In these instances, DTI scans were acquired following the fMRI sequence whilst the participants were still wearing headphones inside the MRI scanner. A paired t-test was used to determine whether the mean difference in FA values in the CC between the day0 and day1 sessions with headphones, and without headphones, was significant. Unfortunately, there was a significant difference between FA values in the two conditions (with headphones or without headphones), as mentioned in the method section. Therefore, the headphone sessions were excluded from analysis in this project. However, even though the diffusion

126

sessions when wearing headphones were excluded, the initial negative spike (steep drop) appearing in FA data over the five sub regions of CC remained. Consequently, these results need to be interpreted with caution. Therefore, the first bins data was excluded from the curve fitting, as shown in Fig.36.
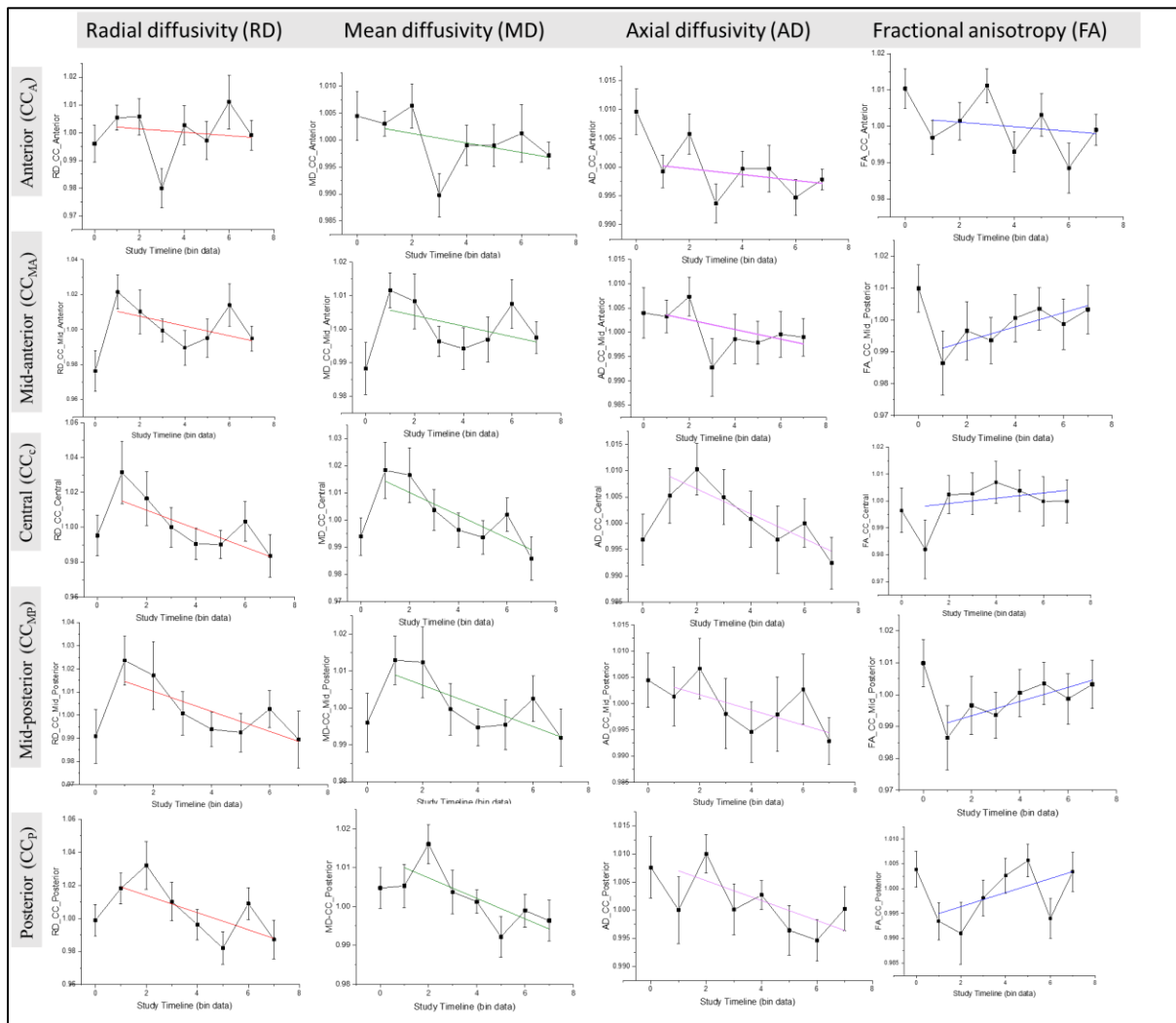


Figure 36. Presents an overview of the line fitting to average changes of the diffusion markers within five sub regions of CC. The curve fitting of MD (green), RD (red), AD (purple) and FA (blue) shows value changes in the five sub regions of CC.

The most interesting finding was that the mean, radial, and axial diffusivity values decreased, whereas fractional anisotropy values changed in the reverse direction and increased over the learning course. The results showed a trend for the long-term increase of FA and decrease of MD measurements in the splenium, the body of the corpus callosum, over the study timeline, although there was no clear pattern of change in the genu of the CC. The results, as shown in Table 17, indicate that the MD, AD and RD significantly decreased in the splenium of and body of the CC.

| DTI parameters | CC regions | slope value | t-value | p value |
|---|---|---|---|---|
| MD | $(CC_P)$ | -0.00264 | -2.70 | .0212 |
|  | $(CC_{MP})$ | -0.00281 | -2.07 | .0461 |
|  | $(CC_C)$ | -0.00421 | -2.61 | .0237 |
|  | $(CC_{MA})$ | -0.00159 | -1.54 | .0913 |
|  | $(CC_A)$ | -8.89E-04 | -1.69 | .0758 |
| AD | $(CC_P)$ | -0.00177 | -2.21 | .0386 |
|  | $(CC_{MP})$ | -0.00145 | -1.43 | .1050 |
|  | $(CC_C)$ | -0.00236 | -2.50 | .0271 |
|  | $(CC_{MA})$ | -9.95E-04 | -1.37 | .1140 |
|  | $(CC_A)$ | -5.07E-04 | -1.06 | .1670 |
| FA | $(CC_P)$ | 0.00141 | 1.87 | .0599 |
|  | $(CC_{MP})$ | 0.00223 | 1.38 | .1120 |
|  | $(CC_C)$ | 9.76E-04 | 0.60 | .2870 |
|  | $(CC_{MA})$ | 0.00304 | 1.91 | .0571 |
|  | $(CC_A)$ | -6.21E-04 | -0.68 | .2630 |
| RD | $(CC_P)$ | -0.00518 | -2.58 | .0247 |
|  | $(CC_{MP})$ | -0.00431 | -2.12 | .0433 |
|  | $(CC_C)$ | -0.00532 | -2.04 | .0482 |
|  | $(CC_{MA})$ | -0.00279 | -1.66 | .0780 |
|  | $(CC_A)$ | -6.12E-04 | -0.58 | .2930 |

Table 17. Presents the statistical results of the line fitting to average changes of the diffusion markers within five sub regions of CC.

## II.         Linear fitting of superior marginal gyrus

Generally speaking, the diffusivity markers (MD and RD) values followed a decreasing pattern over the learning course on both sides of SMG. MD value significantly decreased (p = .0185), as did RD value (p = .00716 in the left side of SMG). MD value decrease was also borderline significant, and FA showed an increase in value on the right side of SMG, but not on the left.

| DTI parameters | SMG regions | Slope value | t-value | p value |
|---|---|---|---|---|
| AD | Left SMG | -9.53E-04 | -1.31 | .1230 |
| RD | | -0.00211 | -3.67 | .0072 |
| MD | | -0.0016 | -2.82 | .0185 |
| FA | | 0.00167 | 1.35 | .1170 |
| AD | Right SMG | -0.00143 | -2.09 | .0449 |
| RD | | -0.00098 | -1.37 | .1138 |
| MD | | -0.00119 | -1.91 | .0567 |
| FA | | -0.00227 | -2.11 | .0443 |

Table 18.Presents the statistical results of the line fitting to average changes of the diffusion markers within SMG.

# III.      Linear fitting of superior and middle temporal gyrus

Closer inspection of the table shows that AD and MD values significantly decreased at probability levels of p = .00491 and p = .0218, respectively, on the left side of STG. In addition, axial diffusively value significantly decreased on the left of MTG, at p = .0393.

| DTI parameters | MTG / STG regions | slope value | t-value | p value |
|---|---|---|---|---|
| AD | Right STG | -0.0008 | -1.79 | .0667 |
| RD | | -0.0005 | -0.78 | .2333 |
| MD | | -0.0006 | -1.17 | .1460 |
| FA | | -0.0004 | -0.35 | .3680 |
| AD | Left STG | -0.0017 | -4.05 | .0049 |
| RD | | -0.0008 | -1.36 | .1148 |
| MD | | -0.0011 | -2.68 | .0218 |
| FA | | -0.0007 | -0.67 | .2650 |
| AD | Right MTG | -0.0005 | -0.85 | .2150 |
| RD | | -0.0002 | -0.33 | .3751 |
| MD | | -0.0003 | -0.61 | .2820 |
| FA | | -0.0001 | -0.09 | .4620 |
| AD | Left MTG | -0.0010 | -2.20 | .0393 |
| RD | | -0.0006 | -0.92 | .1977 |
| MD | | -0.0008 | -1.76 | .0685 |
| FA | | -0.0013 | -0.87 | .2110 |

Table 19. Presents the statistical results of the line fitting to average changes of the diffusion markers within superior and middle temporal gyrus.

# IV.        Linear fitting (of pars triangularis) in IFG

It is apparent from this table that AD, RD, and MD values decreased significantly over the learning course on the left side of pars triangularis, but not on the right side. However, FA value displayed no significant changes on either side of pars triangularis, as shown in Table 20.

| DTI parameters | pars triangularis regions | Slope value | t-value | p value |
|---|---|---|---|---|
| AD | Right pars triangularis | -0.0011 | -1.59 | .0862 |
| RD | | -0.0012 | -1.73 | .0714 |
| MD | | -0.0011 | -1.94 | .0547 |
| FA | | -0.0006 | -0.40 | .3500 |
| AD | Left pars triangularis | -0.0021 | -3.40 | .0096 |
| RD | | -0.0024 | -2.85 | .0178 |
| MD | | -0.0022 | -3.32 | .0105 |
| FA | | 0.0015 | 0.897 | .2050 |

Table 20. Presents the statistical results of the line fitting to average changes of the diffusion markers (of pars triangularis) in IFG.

# V.          Linear fitting of precentral gyrus

The main finding here was that FA value significant increased on the left side of precentral gyrus.

| DTI parameters | Precentral regions | Slope value | t-value | p value |
|:---:|:---:|:---:|:---:|:---:|
| AD | Left precentral | -0.0002 | -0.37 | .3620 |
| RD | | -0.0009 | -0.89 | .2070 |
| MD | | -0.0006 | -0.91 | .2007 |
| FA | | 0.0023 | 2.98 | .0102 |
| AD | Right precentral | -0.0007 | -1.30 | .1240 |
| RD | | -0.0013 | -1.45 | .1022 |
| MD | | -0.0009 | -1.39 | .1120 |
| FA | | 6.49E-04 | 0.65 | .0271 |

Table 21.Presents the statistical results of the line fitting to average changes of the diffusion markers within precentral gyrus.
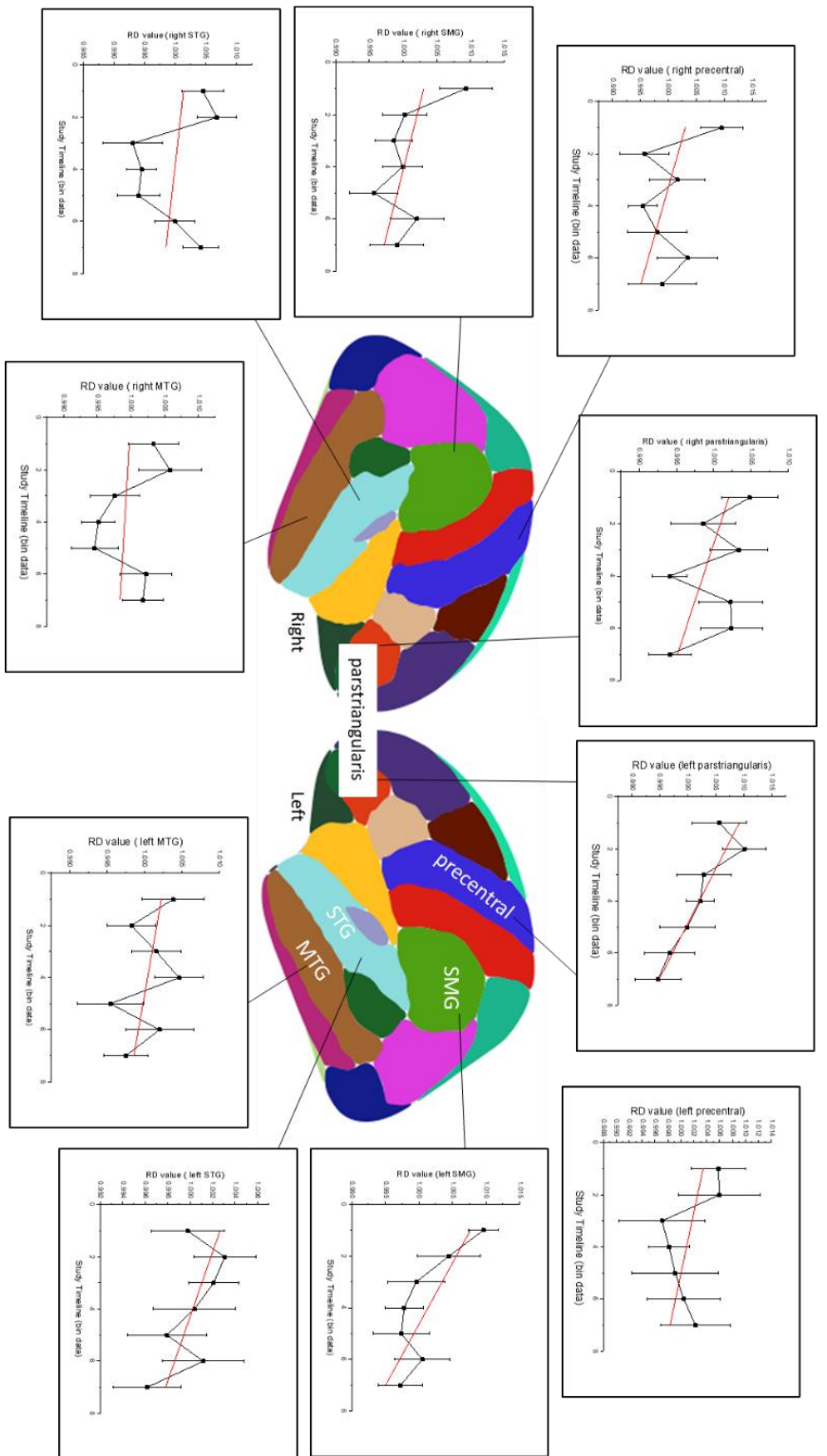
Figure 37. Presents an overview of the line fitting to average changes of (RD) within superior and middle temporal gyrus, superior marginal gyrus, (pars triangularis: BA44) part of IFG, and precentral gyrus, in response to drumming learning.

Figure 38 Presents an overview of the line fitting to average changes of (AD) within superior and middle temporal gyrus, superior marginal gyrus, (pars triangularis: BA44) part of IFG, and precentral gyrus, in response to drumming learning

134
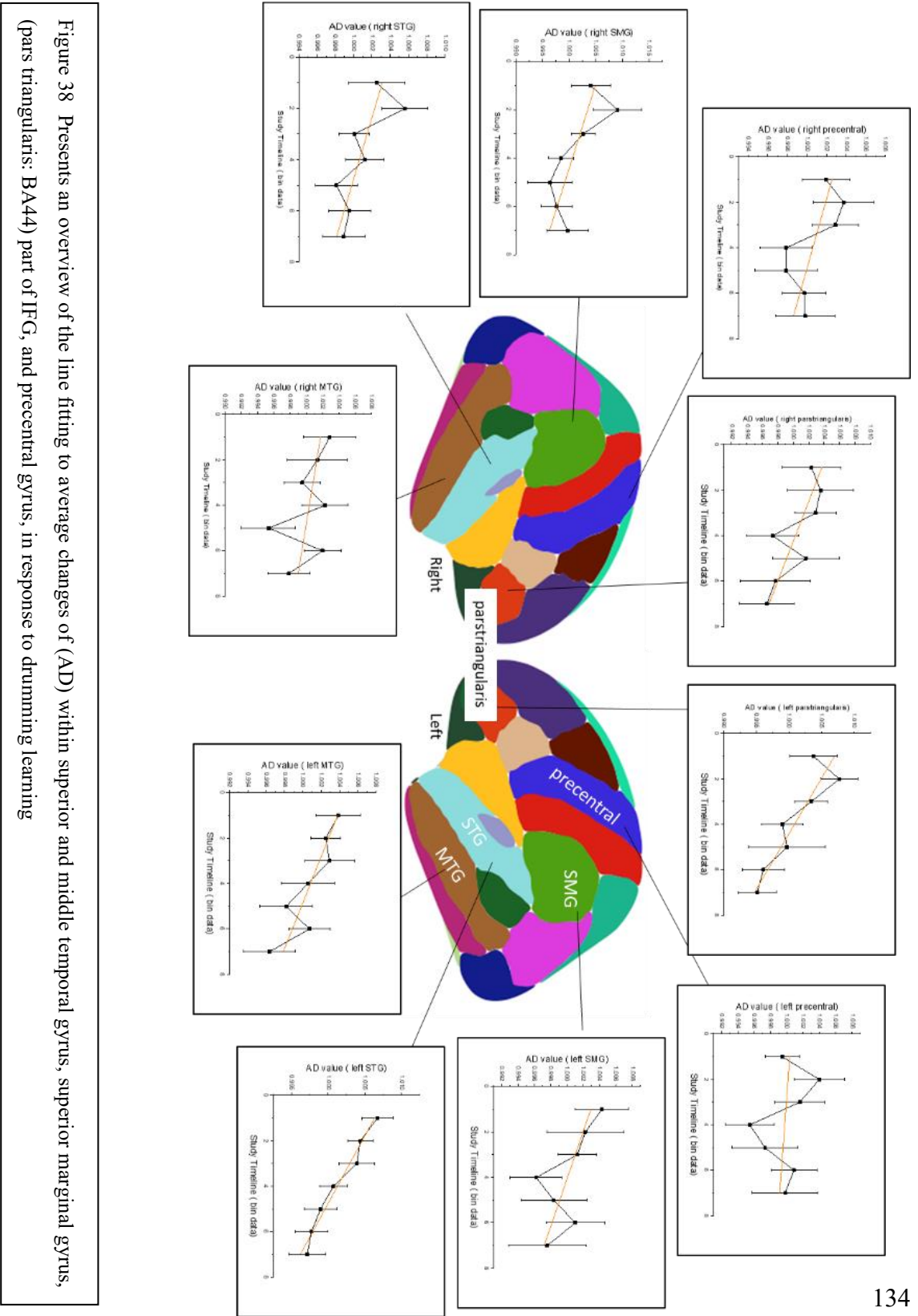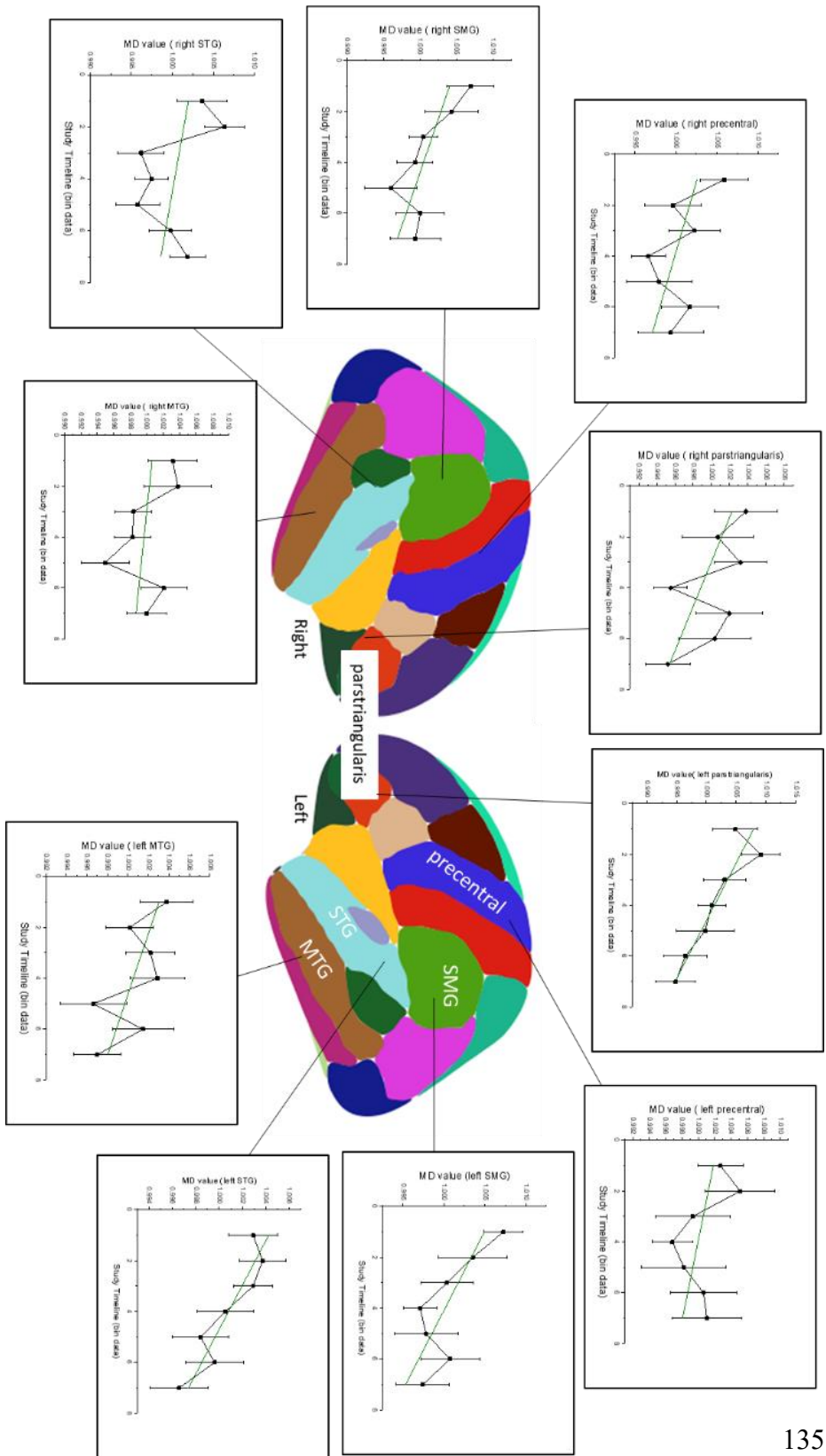
Figure 39. Presents an overview of the line fitting to average changes of (MD) within superior and middle temporal gyrus, superior marginal gyrus, (pars triangularis: BA44) part of IFG, and precentral gyrus, in response to drumming learning.

135
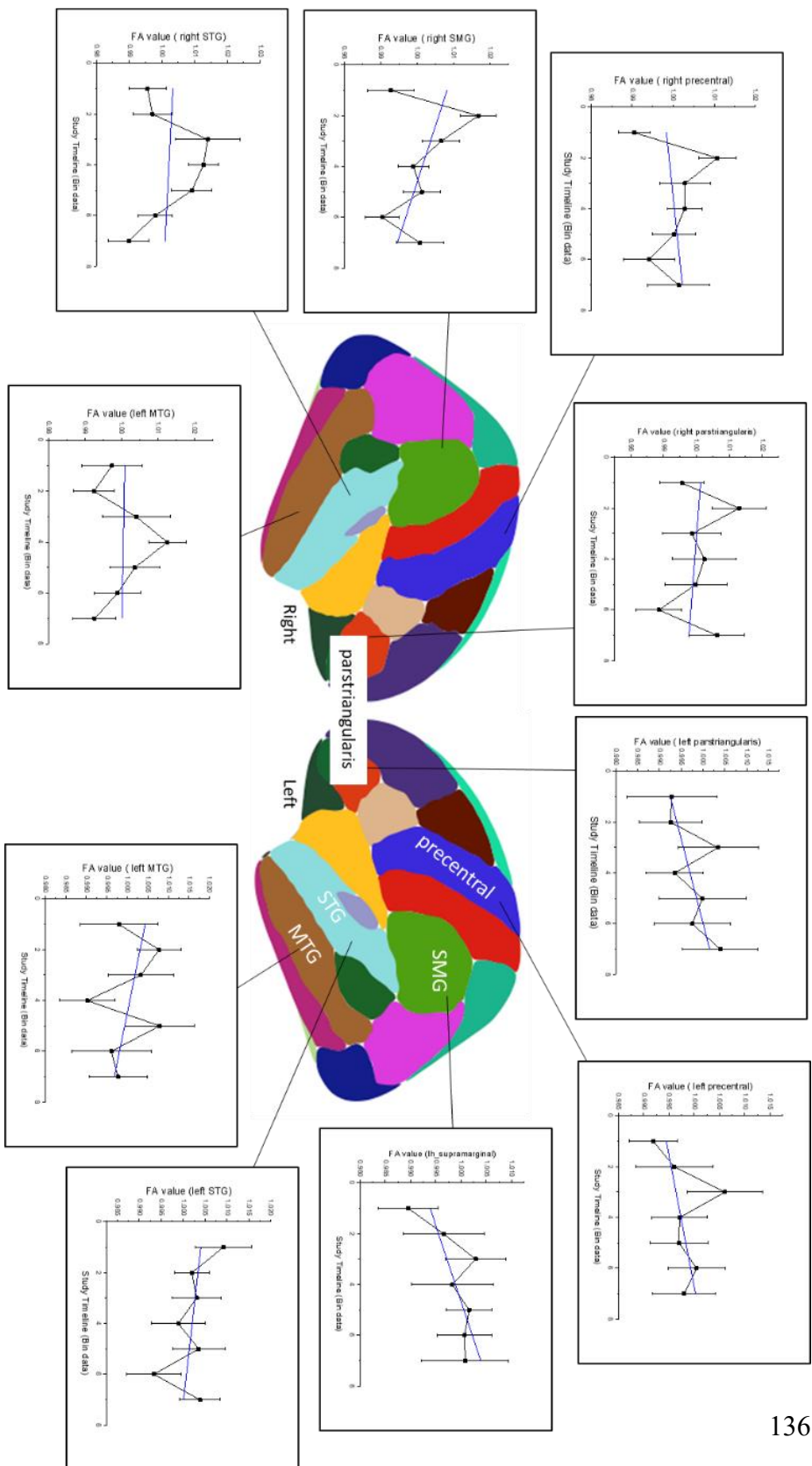
Figure 40. Presents an overview of the line fitting to average changes of (FA) within superior and middle temporal gyrus, superior marginal gyrus, (pars triangularis: BA44) part of IFG, and precentral gyrus, in response to drumming learning.

## 5.4 Discussion

It is well established that human brain structures change in response to musical training, and other forms of learning can also be used to induce neuroplastic changes with which to combat cognitive decline. However, the timescale and spatial distribution of these changes remain uncertain. Structural remodelling of human brain tissue is known to occur following both short-term (hours) and long-term (years) acquisition of a new skill. However, little is known as to what happens structurally when the brain needs to adopt new sequences of procedural rules or memorise a cascade of events within days or weeks. The present study was the first to investigate the timescale of effects of six months daily drumming training on the brain microstructure environment. DTI scans were performed in 15 healthy subjects. The subjects were tested multiple times over a period of six months, and each had around 21 learning sessions delivered by the professional tutor.

The MD, AD and RD values significantly decreased in the splenium and midbody of the CC, whereas there was no clear pattern of change in the anterior part of CC. These are interesting findings, as a reduction in MD, AD and RD are commonly associated with learning, and may represent microstructural alterations (e.g. myelination processing, glio-genesis, angiogenesis and fibre remodelling) in the sub regions of the CC. Recently, longitudinal studies of adults have confirmed experience-related WM changes over short intervals following motor training. In 2010, a study by Lövdén et al. reported a training-related decrease in MD. Interestingly, these patterns contrast the observed age-related trajectories previously described in this chapter, whereby decreasing FA and increasing MD is found to occur with advancing age.

The primary function of the corpus callosum is to integrate and transfer information from both cerebral hemispheres in order to process sensory, motor, and high-level cognitive signals. In 1998, Zarei et al. created a map of the cortical tracts within the CC using probabilistic

diffusion tensor imaging (DTI) tractography. Primary motor and somatosensory tracts were located in the midbody of the CC. In addition, premotor cortical connections were located in the mid body region. Immediately posterior to the premotor region, they found primary motor tracts, followed by somatosensory tracts. Posterior to somatosensory tracts were predominantly posterior parietal cortical connections. The occipital tracts form the most posterior part of the splenium. In addition, visual information is integrated by posterior fibres linking parietal, temporal and occipital lobes across the posterior body and splenium (Fabri et al., 2013 & 2014). The prevailing idea is that the anterior callosal fibres transfer motor information between the frontal lobes, whilst the posterior fibres are involved in the processing of somatosensory (posterior midbody) and visual (splenium) cues by connecting the parietal, temporal, and occipital lobes (Goldstein & Mesfin, 2019). This is in line with the results of the intervention task used in this project, in which playing a drum kit involved the premotor, primary motor, somatosensory and visual brain areas of the participants. In contrast, there were no significant changes in the anterior portion of the corpus callosum. The main function of anterior callosal axons is transfer of motor information between the frontal lobes and somatic sensory and auditory regions.

The most surprising aspect of the data acquired in the present study was the decreasing of mean and radial diffusivity in the supermarginal gyrus (SMG) bilaterally. SMG is located in both the right and left sides of the parietal lobe and plays a key role in spatial processing and motor control (Ben-Shabat et al., 2015). SMG has been shown to have differential lateralisation of function according to whether it's involved in the processing of rhythm or pitch. Jerde and colleagues revealed activation increase in SMG bilaterally for pitch memory, but only right hemisphere SMG activation increase for rhythm memory (Jerde et al., 2011).

In the present study, the mean and axial diffusivity values significantly decreased in the left side of the middle and superior temporal gyrus. This result is interesting, as Wernicke's area is located within the posterior portion of the left superior temporal gyrus. This area's main

role is for speech comprehension, but it is also involved in both musical imagery and perception (Zhang et al., 2017).

Furthermore, AD, RD, and MD values showed a significant decrease over the learning course in left side of pars triangularis, but not the right side. Pars triangularis (BA45) is a sub region of the IFG. IFG is classically subdivided into three regions: the pars opercularis (BA44), pars triangularis (BA45), and pars orbitalis (BA47). Left hemisphere BA44 and BA45 are often collectively referred to as Broca's area based on the landmark study by neurologist Paul Broca, who identified these areas as crucial for language production based on the location of lesions in aphasic patients (Broca, 1861). Broca's area is responsible for language comprehension, and it is involved with action execution and observation, including music execution and listening. Wernicke's area and Broca's area are connected by a large white matter fibre tract known as the arcuate fasciculus, and these areas are known to be critically involved in language learning. Language learning and processing is known to recruit a vast network of mostly left hemispheric brain regions (Schlaffke et al., 2017).

The main interesting finding was the increased FA value on the left side of precentral gyrus. The precentral gyrus is the anatomical location of the primary motor cortex, which is responsible for controlling voluntary motor movement on the body's contralateral side. It is commonly agreed that significant FA value increases in this region are associated with successful training. Scholz et al. (2009) reported increased FA in the precentral gyrus after short intervals of a motor training task, and Takeuchi et al. (2010) found the same result after a cognitive training task.

The main acquired finding of this project was that the model built characterises the DTI markers changing over the study timeline. DTI provides details about the regional microstructure and how diffusion changes during development, learning, and disease. DTI data are primarily reported as mean diffusivity (MD), a value representing water diffusion in

multiple directions, fractional anisotropy (FA), a fraction representing diffusion restricted to a single direction, and radial diffusivity (RD), diffusion perpendicular to barriers such as cell membranes. The MD reduction indicated an increase in tissue density and an up regulation of astrocytes. An increase in FA value may represent microstructural alterations (e.g. myelination processing, glio-genesis, angiogenesis and fibre remodelling). These results suggest that a significant reduction in MD, RD and AD during the drumming training course reflects increased density of cellular membranes, thereby restricting the freedom of water diffusion. This indicates increased axon myelination, which may in turn reflect increased numbers or increased activity of glial cells.

## 5.5 Limitation

There currently are very few longitudinal DTI studies. DTI analysis poses a number of challenges that need to be overcome to produce reliable data. Conventional DTI processing pipelines are currently focussed on single scans (Sampaio-Baptista et al.,2017). One promising area for future work is to optimise DTI analysis for multiple (longitudinal) scans to overcome issues such as individual eddy current correction, the co-registration with a single T1-weighted structural scan, or parameter estimation across time (Assaf & Johansen-Berg, 2019).

For this study, for example, the eigenvectors were estimated for each individual image before computing secondary parameters like AD, RD and MD or FA. It seems reasonable to assume that the estimation of these parameters across scans would significantly reduce noise in the data by assuming that the relative orientation of diffusion parameters changes gradually and systematically. The time course data presented here provides an opportunity to constrain this analysis. Another point is that , the conventional fMRI analysis makes clear assumptions about the observed data, such as the canonical BOLD response, to minimise noise in the data.

The data presented here suggests that a log-linear time course of DTI parameters is appropriate for the type of learning data encountered in the experiments described here. Future work should systematically explore the time course of DTI parameters, and, in particular, to what extend different parameters exhibit the same or different time courses. Finally, DTI analysis co-registers DTI data with T1-weighted data, longitudinal changes, whether they are caused by learning, disease or simply ageing are likely to affect both types of scans. Analysis pipelines that combine time-changing structural data with DTI data may improve the accuracy of results.

## 5.6 Conclusion

In conclusion, our findings indicate that cellular rearrangement of neural tissue can be detected by DTI, and that this modality may allow neuroplasticity to be localised over long/short timescales. The study results demonstrate the important role of white matter neuroplasticity for acquiring a new motor skill. Overall, these findings indicate that plasticity can occur in brain regions that are involved in playing a musical instrument, such as a drumming kit. These findings could help to inform future clinical and cognitive studies regarding the function of white matter microstructure in the human brain.

# Chapter 6    General Discuassion and Conclusion

## 6.1 General Discussion

The main aim of this project was to quantify functional and structural neuroplasticity in response to motor learning, using multiple MRI sequences over six months of a drumming course. More recently, developments in the field of neuroimaging have enabled non-invasive investigation of the living human brain whilst learning new skills or encountering novel experiences, paradigms which have been used for investigating different aspects of brain plasticity. In the current project, learning to use drumming kits was explored due to the fact that musical experiences involve complicated interactions amongst a variety of cognitive, perceptual, affective, and motor processes. The drumming practice sessions were designed for the trainees to be personalised (depending upon individual skill level) 45 minutes/week lessons with the drumming tutor. There was a scores' scale for evaluating the trainees' performance each week, and two tests were done at the mid-training stage of the learning course.

To enable mapping of the functional, macro, and microstructural plasticity, participants were scanned three times at the baseline (pre), mid and post-training course stages using structural and functional MRI techniques. Furthermore, multiple Diffusion Tensor Imaging sessions were performed at different time intervals to characterise the microstructural plasticity.

Firstly, functional MRI techniques were used to localise BOLD signal increases, indicative of heightened brain activation, in response to drumming learning within the human brain. In particular, two task-based fMRI scans were performed: 1) Observation of a drumming task video, and 2) Execution of a drumming task. For the Observation task, the participants had to watch short drumming videos and were asked to press the finger button if they recognised two identical rhythms in a row. The task was repeated three times during the learning drumming course at the before (pre), mid and post-training course stages. For the second fMRI task (Execution), the participants were asked to read musical notes that were displayed on the monitor and then use their hands to play it. This task was completed once participants had

143

become experienced drummers, at the end of the 6-month drumming course. For the Observation task, most clusters produced robust patterns of increase brain activation in the primary visual, audio and motor brain areas, whereas for the Execution task the main clusters of increase brain activation were in the pre, the postcentral and supplementary motor cortex.
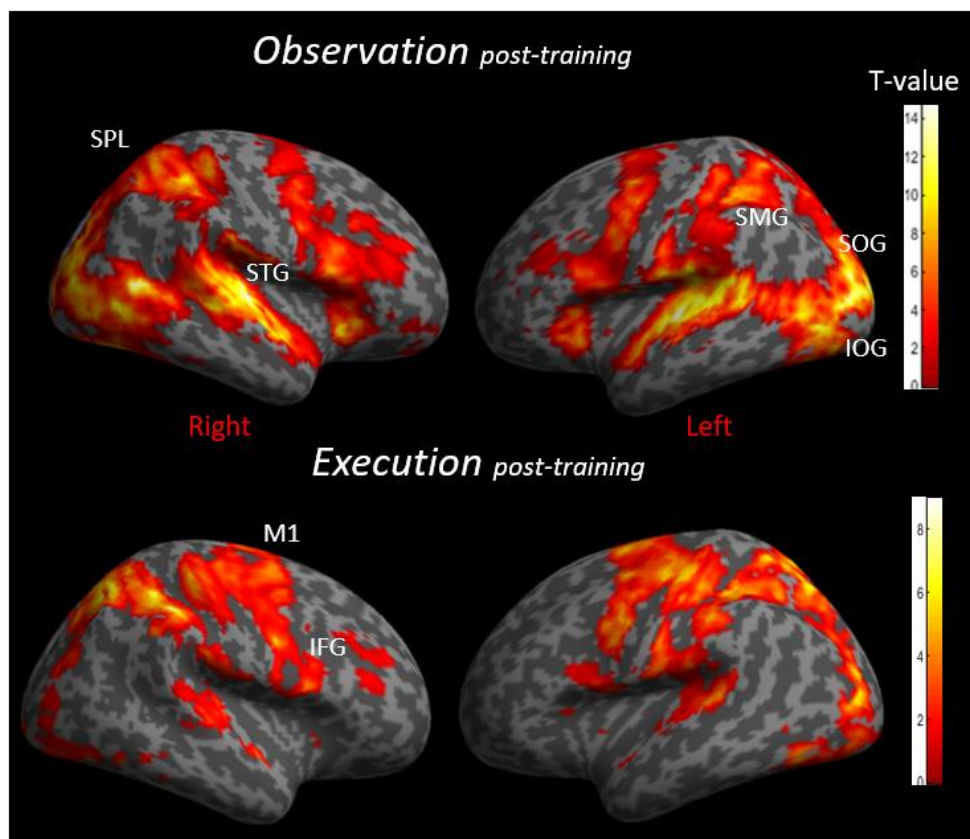


Figure 41. fMRI results. Activation of the group-level found in the whole-brain analysis (task> rest, uncorrected SPMs, a threshold of p ≤ 0.001) with contrast mapping represented on a render view (SPM12).

The conjunction analysis contrast mapping which included both tasks indicated that most of the mirror neurone areas are involved with drumming (i.e. parietal lobe and inferior frontal gyrus) as shown in Fig.42.
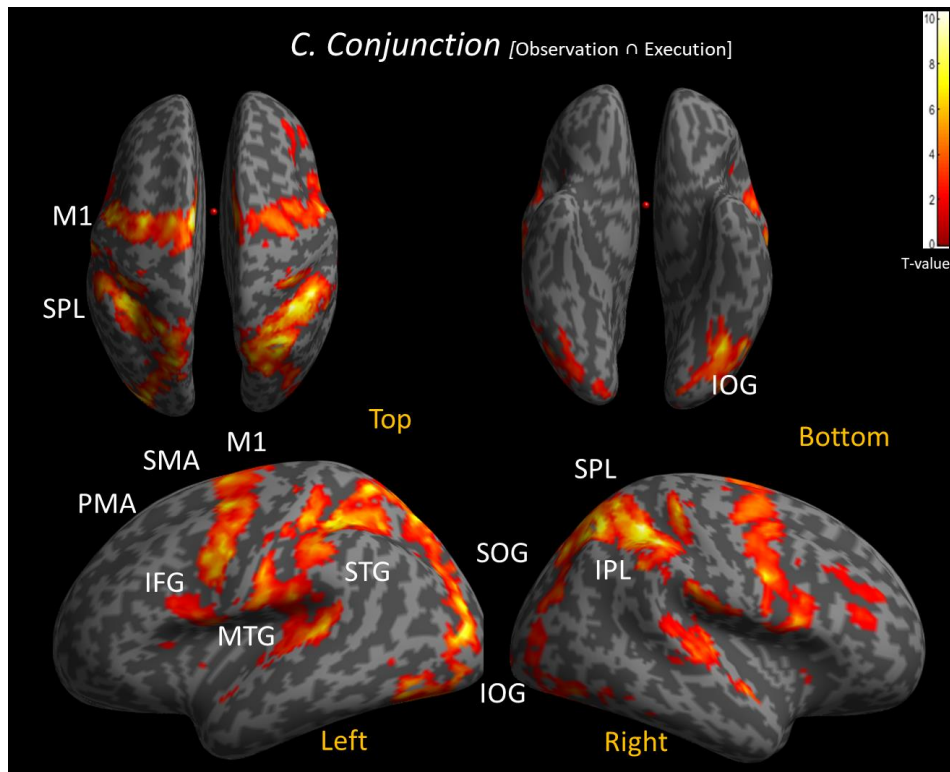


Figure 42. fMRI results: Statistical parametric maps (t values) for the conjunction is – Observation ∩ Execution, contrast mapping represented on a render view (SPM12). Activation of the group-level found in the whole-brain analysis (uncorrected SPMs, a threshold of p ≤ 0.001). Abbreviations: SPL= Superior Parietal Lobe, M1= Primary Motor Area, SOG= Superior Occipital Gyrus, IOG= Inferior Occipital Gyrus.

The fMRI activation clusters from the Execution were used as localisers to define the regions of interest (ROIs). The ROIs identified were the primary motor area, IFG, STG and parietal lobe (SMG), which all showed significant activation changes over time, especially in the midterm fMRI session.

The region of interest analysis was applied to monitor the BOLD signal changes during the observation task over the 6-month drumming course. From this study, we conclude that a complex learning task, such as a beginner learning to play the drum kit in this instance, can lead to an increase in the BOLD signal within motor regions and mirror neuron system regions, indicating increased activity in these areas.

Taken together, these findings are consistent with prior studies, for instance (Herdener et al., 2014) reported that secondary auditory cortex and right posterior STG are involved in the processing of syncopated deviations that are related to the rhythmic structure. Moreover, a higher-order left-hemispheric area (left SMG) shows differential activation for rhythmic variations depending on musical expertise or training. Furthermore, (Schlaffke et al., 2018) found that a professional drummer showed less activation in the motor cortex when performing a finger-tapping task than controls in both hemispheres. In other words, the naïve or the control group showed an increase activation, inconsistent with our previous finding. Several neuroimaging studies have observed that musicians show lower levels of activity in motor regions than non-musicians during the performance of simple motor tasks (Hund-Georgiadis and Von Cramon, 1999; Jäncke et al., 2000; Koeneke et al., 2004).

In 2011, Petrini et al. provide converging evidence that expertise with a certain audio-visual action reduces activation in brain areas crucial for action-sound representation and audio-visual integration. Because both temporal synchrony and temporal congruency of the produced sound may be easily predicted from the observed movements using acquired internal models of that action, a reduction in activation may result as a consequence of perceptual and motor expertise (McKiernan et al., 2003; Parsons et al., 2005).

This indicates that professional drumming/musicians are associated with a more efficient neuronal design of cortical motor areas. This finding is well in line with recent neuroscientific findings on so-called sparse coding, for example having a more efficient neuronal architecture

by using fewer neurons or smaller areas to execute a specific cognitive task (Genç et al., 2018).

The second study in this project was designed to investigate the macrostructural plasticity of grey and white matter volumes (GMV and WMV, respectively). Voxel-based morphometry (VBM), using the CAT12 toolbox, was used to segment the subjects' brains into grey matter (GM), and white matter (WM). Then, these tissues were transformed into MNI space. Two statical analysis methods were then applied: 1) a whole-brain analysis, the purpose being to map GMV and WMV that increased with training, using a paired t-test including the pre-and post-training sessions only, and 2) a regions of interest (ROIs) method, whereby ROIs clusters that showed an increase in BOLD response activations from the Execution fMRI task were identified.

The main findings were that an increase in the gray matter volume, mostly on the right side of the brain. Specifically, following drumming training, gray matter volume had increased in the superior and inferior parietal lobule (BA40), angular gyrus (BA39), superior temporal gyrus, postcentral gyrus (BA6), cuneus, precuneus, superior of the occipital lobe and right side of the insula. Also, there was an increase in gray matter volume on the left side of the brain in the putamen and the middle and inferior of the occipital lobule (BA18 and BA19). The clusters details summary can be found in (Table 11, and Fig. 26. In chapter 4).

And, as expected, the somatosensory cortex (BA2 and BA3) showed a significant increase in GMV when using the line fitting method of analysis. Also, occipital visual areas (BA17 and BA18), as well as BA7 and BA 39 which are part of the parietal cortex in the human brain, showed a significant increase in GMV over the three scanning sessions. The ROIs details summary can be found in (Table 13 and see Fig. 28 and Fig. 29. In chapter 4).

These findings are consistent with prior studies, such as Gaser and Schlaug (2003) concluded that gray matter volume is uppermost in professional musicians, intermediate in amateur

musicians and lowest in controls. Specifically, there was an increase in gray matter volume in the parietal lobe (BA40), and temporal gyrus and correlated with musical skill.

Furthermore, Luders et al. (2004) reported that a gray matter increase in musicians with an absolute pitch in the left temporal gyrus (HG), planum, pre- & post-central gyrus, caudate and occipital pole (BA17/18/19). Bermudez et al. (2009), showed that a greater GM in superior temporal (more on the right), greater cortical thickness in inferior frontal gyrus (BA44/45) and orbital area (BA47) and greater GM and thickness in superior central sulcus in musicians. Also, the Higher GM in left sensorimotor cortex (BA6) in musicians was reported by Han et al. (2009).

The third study in this project was designed to investigate the micro-structural of the gray and white matter plasticity. Diffusion Tensor Imaging was performed in regular time. There were two baseline sessions pre-training, followed by multiple scanning sessions during the training course. Next, the diffusion maps were co-registered to the T1-weighted image in the native space for each subject. In addition, default FSL pre-processing steps were followed to create the four diffusion tensor maps for AD, MD, RD and FA. The Freesurfer software automatically segmented the T1-weighted image into cortical and subcortical brain areas in the native space for each subject. These segmentation areas were used as ROIs to extract the diffusion data, such as for IFG, MTG, STG, SMG and precentral gyrus.

The most interesting finding was that the mean, radial, and axial diffusivity values significantly decreased, whereas fractional anisotropy values increased over the learning course in the sub-regions of the corpus callosum. The results showed a trend for the long-term increase of FA and decrease of MD measurements in the splenium, the body of the corpus callosum, over the study timeline, although there was no clear pattern of change in the genu of the CC. The results, as shown in (Table 17 in chapter 5).

These results further support the idea that motor performance in professional drummers was accompanied by structural differences in the neuroanatomy of the corpus callosum. On the

other word, drummers have higher microstructural diffusion properties in the corpus callosum. In 2019, Schlaffke observed that MD differences between professional drummers and nonmusical controls. All drummers were active members of music bands and/or worked as drumming teachers. Drummers showed significantly higher MD in the anterior section of the corpus callosum than controls. Whereas there were no differences between groups for the other callosal subsegments.

The results of this project are interesting, due to the fact that there was an overlap between the three studies. For example, the supramarginal gyrus (SMG) showed an increase in BOLD response in the functional MRI study and an increase in GMV in the VBM study, as well as a change in the diffusion parameters in the DTI study. SMG is located in the inferior parietal lobule (IPL), and it is part of the mirror neuron system. The inferior frontal gyrus (IFG) and inferior parietal lobule (IPL), as well as the superior temporal sulcus (STS) areas, are engaged in both action observation and execution and are parts of the human mirror system. Mirror neurons are a class of neuron that modulate their activity both when an individual executes a specific motor act and when they observe the same motor act performed by another individual. In addition, the primary motor area (M1) showed BOLD response changes in the fMRI study. M1 lies along the precentral gyrus and has the main role in generating the nerve impulses needed to produce voluntary movements. Secondary to this, it is also responsible for sending orders to the voluntary muscles of the body. The M1 region has a low excitation threshold. Furthermore, the superior and middle temporal gyrus showed BOLD response changes as well as an increase in GMV. These results further support the idea that if particular activities are learned and practised over an adequate period of time, this can result in structural and functional changes that can be measured on a micro and macro-structural level, and which can be visually observed on MR images (Rogenmoser et al., 2018).

Finally, this knowledge will increase understanding of the effects of music (drumming) practise on emotional, cognitive, and perceptual processes. The speed and tone of the beat mediate the type of brainwave stimulated and register a range of patient responses including

increased alertness from fast pulsating beats or relaxation from slow progressive beats. Current studies have shown that can drumming be served as a form of rhythm therapy for all ages of people suffering from neurological disorders. Music can be used as an efficient and cost-effective treatment for individuals affected with hyperactivity disorder (ADHD), Alzheimer's and Parkinson's disease, and stroke-induced neural damage (Deyo, 2016).

For instance, a study with elementary and middle school boys diagnosed with attention deficit hyperactivity disorder (ADHD) concluded that a course of 20-minute treatment sessions with these rhythmic beats yielded results similar to the effects of ADHD medications such as Ritalin and Adderall (Saarman, 2006).

Furthermore, a study evaluates the cognitive performance of elderly with Alzheimer's disease, when adding a set of rhythmic with results showing that the majority had increased accuracy on a range of common tests (Saarman, 2006).

In addition, a study analyzing sensorimotor interaction to music therapy shows that stroke patients experienced increased neurostimulation and function of an affected hand (Grau-Sánchez et al., 2013). Another study showed that listening to music daily increased gray matter volume in the superior frontal gyrus of stroke patients that leads to improved function of working memory and emotional recovery (Särkämö et al., 2016).

## 6.2  General Limitation

There are several limitations to this project. First, the number of participants was relatively small (i.e. 14 participants). It may be argued that participant characteristics, for example the wide age range (20 to 57 years), may have influenced measures of functional and structural plasticity (Aloufi et al.,2021). Future studies with a larger sample population are essential to corroborate our findings.

Performance measures were based on subjective drumming tutor assessment during the lesson rather than at the time of the scans. It is well known that performance in the unusual scanner environment is affected to different degrees in different participants (Yotsumoto et al.,2009; Aloufi et al.,2021). An objective performance assessment during the scan, for example drumming precision while reading music, would be a very useful addition to future studies. It seems reasonable that one of the major driver of functional and structural brain changes is the intensity and duration of engagement with learning tasks. Participants were encouraged to practise daily, but this engagement was not systematically or automatically monitored. Also, it was hard to know that if participants gained another skill during this study. Future studies should include these components. In addition, the generalisability of these results are subject to certain limitations. For instance, a low threshold was used to capture the functional and structural changes over the training course.

A number of different techniques were used independently to quantify functional and structural changes that are linked to learning. One of the recurrent limitations is that for individual techniques, for example VBM or fMRI, learning effects were visible in selected regions, but did not survive rigorous correction. A fusion of MRI analysis methods across modalities, as proposed by (Zhu et al.,2014) may provide much more robust results in future studies.

Another limitation of the present study is that structural non-invasive brain imaging methods cannot identify the underlying neurophysiological mechanisms. Macroscopic alterations may be based on changes at the level of synaptic and neurites, or they might include increased cell genesis, for example, of glial or even neuronal cells. Imaging results need to be compared with histological data for identification of the structural basis at the microscopic level of temporary, training-dependent structural changes in our brains. Thus, animal models in future have to be conducted to understand how and why inter-individual differences in behaviour and learning are related to brain anatomy.

## 6.3 General Conclusion

In this dissertation, I have combined different approaches to study brain structural and functional plasticity with behavioural measurements of music training. We confirmed the results of previous work which demonstrated that skill learning could lead to increased GMV and WMV in some brain regions, as well as to a change in BOLD response and microstructural modification. These findings have potential implications for music therapy and clinical practice. They suggest that long-term musical training shapes several cognitive and perceptual abilities. This has potential implications for music therapy, clinical practice, and theory of emotion inducement from music.

# Chapter 7    References

Aloufi, A. E., Rowe, F. J., & Meyer, G. F. (2021). Behavioural performance improvement in visuomotor learning correlates with functional and microstructural brain changes. *NeuroImage*, *227*(December 2020), 117673. https://doi.org/10.1016/j.neuroimage.2020.117673

Altman, J. (2011). The Discovery of Adult Mammalian Neurogenesis. In *Neurogenesis in the Adult Brain I*. https://doi.org/10.1007/978-4-431-53933-9_1

Amad, A., Seidman, J., Draper, S. B., Bruchhage, M. M. K., Lowry, R. G., Wheeler, J., Robertson, A., Williams, S. C. R., & Smith, M. S. (2017). Motor Learning Induces Plasticity in the Resting Brain-Drumming Up a Connection. *Cerebral Cortex (New York, N.Y. : 1991)*. https://doi.org/10.1093/cercor/bhw048

Amunts, K., Schlaug, G., Jäncke, L., Steinmetz, H., Schleicher, A., Dabringhaus, A., & Zilles, K. (1997). Motor cortex and hand motor skills: Structural compliance in the human brain. *Human Brain Mapping*. https://doi.org/10.1002/(SICI)1097-0193(1997)5:3<206::AID-HBM5>3.0.CO;2-7

Anaya, E. M., Pisoni, D. B., & Kronenberger, W. G. (2017). Visual-spatial sequence learning and memory in trained musicians. *Psychology of Music*. https://doi.org/10.1177/0305735616638942

Ardekani, S., & Sinha, U. (2006). Statistical representation of mean diffusivity and fractional anisotropy brain maps of normal subjects. *Journal of Magnetic Resonance Imaging*, *24*(6), 1243–1251. https://doi.org/10.1002/jmri.20745

Ardila, A., Bernal, B., & Rosselli, M. (2016). How Extended Is Wernicke's Area? Meta-Analytic Connectivity Study of BA20 and Integrative Proposal. *Neuroscience Journal*, *2016*(February), 1–6. https://doi.org/10.1155/2016/4962562

Arima, T., Yanagi, Y., Niddam, D. M., Ohata, N., Arendt-Nielsen, L., Minagi, S., Sessle, B. J., & Svensson, P. (2011). Corticomotor plasticity induced by tongue-task training in humans: a longitudinal fMRI study. *Experimental Brain Research*, *212*(2), 199. https://doi.org/10.1007/s00221-011-2719-7

Ashburner, J., & Friston, K. J. (2005). Unified segmentation. *NeuroImage*. https://doi.org/10.1016/j.neuroimage.2005.02.018

Assaf, Y. (2008). Can we use diffusion MRI as a bio-marker of neurodegenerative processes? *BioEssays*, *30*(11–12), 1235–1245. https://doi.org/10.1002/bies.20851

Assaf, Y., Johansen-Berg, H., & Thiebaut de Schotten, M. (2019). The role of diffusion MRI in neuroscience. *NMR in Biomedicine*, *32*(4), 1–16. https://doi.org/10.1002/nbm.3762

Assaf, Y., & Pasternak, O. (2008). Diffusion tensor imaging (DTI)-based white matter mapping in brain research: A review. *Journal of Molecular Neuroscience*, *34*(1), 51–61. https://doi.org/10.1007/s12031-007-0029-0

Bangert, M., Peschel, T., Schlaug, G., Rotte, M., Drescher, D., Hinrichs, H., Heinze, H. J., & Altenmüller, E. (2006). Shared networks for auditory and motor processing in professional pianists: Evidence from fMRI conjunction. *NeuroImage*. https://doi.org/10.1016/j.neuroimage.2005.10.044

Barrett, K. C., Ashley, R., Strait, D. L., & Kraus, N. (2013). Art and science: how musical training shapes the brain. *Frontiers in Psychology*, *4*(October), 1–13. https://doi.org/10.3389/fpsyg.2013.00713

Baum, G. L., Roalf, D. R., Cook, P. A., Ciric, R., Rosen, A. F. G., Xia, C., Elliott, M. A., Ruparel, K., Verma, R., Tunç, B., Gur, R. E. R. C., Gur, R. E. R. C., Bassett, D. S., & Satterthwaite, T. D. (2018). The impact of in-scanner head motion on structural connectivity derived from diffusion MRI. *NeuroImage*. https://doi.org/10.1016/j.neuroimage.2018.02.041

Beer, A. L., Plank, T., & Greenlee, M. W. (2011). Diffusion tensor imaging shows white matter tracts between human auditory and visual cortex. *Experimental Brain Research*, *213*(2–3), 299–308. https://doi.org/10.1007/s00221-011-2715-y

Beer, A. L., Watanabe, T., Ni, R., Sasaki, Y., & Andersen, G. J. (2009). 3D surface perception from motion involves a temporal-parietal network. *European Journal of Neuroscience*, *30*(4), 703–713. https://doi.org/10.1111/j.1460-9568.2009.06857.x

Behrens, T. E. J., Berg, H. J., Jbabdi, S., Rushworth, M. F. S., & Woolrich, M. W. (2007). Probabilistic diffusion tractography with multiple fibre orientations: What can we gain? *NeuroImage*, *34*(1), 144–155. https://doi.org/10.1016/j.neuroimage.2006.09.018

Behrens, T. E. J., Johansen-Berg, H., Woolrich, M. W., Smith, S. M., Wheeler-Kingshott, C. A. M., Boulby, P. A., Barker, G. J., Sillery, E. L., Sheehan, K., Ciccarelli, O., Thompson, A. J., Brady, J. M., & Matthews, P. M. (2003). Non-invasive mapping of connections between human thalamus and cortex using diffusion imaging. *Nature Neuroscience*, *6*(7), 750–757. https://doi.org/10.1038/nn1075

Behrens, T. E. J., Woolrich, M. W., Jenkinson, M., Johansen-Berg, H., Nunes, R. G., Clare, S., Matthews, P. M., Brady, J. M., & Smith, S. M. (2003). Characterization and Propagation of Uncertainty in Diffusion-Weighted MR Imaging. *Magnetic Resonance in Medicine*, *50*(5), 1077–1088. https://doi.org/10.1002/mrm.10609

Ben-Shabat, E., Matyas, T. A., Pell, G. S., Brodtmann, A., & Carey, L. M. (2015). The right supramarginal gyrus is important for proprioception in healthy and stroke-affected participants: A functional MRI study. *Frontiers in Neurology*. https://doi.org/10.3389/fneur.2015.00248

Bermudez, P., & Zatorre, R. J. (2005). Differences in gray matter between musicians and nonmusicians. *Annals of the New York Academy of Sciences*. https://doi.org/10.1196/annals.1360.057

Bezzola, L., Mérillat, S., Gaser, C., & Jäncke, L. (2011). Training-induced neural plasticity in golf novices. *Journal of Neuroscience*. https://doi.org/10.1523/JNEUROSCI.1996-11.2011

Binder, J. R. (2015). The Wernicke area: Modern evidence and a reinterpretation. *Neurology*.

Blattner, M. M., & Glinert, E. P. (1996). Multimodal integration. *IEEE Multimedia*, *3*(4), 14–24. https://doi.org/10.1109/93.556457

Bliss, T. V. P., & Collingridge, G. L. (1993). A synaptic model of memory: Long-term potentiation in the hippocampus. *Nature*, *361*(6407), 31–39. https://doi.org/10.1038/361031a0

Blumenfeld-Katzir, T., Pasternak, O., Dagan, M., & Assaf, Y. (2011). Diffusion MRI of structural brain plasticity induced by a learning and memory task. *PLoS ONE*, *6*(6). https://doi.org/10.1371/journal.pone.0020678

Bogen, J. E., & Bogen, G. M. (1976). WERNICKE'S REGION–WHERE IS IT? *Annals of the New York Academy of Sciences*. https://doi.org/10.1111/j.1749-6632.1976.tb25546.x

Brodal, H. P., Osnes, B., & Specht, K. (2017). Listening to rhythmic music reduces connectivity within the basal ganglia and the reward system. *Frontiers in Neuroscience*, *11*(MAR), 1–7. https://doi.org/10.3389/fnins.2017.00153

Brown, S., Martinez, M. J., & Parsons, L. M. (2006). Music and language side by side in the brain: A PET study of the generation of melodies and sentences. *European Journal of Neuroscience*, *23*(10), 2791–2803. https://doi.org/10.1111/j.1460-9568.2006.04785.x

Bruce Fischl, Martin I. Sereno, Roger B.H. Tootell, Anders M. Dale, Fischl, B., Sereno, M. I., Tootell, R. B. H., & Dale, A. M. (1999). High-resolution intersubject averaging and a coordinate system for the cortical surface. *Human Brain Mapping*, *8*(4), 272–284. https://doi.org/10.1002/(SICI)1097-0193(1999)8:4<272::AID-HBM10>3.0.CO;2-4

Bruchhage, M. M. K., Amad, A., Draper, S. B., Seidman, J., Lacerda, L., Laguna, P. L., Lowry, R. G., Wheeler, J., Robertson, A., Dell'Acqua, F., Smith, M. S., & Williams, S. C. R. (2020). Drum training induces long-term plasticity in the cerebellum and connected cortical thickness. *Scientific Reports*. https://doi.org/10.1038/s41598-020-65877-2

Bunge, S. A., & Kahn, I. (2009). Cognition: An Overview of Neuroimaging Techniques. *Encyclopedia of Neuroscience*, *2*, 1063–1067. https://doi.org/10.1016/B978-008045046-9.00298-9

Cabeen, R. P., Bastin, M. E., & Laidlaw, D. H. (2017). A Comparative evaluation of voxel-based spatial mapping in diffusion tensor imaging. *NeuroImage*, *146*, 100–112. https://doi.org/10.1016/j.neuroimage.2016.11.020

Cannonieri, G. C., Bonilha, L., Fernandes, P. T., Cendes, F., & Li, L. M. (2007). Practice and perfect: Length of training and structural brain changes in experienced typists. *NeuroReport*. https://doi.org/10.1097/WNR.0b013e3281a030e5

Cao, X., Yao, Y., Li, T., Cheng, Y., Feng, W., Shen, Y., Li, Q., Jiang, L., Wu, W., Wang, J., Sheng, J., Feng, J., & Li, C. (2016). The Impact of Cognitive Training on Cerebral White Matter in Community-Dwelling Elderly: One-Year Prospective Longitudinal Diffusion Tensor Imaging Study. *Scientific Reports*, *6*(April), 1–13. https://doi.org/10.1038/srep33212

Carter, C. S., Braver, T. S., Barch, D. M., Botvinick, M. M., Noll, D., & Cohen, J. D. (1998). Anterior cingulate cortex, error detection, and the online monitoring of performance. *Science*. https://doi.org/10.1126/science.280.5364.747

Casella, C., Bourbon-Teles, J., Bells, S., Coulthard, E., Parker, G., Rosser, A., Jones, D., & Metzler-Baddeley, C. (2020). Drumming Motor Sequence Training Induces Apparent Myelin Remodelling in Huntington's Disease: A Longitudinal Diffusion MRI and Quantitative Magnetization Transfer Study. *Journal of Huntington's Disease*. https://doi.org/10.1101/2019.12.24.887406

Censor, N., Sagi, D., & Cohen, L. G. (2012). Common mechanisms of human perceptual and motor learning. In *Nature Reviews Neuroscience*. https://doi.org/10.1038/nrn3315

Colom, R., Quiroga, M. Á., Solana, A. B., Burgaleta, M., Román, F. J., Privado, J., Escorial, S., Martínez, K., Álvarez-Linera, J., Alfayate, E., García, F., Lepage, C., Hernández-Tamames, J. A., & Karama, S. (2012). Structural changes after videogame practice related to a brain network associated with intelligence. *Intelligence*. https://doi.org/10.1016/j.intell.2012.05.004

Corporation, O. (n.d.). *Origin 8 User Guide*.

Cui, L., Yin, H. C., Lyu, S. J., Shen, Q. Q., Wang, Y., Li, X. J., Li, J., Li, Y. F., & Zhu, L. N. (2019). Tai Chi Chuan vs General Aerobic Exercise in Brain Plasticity: A Multimodal MRI Study. *Scientific Reports*. https://doi.org/10.1038/s41598-019-53731-z

D, R., BT, B., & DJ, H. (2000). Activity in primary visual cortex predicts performance in a visual detection task. *Nature Neuroscience*, *3*(9), 940–945.

Dahlin, E., Neely, A. S., Larsson, A., Bäckman, L., & Nyberg, L. (2008). Transfer of learning after updating training mediated by the striatum. *Science*. https://doi.org/10.1126/science.1155466

De La Rue, S. E., Draper, S. B., Potter, C. R., & Smith, M. S. (2013). Energy Expenditure in Rock/Pop Drumming. *Int J Sports Med*, *34*(10), 868–872.

De Souza, R. S. M., Rosa, M., Escobar, T. D. C., Gasparetto, E. L., & Nakamura-Palacios, E. M. (2019). Anterior to midposterior corpus callosum subregions are volumetrically reduced in Male alcoholics but only the anterior segment is associated to alcohol use. *Frontiers in Psychiatry*, *10*(APR), 1–5. https://doi.org/10.3389/fpsyt.2019.00196

Debowska, W., Wolak, T., Nowicka, A., Kozak, A., Szwed, M., & Kossut, M. (2016). Functional and structural neuroplasticity induced by short-term tactile training based on braille reading. *Frontiers in Neuroscience*. https://doi.org/10.3389/fnins.2016.00460

Decety, J., & Grèzes, J. (1999). Neural mechanisms subserving the perception of human actions. In *Trends in Cognitive Sciences*. https://doi.org/10.1016/S1364-6613(99)01312-1

Degé, F., & Kerkovius, K. (2018). The effects of drumming on working memory in older adults. *Annals of the New York Academy of Sciences*, *1423*(1), 242–250. https://doi.org/10.1111/nyas.13685

Dehaene-Lambertz, G., Monzalvo, K., & Dehaene, S. (2018). The emergence of the visual word form: Longitudinal evolution of category-specific ventral visual areas during reading acquisition. In *PLoS Biology* (Vol. 16, Issue 3). https://doi.org/10.1371/journal.pbio.2004103

Desikan, R. S., Ségonne, F., Fischl, B., Quinn, B. T., Dickerson, B. C., Blacker, D., Buckner, R. L., Dale, A. M., Maguire, R. P., Hyman, B. T., Albert, M. S., & Killiany, R. J. (2006). An automated labeling system for subdividing the human cerebral cortex on MRI scans into gyral based regions of interest. *NeuroImage*, *31*(3), 968–980. https://doi.org/10.1016/j.neuroimage.2006.01.021

Destrieux, C., Fischl, B., Dale, A., & Halgren, E. (2010). Automatic parcellation of human cortical gyri and sulci using standard anatomical nomenclature. *NeuroImage*, *53*(1), 1–15. https://doi.org/10.1016/j.neuroimage.2010.06.010

di Pellegrino, G., Fadiga, L., Fogassi, L., Gallese, V., & Rizzolatti, G. (1992). Understanding motor events: a neurophysiological study. *Experimental Brain Research*. https://doi.org/10.1007/BF00230027

Doan, N. T., Engvig, A., Persson, K., Alnæs, D., Kaufmann, T., Rokicki, J., Córdova-Palomera, A., Moberget, T., Bræhkus, A., Barca, M. L., Engedal, K., Andreassen, O. A., Selbæk, G., & Westlye, L. T. (2017). Dissociable diffusion MRI patterns of white matter microstructure and connectivity in Alzheimer's disease spectrum. *Scientific Reports*, *7*(March), 1–12. https://doi.org/10.1038/srep45131

Doyon, J., Penhune, V., & Ungerleider, L. G. (2003). Distinct contribution of the cortico-striatal and cortico-cerebellar systems to motor skill learning. *Neuropsychologia*. https://doi.org/10.1016/S0028-3932(02)00158-6

Draganski, B., Gaser, C., Busch, V., Schuierer, G., Bogdahn, U., & May, A. (2004). Neuroplasticity: Changes in grey matter induced by training. *Nature*.

Driemeyer, J., Boyke, J., Gaser, C., Büchel, C., & May, A. (2008). Changes in gray matter induced by learning - Revisited. *PLoS ONE*. https://doi.org/10.1371/journal.pone.0002669

Drijkoningen, D., Caeyenberghs, K., Leunissen, I., Vander Linden, C., Sunaert, S., Duysens, J., & Swinnen, S. P. (2015). Training-induced improvements in postural control are accompanied by alterations in cerebellar white matter in brain injured patients. *NeuroImage: Clinical*, *7*, 240–251. https://doi.org/10.1016/j.nicl.2014.12.006

Drobyshevsky, A., Back, S., Wyrwicz, A. M., Li, L., Derrick, M., Ji, X., Kotlajich, M., & Tan, S. (2004). Diffusion tensor imaging of the developing rabbit brain. *Magnetic Resonance in Medicine*, *11*(July), 2004–2004. https://www.sciencedirect.com/science/article/pii/S1933721307000955

Duff, E. P., Cunnington, R., & Egan, G. F. (2007). REX: Response exploration for neuroimaging datasets. *Neuroinformatics*, *5*(4), 223–234. https://doi.org/10.1007/s12021-007-9001-y

Eickhoff, S. (2007). SPM Anatomy toolbox. *NeuroImage*, *91*(14), 1–21.

Ellis, R. J., Bruijn, B., Norton, A. C., Winner, E., & Schlaug, G. (2013). Training-mediated leftward asymmetries during music processing: A cross-sectional and longitudinal fMRI analysis. *NeuroImage*. https://doi.org/10.1016/j.neuroimage.2013.02.045

Erickson, K. I., Voss, M. W., Prakash, R. S., Basak, C., Szabo, A., Chaddock, L., Kim, J. S., Heo, S., Alves, H., White, S. M., Wojcicki, T. R., Mailey, E., Vieira, V. J., Martin, S. A., Pence, B. D., Woods, J. A., McAuley, E., & Kramer, A. F. (2011). Exercise training increases size of hippocampus and improves memory. *Proceedings of the National Academy of Sciences of the United States of America*. https://doi.org/10.1073/pnas.1015950108

Eriksen, A. D., Lorås, H., Pedersen, A. V., & Sigmundsson, H. (2018). Proximal–Distal Motor Control in Skilled Drummers: The Effect on Tapping Frequency of Mechanically Constraining Joints of the Arms in Skilled Drummers and Unskilled Controls. *SAGE Open*. https://doi.org/10.1177/2158244018791220

Eriksson, P. S., Perfilieva, E., Björk-Eriksson, T., Alborn, A. M., Nordborg, C., Peterson, D. A., & Gage, F. H. (1998). Neurogenesis in the adult human hippocampus. *Nature Medicine*. https://doi.org/10.1038/3305

Fabri, M. (2014). Functional topography of the corpus callosum investigated by DTI and fMRI. *World Journal of Radiology*. https://doi.org/10.4329/wjr.v6.i12.895

Fabri, M., & Polonara, G. (2013). Functional topography of human corpus callosum: an FMRI mapping study. *Neural Plasticity*. https://doi.org/10.1155/2013/251308

Fadiga, L., Craighero, L., & D'Ausilio, A. (2009). Broca's area in language, action, and music. *Annals of the New York Academy of Sciences*. https://doi.org/10.1111/j.1749-6632.2009.04582.x

Fischl, B., Liu, A., & Dale, A. M. (2001). Automated manifold surgery: Constructing geometrically accurate and topologically correct models of the human cerebral cortex. *IEEE Transactions on Medical Imaging*, *20*(1), 70–80. https://doi.org/10.1109/42.906426

Fischl, B., Rajendran, N., Busa, E., Augustinack, J., Hinds, O., Yeo, B. T. T., Mohlberg, H., Amunts, K., & Zilles, K. (2008). Cortical folding patterns and predicting cytoarchitecture. *Cerebral Cortex*, *18*(8), 1973–1980. https://doi.org/10.1093/cercor/bhm225

Fischl, B., Salat, D. H., Busa, E., Albert, M., Dieterich, M., Haselgrove, C., van der Kouwe, A., Killiany, R., Kennedy, D., Klaveness, S., Montillo, A., Makris, N., Rosen, B., & Dale, A. M. (2002). Whole Brain Segmentation. *Neuron*, *33*(3), 341–355. https://doi.org/10.1016/s0896-6273(02)00569-x

Fischl, B., Salat, D. H., Van Der Kouwe, A. J. W., Makris, N., Ségonne, F., Quinn, B. T., & Dale, A. M. (2004). Sequence-independent segmentation of magnetic resonance images. *NeuroImage*, *23*(SUPPL. 1), 69–84. https://doi.org/10.1016/j.neuroimage.2004.07.016

Fischl, B., Van Der Kouwe, A., Destrieux, C., Halgren, E., Ségonne, F., Salat, D. H., Busa, E., Seidman, L. J., Goldstein, J., Kennedy, D., Caviness, V., Makris, N., Rosen, B., & Dale, A. M. (2004). Automatically Parcellating the Human Cerebral Cortex. *Cerebral Cortex*, *14*(1), 11–22. https://doi.org/10.1093/cercor/bhg087

Fjell, A. M., Westlye, L. T., Greve, D. N., Fischl, B., Benner, T., Van Der Kouwe, A. J. W., Salat, D., Bjørnerud, A., Due-Tønnessen, P., & Walhovd, K. B. (2008). The relationship between diffusion tensor imaging and volumetry as measures of white matter properties. *NeuroImage*, *42*(4), 1654–1668. https://doi.org/10.1016/j.neuroimage.2008.06.005

Floyer-Lea, A., & Matthews, P. M. (2005). Distinguishable brain activation networks for short- and long-term motor skill learning. *Journal of Neurophysiology*. https://doi.org/10.1152/jn.00717.2004

François, C., Grau-Sánchez, J., Duarte, E., & Rodriguez-Fornells, A. (2015). Musical training as an alternative and effective method for neuro-education and neuro-rehabilitation. *Frontiers in Psychology*, *6*(APR), 1–15. https://doi.org/10.3389/fpsyg.2015.00475

Friedrich, P., Fraenz, C., Schlüter, C., Ocklenburg, S., Mädler, B., Güntürkün, O., & Genç, E. (2020). The Relationship between Axon Density, Myelination, and Fractional

Anisotropy in the Human Corpus Callosum. *Cerebral Cortex*, *30*(4), 2042–2056. https://doi.org/10.1093/cercor/bhz221

Gaab, N., Gaser, C., & Schlaug, G. (2006). Improvement-related functional plasticity following pitch memory training. *NeuroImage*. https://doi.org/10.1016/j.neuroimage.2005.11.046

Gallese, V., Fadiga, L., Fogassi, L., & Rizzolatti, G. (1996). Action recognition in the premotor cortex. *Brain*. https://doi.org/10.1093/brain/119.2.593

Ganaye, P., & Umr, I. C. (2018). Semi-supervised Learning for Segmentation Under Semantic Constraint Pierre-Antoine. *MICCAI (Oral Segmentation)*, *1*(August 2019), 595–602. https://doi.org/10.1007/978-3-030-00931-1

Gaser, C., & Schlaug, G. (2003). Gray Matter Differences between Musicians and Nonmusicians. *Annals of the New York Academy of Sciences*. https://doi.org/10.1196/annals.1284.062

Gaser, C., & Schlaug, G. (2003). Brain structures differ between musicians and non-musicians. *Journal of Neuroscience*, *23*(27), 9240–9245. https://doi.org/10.1523/jneurosci.23-27-09240.2003

Gebauer, D., Fink, A., Filippini, N., Johansen-Berg, H., Reishofer, G., Koschutnig, K., Kargl, R., Purgstaller, C., Fazekas, F., & Enzinger, C. (2012). Differences in integrity of white matter and changes with training in spelling impaired children: A diffusion tensor imaging study. *Brain Structure and Function*, *217*(3), 747–760. https://doi.org/10.1007/s00429-011-0371-4

Genovese, C. R., Lazar, N. A., & Nichols, T. (2002). Thresholding of statistical maps in functional neuroimaging using the false discovery rate. *NeuroImage*, *15*(4), 870–878. https://doi.org/10.1006/nimg.2001.1037

Giacosa, C. (2019). *White Matter Plasticity in Dancers and Musicians*. *May*.

Goldberg, G. (1985). Supplementary motor area structure and function: Review and hypotheses. *Behavioral and Brain Sciences*. https://doi.org/10.1017/S0140525X00045167

Goldstein, A., & Mesfin, F. B. (2019). Neuroanatomy, Corpus Callosum. In *StatPearls*.

Golland, P., & Fischl, B. (2003). Permutation tests for classification: Towards statistical significance in image-based studies. *Lecture Notes in Computer Science (Including*

*Subseries Lecture Notes in Artificial Intelligence and Lecture Notes in Bioinformatics)*, *2732*, 330–341. https://doi.org/10.1007/978-3-540-45087-0_28

Golland, P., Fischl, B., Spiridon, M., Kanwisher, N., Buckner, R. L., Shenton, M. E., Kikinis, R., Dale, A., & Grimson, W. E. L. (2002). Discriminative analysis for image-based studies. *Lecture Notes in Computer Science (Including Subseries Lecture Notes in Artificial Intelligence and Lecture Notes in Bioinformatics)*, *2488*, 508–515. https://doi.org/10.1007/3-540-45786-0_63

Greco, V., Frijia, F., Mikellidou, K., Montanaro, D., Farini, A., D'Uva, M., Poggi, P., Pucci, M., Sordini, A., Morrone, M. C., & Burr, D. C. (2016). A low-cost and versatile system for projecting wide-field visual stimuli within fMRI scanners. *Behavior Research Methods*, *48*(2), 614–620. https://doi.org/10.3758/s13428-015-0605-0

Greve, D. N. (1999). *Signal Processing and Statistical Analysis for Event-Related fMRI Model of the Hemodynamic Response*. 1–8.

Greve, D. N. (2005). fMRI Analysis 101 - Univariate Analysis 1 Generalized Least Squares ( GLS ) Solution. *NeuroImage*, 1–6.

Groussard, M., Viader, F., Landeau, B., Desgranges, B., Eustache, F., & Platel, H. (2014). The effects of musical practice on structural plasticity: The dynamics of grey matter changes. *Brain and Cognition*, *90*, 174–180. https://doi.org/10.1016/j.bandc.2014.06.013

Grover, V. P. B., Tognarelli, J. M., Crossey, M. M. E., Cox, I. J., Taylor-Robinson, S. D., & McPhail, M. J. W. (2015). Magnetic Resonance Imaging: Principles and Techniques: Lessons for Clinicians. *Journal of Clinical and Experimental Hepatology*, *5*(3), 246–255. https://doi.org/10.1016/j.jceh.2015.08.001

Hagler, D. J., Saygin, A. P., & Sereno, M. I. (2006). Smoothing and cluster thresholding for cortical surface-based group analysis of fMRI data. *NeuroImage*, *33*(4), 1093–1103. https://doi.org/10.1016/j.neuroimage.2006.07.036

Hall, G. (2016). Perceptual learning. In *The Curated Reference Collection in Neuroscience and Biobehavioral Psychology*. https://doi.org/10.1016/B978-0-12-809324-5.21005-5

Han, X., & Fischl, B. (2007). Atlas renormalization for improved brain MR image segmentation across scanner platforms. *IEEE Transactions on Medical Imaging*, *26*(4), 479–486. https://doi.org/10.1109/TMI.2007.893282

Han, X., Jovicich, J., Salat, D., van der Kouwe, A., Quinn, B., Czanner, S., Busa, E., Pacheco, J., Albert, M., Killiany, R., Maguire, P., Rosas, D., Makris, N., Dale, A., Dickerson, B., & Fischl, B. (2006). Reliability of MRI-derived measurements of human cerebral cortical thickness: The effects of field strength, scanner upgrade and manufacturer. *NeuroImage*, *32*(1), 180–194. https://doi.org/10.1016/j.neuroimage.2006.02.051

Han, Y., Yang, H., Lv, Y. T., Zhu, C. Z., He, Y., Tang, H. H., Gong, Q. Y., Luo, Y. J., Zang, Y. F., & Dong, Q. (2009). Gray matter density and white matter integrity in pianists' brain: A combined structural and diffusion tensor MRI study. *Neuroscience Letters*. https://doi.org/10.1016/j.neulet.2008.07.056

Haslinger, B., Erhard, P., Altenmüller, E., Schroeder, U., Boecker, H., & Ceballos-Baumann, A. O. (2005). Transmodal sensorimotor networks during action observation in professional pianists. *Journal of Cognitive Neuroscience*. https://doi.org/10.1162/0898929053124893

Henson, R. (2010). *fMRI Basics: Spatial pre-processing*. *6*, 1–10. http://imaging.mrc-cbu.cam.ac.uk/imaging/Introduction_to_fMRI_2010?action=AttachFile&do=get&target=Intro_fMRI_2010_01_preprocessing.pdf

Herdener, M., Esposito, F., Di Salle, F., Boller, C., Hilti, C. C., Habermeyer, B., Scheffler, K., Wetzel, S., Seifritz, E., & Cattapan-Ludewig, K. (2010). Musical training induces functional plasticity in human hippocampus. *Journal of Neuroscience*. https://doi.org/10.1523/JNEUROSCI.4513-09.2010

Herholz, S. C., & Zatorre, R. J. (2012). Musical Training as a Framework for Brain Plasticity: Behavior, Function, and Structure. *Neuron*, *76*(3), 486–502. https://doi.org/10.1016/j.neuron.2012.10.011

Hill, R. A. (2013). Do short-term changes in white matter structure indicate learning-induced myelin plasticity? *Journal of Neuroscience*, *33*(50), 19393–19395. https://doi.org/10.1523/JNEUROSCI.4122-13.2013

Hofstetter, S., Tavor, I., Moryosef, S. T., & Assaf, Y. (2013). Short-term learning induces white matter plasticity in the fornix. *Journal of Neuroscience*. https://doi.org/10.1523/JNEUROSCI.4520-12.2013

Hospital, M. G. (n.d.). *The NMR-MGH fMRI Processing Stream Rapid-Presenation Event-Related Experimental Design*. *0*, 1–3.

Jäncke, L., Gaab, N., Wüstenberg, T., Scheich, H., & Heinze, H. J. (2001). Short-term functional plasticity in the human auditory cortex: An fMRI study. *Cognitive Brain Research*. https://doi.org/10.1016/S0926-6410(01)00092-1

Jäncke, L. (2009). Music drives brain plasticity. *F1000 Biology Reports*. https://doi.org/10.3410/b1-78

Jäncke, L., Koeneke, S., Hoppe, A., Rominger, C., & Hänggi, J. (2009). The architecture of the golfer's brain. *PLoS ONE*. https://doi.org/10.1371/journal.pone.0004785

Jerde, T. A., Childs, S. K., Handy, S. T., Nagode, J. C., & Pardo, J. V. (2011). Dissociable systems of working memory for rhythm and melody. *NeuroImage*. https://doi.org/10.1016/j.neuroimage.2011.05.061

Johansen-berg, H. (2008). *Europe PMC Funders Group The future of functionally-related structural change assessment*. *62*(2), 1293–1298. https://doi.org/10.1016/j.neuroimage.2011.10.073.The

Johansen-Berg, H. (2012). The future of functionally-related structural change assessment. *NeuroImage*, *62*(2), 1293–1298. https://doi.org/10.1016/j.neuroimage.2011.10.073

Jolles, D. D., & Crone, E. A. (2012). Training the developing brain: A neurocognitive perspective. *Frontiers in Human Neuroscience*, *6*(MARCH 2012), 1–29. https://doi.org/10.3389/fnhum.2012.00076

Jolles, D. D., Grol, M. J., Van Buchem, M. A., Rombouts, S. A. R. B., & Crone, E. A. (2010). Practice effects in the brain: Changes in cerebral activation after working memory practice depend on task demands. *NeuroImage*, *52*(2), 658–668. https://doi.org/10.1016/j.neuroimage.2010.04.028

Keller, T. A., & Just, M. A. (2016). Structural and functional neuroplasticity in human learning of spatial routes. *NeuroImage*. https://doi.org/10.1016/j.neuroimage.2015.10.015

Kelly, A. M. C., & Garavan, H. (2005). Human functional neuroimaging of brain changes associated with practice. *Cerebral Cortex*, *15*(8), 1089–1102. https://doi.org/10.1093/cercor/bhi005

Kent, M. (ed). (2006). Fitts and Posner's stages of learning. In *Oxford Dictionary of Sports and Medicine*.

Klasen, M., Kreifelts, B., Chen, Y., Seubert, J., Mathiak, K., & Neuroscience, H. (n.d.). *NEURAL PROCESSING OF EMOTION Topic Editors*. https://doi.org/10.3389/978-2-88919-414-8

Kleim, J. A., & Jones, T. A. (2008). Principles of experience-dependent neural plasticity: Implications for rehabilitation after brain damage. In *Journal of Speech, Language, and Hearing Research*. https://doi.org/10.1044/1092-4388(2008/018)

Klein, C., Liem, F., Hänggi, J., Elmer, S., & Jäncke, L. (2016). The "silent" imprint of musical training. *Human Brain Mapping*. https://doi.org/10.1002/hbm.23045

Kodama, M., Ono, T., Yamashita, F., Ebata, H., Liu, M., Kasuga, S., & Ushiba, J. (2018). Structural Gray Matter Changes in the Hippocampus and the Primary Motor Cortex on An-Hour-to-One- Day Scale Can Predict Arm-Reaching Performance Improvement. *Frontiers in Human Neuroscience*. https://doi.org/10.3389/fnhum.2018.00209

Koelsch, S. (2010). Towards a neural basis of music-evoked emotions. *Trends in Cognitive Sciences*, *14*(3), 131–137. https://doi.org/10.1016/j.tics.2010.01.002

Kokal, I., Engel, A., Kirschner, S., & Keysers, C. (2011). Synchronized drumming enhances activity in the caudate and facilitates prosocial commitment - If the rhythm comes easily. *PLoS ONE*, *6*(11), 1–12. https://doi.org/10.1371/journal.pone.0027272

Krogsrud, S. K., Fjell, A. M., Tamnes, C. K., Grydeland, H., Mork, L., Due-Tønnessen, P., Bjørnerud, A., Sampaio-Baptista, C., Andersson, J., Johansen-Berg, H., & Walhovd, K. B. (2016). Changes in white matter microstructure in the developing brain-A longitudinal diffusion tensor imaging study of children from 4 to 11years of age. *NeuroImage*, *124*, 473–486. https://doi.org/10.1016/j.neuroimage.2015.09.017

Kurth, F., Luders, E., & Gaser, C. (2015). Voxel-Based Morphometry. *Brain Mapping: An Encyclopedic Reference*, *1*, 345–349. https://doi.org/10.1016/B978-0-12-397025-1.00304-3

Kwok, V., Niu, Z., Kay, P., Zhou, K., Mo, L., Jin, Z., So, K. F., & Tan, L. H. (2011). Learning new color names produces rapid increase in gray matter in the intact adult human cortex. *Proceedings of the National Academy of Sciences of the United States of America*. https://doi.org/10.1073/pnas.1103217108

Le Bihan, D., & Iima, M. (2015). Diffusion magnetic resonance imaging: What water tells us about biological tissues. *PLoS Biology*, *13*(7), 1–13. https://doi.org/10.1371/journal.pbio.1002203

Le Bihan, D., Urayama, S. I., Aso, T., Hanakawa, T., & Fukuyama, H. (2006). Direct and fast detection of neuronal activation in the human brain with diffusion MRI. *Proceedings of the National Academy of Sciences of the United States of America*. https://doi.org/10.1073/pnas.0600644103

Lebel, C., & Deoni, S. (2018). The development of brain white matter microstructure. *NeuroImage*, *182*(June 2017), 207–218. https://doi.org/10.1016/j.neuroimage.2017.12.097

Lebel, C., Treit, S., & Beaulieu, C. (2019). A review of diffusion MRI of typical white matter development from early childhood to young adulthood. In *NMR in Biomedicine*. https://doi.org/10.1002/nbm.3778

Lee, D. W. H., Lee, D. W. H., & Han, B. S. (2016). Brodmann's area template based region of interest setting and probabilistic pathway map generation in diffusion tensor tractography: Application to the arcuate fasciculus fiber tract in the human brain. *Frontiers in Neuroanatomy*, *10*(JAN), 1–5. https://doi.org/10.3389/fnana.2016.00004

Lepousez, G., Nissant, A., & Lledo, P. M. (2015). Adult neurogenesis and the future of the rejuvenating brain circuits. In *Neuron*. https://doi.org/10.1016/j.neuron.2015.01.002

Lindquist, M. A. (2008). The Statistical Analysis of fMRI Data. *Statistical Science*, *23*(4), 439–464. https://doi.org/10.1214/09-STS282

Loui, P., Raine, L. B., Chaddock-Heyman, L., Kramer, A. F., & Hillman, C. H. (2019). Musical instrument practice predicts white matter microstructure and cognitive abilities in childhood. *Frontiers in Psychology*, *10*(MAY), 1–10. https://doi.org/10.3389/fpsyg.2019.01198

Lövdén, M., Wenger, E., Mårtensson, J., Lindenberger, U., & Bäckman, L. (2013). Structural brain plasticity in adult learning and development. *Neuroscience and Biobehavioral Reviews*, *37*(9), 2296–2310. https://doi.org/10.1016/j.neubiorev.2013.02.014

Luders, E., Gaser, C., Jancke, L., & Schlaug, G. (2004). A voxel-based approach to gray matter asymmetries. *NeuroImage*, *22*(2), 656–664. https://doi.org/10.1016/j.neuroimage.2004.01.032

Maguire, E. A., Gadian, D. G., Johnsrude, I. S., Good, C. D., Ashburner, J., Frackowiak, R. S. J., & Frith, C. D. (2000). Navigation-related structural change in the hippocampi of taxi drivers. *Proceedings of the National Academy of Sciences of the United States of America*. https://doi.org/10.1073/pnas.070039597

Maguire, E. A., Woollett, K., & Spiers, H. J. (2006). London taxi drivers and bus drivers: A structural MRI and neuropsychological analysis. *Hippocampus*. https://doi.org/10.1002/hipo.20233

Mar, F., & Pdf, H. (2014). *Swift v. Tyson*. *1*(2), 1–23. https://doi.org/10.1016/j.nec.2010.12.004.An

Mason, M. F., Norton, M. I., Van Horn, J. D., Wegner, D. M., Grafton, S. T., & Macrae, C. N. (2007). Wandering minds: The default network and stimulus-independent thought. *Science*. https://doi.org/10.1126/science.1131295

Miendlarzewska, E. A., & Trost, W. J. (2014). How musical training affects cognitive development: Rhythm, reward and other modulating variables. *Frontiers in Neuroscience*, *7*(8 JAN), 1–18. https://doi.org/10.3389/fnins.2013.00279

Mihailoff, G. A., & Haines, D. E. (2018). Motor System II: Corticofugal Systems and the Control of Movement. In *Fundamental Neuroscience for Basic and Clinical Applications: Fifth Edition* (Fifth Edit). Elsevier Inc. https://doi.org/10.1016/B978-0-323-39632-5.00025-6

Minjáres, G. (2014). Edifican "Las Arecas" en territorio arcilloso. *El Diario*, *15*(4), 528–536. https://doi.org/10.1038/nn.3045.Plasticity

Moore, E., Schaefer, R. S., Bastin, M. E., Roberts, N., & Overy, K. (2014). Can musical training influence brain connectivity? Evidence from diffusion tensor MRI. *Brain Sciences*, *4*(2), 405–427. https://doi.org/10.3390/brainsci4020405

Mori, S., & Barker, P. B. (1999). Diffusion magnetic resonance imaging: Its principle and applications. *The Anatomical Record*, *257*(3), 102–109. https://doi.org/10.1002/(SICI)1097-0185(19990615)257:33.0.CO;2-6

Newman-Norlund, R. D., Frey, S. H., Petitto, L. A., & Grafton, S. T. (2006). Anatomical substrates of visual and auditory miniature second-language learning. *Journal of Cognitive Neuroscience*. https://doi.org/10.1162/jocn.2006.18.12.1984

O'Donnell, L. J., & Westin, C. F. (2011). An introduction to diffusion tensor image analysis. In *Neurosurgery Clinics of North America*. https://doi.org/10.1016/j.nec.2010.12.004

Oechslin, M. S., Gschwind, M., & James, C. E. (2018). Tracking Training-Related Plasticity by Combining fMRI and DTI: The Right Hemisphere Ventral Stream Mediates

Musical Syntax Processing. *Cerebral Cortex (New York, N.Y. : 1991)*, *28*(4), 1209–1218. https://doi.org/10.1093/cercor/bhx033

Orgogozo, J. M., & Larsen, B. (1979). Activation of the supplementary motor area during voluntary movement in man suggests it works as a supramotor area. *Science*. https://doi.org/10.1126/science.493986

OriginLab. (2016). *Tutorials for Origin*. 2118.

Overy, K., & Molnar-Szakacs, I. (2009). Being together in time: Musical experience and the mirror neuron system. *Music Perception*, *26*(5), 489–504. https://doi.org/10.1525/mp.2009.26.5.489

Pantelyat, A., Syres, C., Reichwein, S., & Willis, A. (2016). DRUM-PD: The Use of a Drum Circle to Improve the Symptoms and Signs of Parkinson's Disease (PD). *Movement Disorders Clinical Practice*. https://doi.org/10.1002/mdc3.12269

Park, I. S., Lee, K. J., Han, J. W., Lee, N. J., Lee, W. T., Park, K. A., & Rhyu, I. J. (2009). Experience-dependent plasticity of cerebellar vermis in basketball players. *Cerebellum*. https://doi.org/10.1007/s12311-009-0100-1

Patel, R., Spreng, R. N., & Turner, G. R. (2013). Functional brain changes following cognitive and motor skills training: A quantitative meta-analysis. *Neurorehabilitation and Neural Repair*. https://doi.org/10.1177/1545968312461718

Penhune, V. B., & Doyon, J. (2002). Dynamic cortical and subcortical networks in learning and delayed recall of timed motor sequences. *Journal of Neuroscience*. https://doi.org/10.1523/jneurosci.22-04-01397.2002

Penhune, V. B., & Penhune, V. B. (2019). Musical Expertise and Brain Structure: The Causes and Consequences of Training. In *The Oxford Handbook of Music and the Brain*. https://doi.org/10.1093/oxfordhb/9780198804123.013.17

Petersen, S. E., Van Mier, H., Fiez, J. A., & Raichle, M. E. (1998). The effects of practice on the functional anatomy of task performance. *Proceedings of the National Academy of Sciences of the United States of America*. https://doi.org/10.1073/pnas.95.3.853

Petrini, K., Dahl, S., Rocchesso, D., Waadeland, C. H., Avanzini, F., Puce, A., & Pollick, F. E. (2009). Multisensory integration of drumming actions: Musical expertise affects perceived audiovisual asynchrony. *Experimental Brain Research*. https://doi.org/10.1007/s00221-009-1817-2

Piervincenzi, C., Ben-Soussan, T. D., Mauro, F., Mallio, C. A., Errante, Y., Quattrocchi, C. C., & Carducci, F. (2017). White matter microstructural changes following quadrato motor training: A longitudinal study. *Frontiers in Human Neuroscience*, *11*(December), 1–16. https://doi.org/10.3389/fnhum.2017.00590

Raboyeau, G., Marcotte, K., Adrover-Roig, D., & Ansaldo, A. I. (2010). Brain activation and lexical learning: The impact of learning phase and word type. *NeuroImage*. https://doi.org/10.1016/j.neuroimage.2009.10.007

Ramanoël, S., Hoyau, E., Kauffmann, L., Renard, F., Pichat, C., Boudiaf, N., Krainik, A., Jaillard, A., & Baciu, M. (2018). Gray matter volume and cognitive performance during normal aging. A voxel-based morphometry study. *Frontiers in Aging Neuroscience*, *10*(AUG), 1–10. https://doi.org/10.3389/fnagi.2018.00235

Reybrouck, M., Vuust, P., & Brattico, E. (2018). Music and Brain Plasticity: How Sounds Trigger Neurogenerative Adaptations. In *Neuroplasticity - Insights of Neural Reorganization*. https://doi.org/10.5772/intechopen.74318

Rilling, J. K. (2014). Comparative primate neurobiology and the evolution of brain language systems. In *Current Opinion in Neurobiology*. https://doi.org/10.1016/j.conb.2014.04.002

Rizzolatti, G., Fadiga, L., Gallese, V., & Fogassi, L. (1996). Premotor cortex and the recognition of motor actions. *Cognitive Brain Research*. https://doi.org/10.1016/0926-6410(95)00038-0

Rodrigues, A. C., Loureiro, M. A., & Caramelli, P. (2010). Musical training, neuroplasticity and cognition. *Dementia & Neuropsychologia*. https://doi.org/10.1590/s1980-57642010dn40400005

Rojo, N., Amengual, J., Juncadella, M., Rubio, F., Camara, E., Marco-Pallares, J., Schneider, S., Veciana, M., Montero, J., Mohammadi, B., Altenmüller, E., Grau, C., Münte, T. F., & Rodriguez-Fornells, A. (2011). Music-Supported Therapy induces plasticity in the sensorimotor cortex in chronic stroke: A single-case study using multimodal imaging (fMRI-TMS). *Brain Injury*. https://doi.org/10.3109/02699052.2011.576305

Roland, P. E., Larsen, B., Lassen, N. A., & Skinhoj, E. (1980). Supplementary motor area and other cortical areas in organization of voluntary movements in man. *Journal of Neurophysiology*. https://doi.org/10.1152/jn.1980.43.1.118

Ronsse, R., Puttemans, V., Coxon, J. P., Goble, D. J., Wagemans, J., Wenderoth, N., & Swinnen, S. P. (2011). Motor learning with augmented feedback: Modality-dependent behavioral and neural consequences. *Cerebral Cortex*. https://doi.org/10.1093/cercor/bhq209

Rusznák, Z., Henskens, W., Schofield, E., Kim, W. S., & Fu, Y. H. (2016). Adult neurogenesis and gliogenesis: Possible mechanisms for neurorestoration. *Experimental Neurobiology*. https://doi.org/10.5607/en.2016.25.3.103

S, M., & A, M. (2018). Rehabilitation Medicine for Elderly Patients, a further note. In *Biology, Engineering and Medicine* (Vol. 3, Issue 3). https://doi.org/10.15761/bem.1000s1006

Sagi, Y., Tavor, I., Hofstetter, S., Tzur-Moryosef, S., Blumenfeld-Katzir, T., & Assaf, Y. (2012). Learning in the Fast Lane: New Insights into Neuroplasticity. *Neuron*, *73*(6), 1195–1203. https://doi.org/10.1016/j.neuron.2012.01.025

Sakai, K., Hikosaka, O., Miyauchi, S., Takino, R., Sasaki, Y., & Pütz, B. (1998). Transition of brain activation from frontal to parietal areas in visuomotor sequence learning. *Journal of Neuroscience*. https://doi.org/10.1523/jneurosci.18-05-01827.1998

Salat, D. H., Buckner, R. L., Snyder, A. Z., Greve, D. N., Desikan, R. S. R., Busa, E., Morris, J. C., Dale, A. M., & Fischl, B. (2004). Thinning of the cerebral cortex in aging. *Cerebral Cortex*, *14*(7), 721–730. https://doi.org/10.1093/cercor/bhh032

Salminen, T., Mårtensson, J., Schubert, T., & Kühn, S. (2016). Increased integrity of white matter pathways after dual n-back training. *NeuroImage*, *133*, 244–250. https://doi.org/10.1016/j.neuroimage.2016.03.028

Sampaio-Baptista, C., & Johansen-Berg, H. (2017). White Matter Plasticity in the Adult Brain. *Neuron*, *96*(6), 1239–1251. https://doi.org/10.1016/j.neuron.2017.11.026

Sampaio-Baptista, C., Khrapitchev, A. A., Foxley, S., Schlagheck, T., Scholz, J., Jbabdi, S., DeLuca, G. C., Miller, K. L., Taylor, A., Thomas, N., Kleim, J., Sibson, N. R., Bannerman, D., & Johansen-Berg, H. (2013). Motor skill learning induces changes in white matter microstructure and myelination. *Journal of Neuroscience*, *33*(50), 19499–19503. https://doi.org/10.1523/JNEUROSCI.3048-13.2013

Särkämö, T., & Sihvonen, A. J. (2018). Golden oldies and silver brains: Deficits, preservation, learning, and rehabilitation effects of music in ageing-related neurological disorders. In *Cortex*. https://doi.org/10.1016/j.cortex.2018.08.034

Särkämö, T., Tervaniemi, M., & Huotilainen, M. (2013). Music perception and cognition: Development, neural basis, and rehabilitative use of music. *Wiley Interdisciplinary Reviews: Cognitive Science*. https://doi.org/10.1002/wcs.1237

Schlaffke, L., Leemans, A., Schweizer, L. M., Ocklenburg, S., & Schmidt-Wilcke, T. (2017). Learning morse code alters microstructural properties in the inferior longitudinal fasciculus: A DTI study. *Frontiers in Human Neuroscience*. https://doi.org/10.3389/fnhum.2017.00383

Schlaug, G. (2015). Musicians and music making as a model for the study of brain plasticity. In *Progress in Brain Research*. https://doi.org/10.1016/bs.pbr.2014.11.020

Schlaug, G. (2001). The brain of musicians: A model for functional and structural adaptation. *Annals of the New York Academy of Sciences*. https://doi.org/10.1111/j.1749-6632.2001.tb05739.x

Schlaug, G., Forgeard, M., Zhu, L., Norton, A., Norton, A., & Winner, E. (2009). Training-induced neuroplasticity in young children. *Annals of the New York Academy of Sciences*, *1169*(Cc), 205–208. https://doi.org/10.1111/j.1749-6632.2009.04842.x

Schlaug, G., Laboratories, R., Israel, B., & Medical, D. (2015). *plasticity*. 37–55. https://doi.org/10.1016/bs.pbr.2014.11.020.Musicians

Schmithorst, V. J., & Wilke, M. (2002). Differences in white matter architecture between musicians and non-musicians: A diffusion tensor imaging study. *Neuroscience Letters*, *321*(1–2), 57–60. https://doi.org/10.1016/S0304-3940(02)00054-X

Scholl, B., & Priebe, N. J. (2015). Neuroscience : the cortical connection. In *Nature*. https://doi.org/10.1038/nature14201

Scholz, J., Klein, M. C., Behrens, T. E. J., & Johansen-Berg, H. (2009). Training induces changes in white-matter architecture. *Nature Neuroscience*. https://doi.org/10.1038/nn.2412

Scholz, J., Klein, M. C., Behrens, T. E. J., & Johansen-berg, H. (2010). Europe PMC Funders Group Training induces changes in white matter architecture. *Nat Neurosci.*, *12*(11), 1370–1371. https://doi.org/10.1038/nn.2412.Training

Ségonne, F., Dale, A. M., Busa, E., Glessner, M., Salat, D., Hahn, H. K., & Fischl, B. (2004). A hybrid approach to the skull stripping problem in MRI. *NeuroImage*, *22*(3), 1060–1075. https://doi.org/10.1016/j.neuroimage.2004.03.032

Ségonne, F., Grimson, E., & Fischl, B. (2005). A genetic algorithm for the topology correction of cortical surfaces. *Lecture Notes in Computer Science*, *3565*, 393–405. https://doi.org/10.1007/11505730_33

Sexton, C. E., Walhovd, K. B., Storsve, A. B., Tamnes, C. K., Westlye, L. T., Johansen-Berg, H., & Fjell, A. M. (2014). Accelerated changes in white matter microstructure during aging: A longitudinal diffusion tensor imaging study. *Journal of Neuroscience*, *34*(46), 15425–15436. https://doi.org/10.1523/JNEUROSCI.0203-14.2014

Shen, Y., Lin, Y., Liu, S., Fang, L., & Liu, G. (2019). Sustained effect of music training on the enhancement of executive function in preschool children. *Frontiers in Psychology*, *10*(AUG), 1–14. https://doi.org/10.3389/fpsyg.2019.01910

Shenton, M., Hamoda, H., & Zafonte, R. (2012). A review of MRI and DTI Findings in Mild Traumatic Brain Injury. *Brain Imaging Behav*, *6*(2), 137–192. https://doi.org/10.1007/s11682-012-9156-5.A

Sikka, R., Cuddy, L. L., Johnsrude, I. S., & Vanstone, A. D. (2015). An fMRI comparison of neural activity associated with recognition of familiar melodies in younger and older adults. *Frontiers in Neuroscience*, *9*(OCT), 1–10. https://doi.org/10.3389/fnins.2015.00356

Smith, S. M., Jenkinson, M., Woolrich, M. W., Beckmann, C. F., Behrens, T. E. J., Johansen-Berg, H., Bannister, P. R., De Luca, M., Drobnjak, I., Flitney, D. E., Niazy, R. K., Saunders, J., Vickers, J., Zhang, Y., De Stefano, N., Brady, J. M., & Matthews, P. M. (2004). Advances in functional and structural MR image analysis and implementation as FSL. *NeuroImage*, *23*(SUPPL. 1), 208–219. https://doi.org/10.1016/j.neuroimage.2004.07.051

Smith, S. M., & Nichols, T. E. (2009). Threshold-free cluster enhancement: Addressing problems of smoothing, threshold dependence and localisation in cluster inference. *NeuroImage*, *44*(1), 83–98. https://doi.org/10.1016/j.neuroimage.2008.03.061

Soares, J. M., Marques, P., Alves, V., & Sousa, N. (2013). A hitchhiker's guide to diffusion tensor imaging. *Frontiers in Neuroscience*, *7*(7 MAR), 1–14. https://doi.org/10.3389/fnins.2013.00031

Staigeri, J. F., & Steinmetz, H. (1995). Pergamon SIZE IN MUSICIANS GOTTFRIED SCHLAUG ,* ~ f LUTZ J , ANCKE , $ YANXIONG HUANG , t The corpus callosum ( CC ) as the main interhemispheric fiber tract plays an important role. *Neurology*, *33*(8), 1047–1055.

Steele, C. J., Bailey, J. A., Zatorre, R. J., & Penhune, V. B. (2013). Early musical training and white-matter plasticity in the corpus callosum: Evidence for a sensitive period. *Journal of Neuroscience*, *33*(3), 1282–1290. https://doi.org/10.1523/JNEUROSCI.3578-12.2013

Sui, J., & Calhoun, V. D. (2009). *fMRI Techniques and Protocols* (Vol. 41). https://doi.org/10.1007/978-1-60327-919-2

Sylvaine, A., Mortamais, M., Poulain, V., Maller, J., Meslin, C., Bonafé, A., Le Bars, E., Touchon, J., Berr, C., & Ritchie, K. (2013). P2-170: Structural changes of the corpus callosum predicts severe cognitive decline and dementia: A longitudinal 7-year study. *Alzheimer's & Dementia*, *9*(3), P411–P411. https://doi.org/10.1016/j.jalz.2013.05.815

Takeuchi, H., Sekiguchi, A., Taki, Y., Yokoyama, S., Yomogida, Y., Komuro, N., Yamanouchi, T., Suzuki, S., & Kawashima, R. (2010). Training of working memory impacts structural connectivity. *Journal of Neuroscience*, *30*(9), 3297–3303. https://doi.org/10.1523/JNEUROSCI.4611-09.2010

Takeuchi, H., Taki, Y., Hashizume, H., Sassa, Y., Nagase, T., Nouchi, R., & Kawashima, R. (2011). Effects of training of processing speed on neural systems. *Journal of Neuroscience*. https://doi.org/10.1523/JNEUROSCI.2948-11.2011

Tanaka, S., & Kirino, E. (2019). Increased functional connectivity of the angular gyrus during imagined music performance. *Frontiers in Human Neuroscience*, *13*(March), 1–8. https://doi.org/10.3389/fnhum.2019.00092

Tanji, J. (2001). Sequential organization of multiple movements: Involvement of cortical motor areas. In *Annual Review of Neuroscience*. https://doi.org/10.1146/annurev.neuro.24.1.631

Tanji, J. (1994). The supplementary motor area in the cerebral cortex. In *Neuroscience Research*. https://doi.org/10.1016/0168-0102(94)90038-8

Target, R., & Average, I. (2005). *Intesity Normalization and Data Integrity Analysis with Intensity Normalization Implementation Usage*. 1–5.

Taubert, M., Draganski, B., Anwander, A., Müller, K., Horstmann, A., Villringer, A., & Ragert, P. (2010). Dynamic properties of human brain structure: Learning-related changes in cortical areas and associated fiber connections. *Journal of Neuroscience*, *30*(35), 11670–11677. https://doi.org/10.1523/JNEUROSCI.2567-10.2010

Taubert, M., Mehnert, J., Pleger, B., & Villringer, A. (2016). Rapid and specific gray matter changes in M1 induced by balance training. *NeuroImage*. https://doi.org/10.1016/j.neuroimage.2016.03.017

Taubert, M., Villringer, A., & Ragert, P. (2012). Learning-related gray and white matter changes in humans: An update. *Neuroscientist*. https://doi.org/10.1177/1073858411419048

Thaut, M. H., Trimarchi, P. D., & Parsons, L. M. (2014). Human brain basis of musical rhythm perception: Common and distinct neural substrates for meter, tempo, and patter. *Brain Sciences*. https://doi.org/10.3390/brainsci4020428

Thiebaut de Schotten, M., ffytche, D. H., Bizzi, A., Dell'Acqua, F., Allin, M., Walshe, M., Murray, R., Williams, S. C., Murphy, D. G. M., & Catani, M. (2011). Atlasing location, asymmetry and inter-subject variability of white matter tracts in the human brain with MR diffusion tractography. *NeuroImage*, *54*(1), 49–59. https://doi.org/10.1016/j.neuroimage.2010.07.055

Thomas Yeo, B. T., Krienen, F. M., Sepulcre, J., Sabuncu, M. R., Lashkari, D., Hollinshead, M., Roffman, J. L., Smoller, J. W., Zöllei, L., Polimeni, J. R., Fisch, B., Liu, H., & Buckner, R. L. (2011). The organization of the human cerebral cortex estimated by intrinsic functional connectivity. *Journal of Neurophysiology*, *106*(3), 1125–1165. https://doi.org/10.1152/jn.00338.2011

Thomas Yeo, B. T., Sabuncu, M. R., Desikan, R., Fischl, B., & Golland, P. (2008). Effects of registration regularization and atlas sharpness on segmentation accuracy. *Medical Image Analysis*, *12*(5), 603–615. https://doi.org/10.1016/j.media.2008.06.005

Thomas, C., & Baker, C. I. (2013). Teaching an adult brain new tricks: A critical review of evidence for training-dependent structural plasticity in humans. *NeuroImage*, *73*, 225–236. https://doi.org/10.1016/j.neuroimage.2012.03.069

Thomas, C., & Baker, C. I. (2012). Remodeling human cortex through training: Comment on May. In *Trends in Cognitive Sciences*. https://doi.org/10.1016/j.tics.2011.12.005

Tracy, J., Flanders, A., Madi, S., Laskas, J., Stoddard, E., Pyrros, A., Natale, P., & DelVecchio, N. (2003). Regional brain activation associated with different performance patterns during learning of a complex motor skill. *Cerebral Cortex*, *13*(9), 904–910. https://doi.org/10.1093/cercor/13.9.904

Valkanova, V., Eguia Rodriguez, R., & Ebmeier, K. P. (2014). Mind over matter - What do we know about neuroplasticity in adults? *International Psychogeriatrics*, *26*(6), 891–909. https://doi.org/10.1017/S1041610213002482

Vaquero, L., Hartmann, K., Ripollés, P., Rojo, N., Sierpowska, J., François, C., Càmara, E., van Vugt, F. T., Mohammadi, B., Samii, A., Münte, T. F., Rodríguez-Fornells, A., & Altenmüller, E. (2016). Structural neuroplasticity in expert pianists depends on the age of musical training onset. *NeuroImage*, *126*, 106–119. https://doi.org/10.1016/j.neuroimage.2015.11.008

Vikene, K., Skeie, G. O., & Specht, K. (2019). Subjective judgments of rhythmic complexity in Parkinson's disease: Higher baseline, preserved relative ability, and modulated by tempo. *PLoS ONE*. https://doi.org/10.1371/journal.pone.0221752

Wan, C. Y., & Schlaug, G. (2010). Making music as a tool for brain plasticity. *Neuroscientist*, *16*(5), 566–577. https://doi.org/10.1177/1073858410377805.Music

Wedeen, V. J., Hagmann, P., Tseng, W. Y. I., Reese, T. G., & Weisskoff, R. M. (2005). Mapping complex tissue architecture with diffusion spectrum magnetic resonance imaging. *Magnetic Resonance in Medicine*. https://doi.org/10.1002/mrm.20642

Werner, K., & Frotscher, M. (2010). Color Atlas and Textbook of Human Anatomy: Nervous system and sensory organs. *The British Journal of Ophthalmology*, *94*(9), i. https://doi.org/10.1136/bjo.2010.193169

Whitfield-Gabrieli, While, I., Matlab, S., Path-, S., Folder, A., Save, C., Step, S. B. Y., & To, G. U. I. (2009). *REX Manual*. 1–9.

Wong, P. C. M., Perrachione, T. K., & Parrish, T. B. (2007). Neural characteristics of successful and less successful speech and word learning in adults. *Human Brain Mapping*. https://doi.org/10.1002/hbm.20330

Xu, X., Yuan, H., & Lei, X. (2016). Activation and Connectivity within the Default Mode Network Contribute Independently to Future-Oriented Thought. *Scientific Reports*. https://doi.org/10.1038/srep21001

Yousry, T. A., Schmid, U. D., Alkadhi, H., Schmidt, D., Peraud, A., Buettner, A., & Winkler, P. (1997). Localization of the motor hand area to a knob on the precentral gyrus. A new landmark. *Brain*, *120*(1), 141–157. https://doi.org/10.1093/brain/120.1.141

Yuko Yotsumoto Takeo Watanabe, and Y. S. (2009). *Different dynamics of performance and brain activation in the time course of perceptual learning*. *57*(6), 827–833. https://doi.org/10.1016/j.neuron.2008.02.034.Different

Zafar, R., Malik, A. S., Kamel, N., & Dass, S. C. (2016). Role of voxel selection and ROI in fMRI data analysis. *2016 IEEE International Symposium on Medical Measurements and Applications, MeMeA 2016 - Proceedings*, 1–6. https://doi.org/10.1109/MeMeA.2016.7533739

Zarei, M., Johansen-Berg, H., Smith, S., Ciccarelli, O., Thompson, A. J., & Matthews, P. M. (2006). Functional anatomy of interhemispheric cortical connections in the human brain. *Journal of Anatomy*. https://doi.org/10.1111/j.1469-7580.2006.00615.x

Zatorre, R. J. (2013). Predispositions and plasticity in music and speech learning: Neural correlates and implications. In *Science*. https://doi.org/10.1126/science.1238414

Zatorre, R. J., Chen, J. L., & Penhune, V. B. (2007). When the brain plays music: Auditory-motor interactions in music perception and production. *Nature Reviews Neuroscience*, *8*(7), 547–558. https://doi.org/10.1038/nrn2152

Zatorre, R. J., Delhommeau, K., & Zarate, J. M. (2012). Modulation of auditory cortex response to pitch variation following training with microtonal melodies. *Frontiers in Psychology*, *3*(DEC), 1–17. https://doi.org/10.3389/fpsyg.2012.00544

Zatorre, R. J., Fields, R. D., & Johansen-Berg, H. (2012). Plasticity in gray and white: Neuroimaging changes in brain structure during learning. In *Nature Neuroscience*. https://doi.org/10.1038/nn.3045

Zhang, H., Xu, L., Wang, S., Xie, B., Guo, J., Long, Z., & Yao, L. (2011). Behavioral improvements and brain functional alterations by motor imagery training. *Brain Research*. https://doi.org/10.1016/j.brainres.2011.06.038

Zhang, Y., Chen, G., Wen, H., Lu, K. H., & Liu, Z. (2017). Musical Imagery Involves Wernicke's Area in Bilateral and Anti-Correlated Network Interactions in Musicians. *Scientific Reports*, *7*(1), 1–13. https://doi.org/10.1038/s41598-017-17178-4

Zhu, D., Zhang, T., Jiang, X., Hu, X., Chen, H., Yang, N., Lv, J., Han, J., Guo, L., & Liu, T. (2014). Fusing DTI and fMRI data: A survey of methods and applications. *NeuroImage*, *102*(P1), 184–191. https://doi.org/10.1016/j.neuroimage.2013.09.071

Zilles, K. (1992). Neuronal plasticity as an adaptive property of the central nervous system.

# Chapter 8　Appendix

| The inclusion criteria | The exclusion criteria |
|---|---|
| if you are: | if you have any of the following: |
| Above 18 years | Cardiac pacemaker |
| No prior drumming experience | Certain artificial heart valves and stents |
| | Brain clips |
| | Certain intra-uterine contraceptive coils |
| | Wires directly into your heart |
| | Metal fragments in the eye or head |
| | Certain ear implants |
| | Neuro-electrical stimulators |
| | Pregnancy |

Table 22. provide an overview of the inclusion and exclusion criteria for healthy volunteers.

| S01 | | S02 | | S03 | | S04 | | S05 | |
|---|---|---|---|---|---|---|---|---|---|
| Timeline (days) | -/+ headph one | Timeline (days) | -/+ headph one | Timeline (days) | -/+ headph one | Timeline (days ) | -/+ headph one | Timeline (days ) | -/+ headph one |
| -18 | 0 | -18 | 0 | -13 | 0 | -13 | 0 | -22 | 1* |
| -4 | 1* | -4 | 1* | -4 | 1* | -4 | 1* | -4 | 0 |
| 1 | 0 | 1 | 0 | 1 | 0 | 1 | 0 | 1 | 0 |
| 2 | 0 | 2 | 0 | 2 | 0 | 2 | 0 | 3 | 0 |
| 4 | 0 | 7 | 0 | 7 | 0 | 7 | 0 | 6 | 0 |
| 7 | 0 | 10 | 0 | 9 | 0 | 9 | 0 | 10 | 0 |
| 10 | 0 | 18 | 0 | 17 | 0 | 17 | 0 | 17 | 0 |
| 18 | 0 | 25 | 0 | 24 | 0 | 24 | 0 | 22 | 0 |
| 25 | 0 | 39 | 0 | 37 | 0 | 37 | 0 | 30 | 0 |
| 39 | 0 | 51 | 0 | 56 | 0 | 56 | 0 | 69 | 0 |
| 51 | 0 | 84 | 0 | 84 | 0 | 84 | 0 | 99 | 1* |
| 70 | 0 | 113 | 1* | 106 | 1* | 106 | 1* | 136 | 0 |
| 93 | 0 | 151 | 0 | 136 | 0 | 136 | 0 | 168 | 1* |
| 113 | 1* | 183 | 1* | 183 | 1* | 183 | 1* | X | X |
| 151 | 0 | X | X | X | X | X | X | X | X |
| X | X | X | X | X | X | X | X | X | X |
| X | X | X | X | X | X | X | X | X | X |
| S06 | | S07 | | S08 | | S09 | | S10 | |
| Timeline (days ) | -/+ headph one | Timeline (days ) | -/+ headph one | Timeline (days ) | -/+ headph one | Timeline (days ) | -/+ headph one | Timeline (days ) | -/+ headph one |
| -6 | 0 | -8 | 0 | -8 | 0 | -2 | 0 | -41 | 0 |
| -4 | 1* | -4 | 1* | -4 | 1* | -1 | 1* | -1 | 1* |
| 1 | 0 | 1 | 0 | 1 | 0 | 1 | 0 | 0 | 0 |
| 3 | 0 | 3 | 0 | 3 | 0 | 5 | 0 | 1 | 0 |
| 6 | 0 | 8 | 0 | 8 | 0 | 9 | 0 | 7 | 0 |
| 10 | 0 | 30 | 0 | 10 | 0 | 15 | 0 | 9 | 0 |
| 17 | 0 | 37 | 0 | 16 | 0 | 19 | 0 | 13 | 0 |
| 24 | 0 | 48 | 0 | 24 | 0 | 23 | 0 | 20 | 0 |
| 30 | 0 | 69 | 0 | 30 | 0 | 42 | 0 | 28 | 0 |
| 41 | 0 | 77 | 0 | 48 | 0 | 51 | 0 | 37 | 0 |
| 69 | 0 | 86 | 0 | 77 | 0 | 77 | 0 | 42 | 0 |

| | | | | | | | | | |
|---|---|---|---|---|---|---|---|---|---|
| 99 | 1* | 105 | 1* | 91 | 0 | 111 | 1* | 58 | 0 |
| 136 | 0 | 140 | 0 | 105 | 1* | 125 | 0 | 77 | 0 |
| 168 | 1* | X | X | 140 | 0 | X | X | X | X |
| X | X | X | X | X | X | X | X | X | X |
| **S11** | | **S12** | | **S13** | | **S14** | | **S15** | |
| Timeline (days) | -/+ headphone | Timeline (days) | -/+ headphone | Timeline (days) | -/+ headphone | Timeline (days) | -/+ headphone | Timeline (days) | -/+ headphone |
| -41 | 0 | -6 | 0 | -4 | 0 | -7 | 0 | -8 | 0 |
| -4 | 1* | -1 | 1* | -1 | 1* | -6 | 1* | -7 | 1* |
| -1 | 0 | 1 | 0 | 1 | 0 | 1 | 0 | 1 | 0 |
| 1 | 0 | 7 | 0 | 7 | 0 | 3 | 0 | 3 | 0 |
| 6 | 0 | 9 | 0 | 9 | 0 | 7 | 0 | 17 | 0 |
| 9 | 0 | 13 | 0 | 16 | 0 | 10 | 0 | 23 | 0 |
| 13 | 0 | 20 | 0 | 20 | 0 | 17 | 0 | 28 | 0 |
| 20 | 0 | 28 | 0 | 28 | 0 | 22 | 0 | 38 | 0 |
| 28 | 0 | 37 | 0 | 37 | 0 | 31 | 0 | 44 | 0 |
| 37 | 0 | 42 | 0 | 42 | 0 | 38 | 0 | 58 | 0 |
| 44 | 0 | 56 | 0 | 62 | 0 | 51 | 0 | 79 | 0 |
| 56 | 0 | X | X | 72 | 0 | X | X | X | X |
| 72 | 0 | X | X | X | X | X | X | X | X |
| X | X | X | X | X | X | X | X | X | X |

Table 23. presents the individual timelime of the diffusion scanning sessions including all the participants.